

1 **Supplementary Information for:**

2 **Effects of individual base-pairs on in vivo target search and destruction**

3 **kinetics of bacterial small RNA**

4
5 **Anustup Poddar¹, Muhammad S. Azam^{2,3}, Tunc Kayikcioglu¹, Maksym Bobrovskyy^{2,4},**
6 **Jichuan Zhang¹, Xiangqian Ma², Piyush Labhsetwar^{5,6}, Jingyi Fei⁷, Digvijay Singh^{1,8}, Zaida**
7 **Luthey-Schulten⁵, Carin K. Vanderpool^{2,*} and Taekjip Ha^{1,9,*}**

8
9 ¹Department of Biophysics and Biophysical Chemistry, Johns Hopkins University School of
10 Medicine, Baltimore, Maryland 21205

11 ²Department of Microbiology, University of Illinois at Urbana-Champaign, Urbana, Illinois 61801

12 ³Present Address: Department of Biochemistry and Molecular Biology, University of Chicago,
13 Chicago, Illinois 60637

14 ⁴Present Address: Department of Microbiology, University of Chicago, Chicago, Illinois 60637

15 ⁵Department of Chemistry, University of Illinois at Urbana-Champaign, Urbana, Illinois 61801

16 ⁶Present Address: The Land Institute, Salina, Kansas 67401

17 ⁷Department of Biochemistry and Molecular Biology, University of Chicago, Chicago, Illinois
18 60637

19 ⁸Present Address: Division of Biological Sciences, University of California, San Diego, San
20 Diego, California 92093

21 ⁹Howard Hughes Medical Institute, Baltimore, Maryland 21205

22

23 * Corresponding authors

24 Taekjip Ha, Ph.D. (tjha@jhu.edu)

25 Carin K. Vanderpool, Ph.D. (cvanderp@illinois.edu)

26

27 This document includes:

28 **Supplementary Figures 1-54**

29 **Supplementary Tables 1-4**

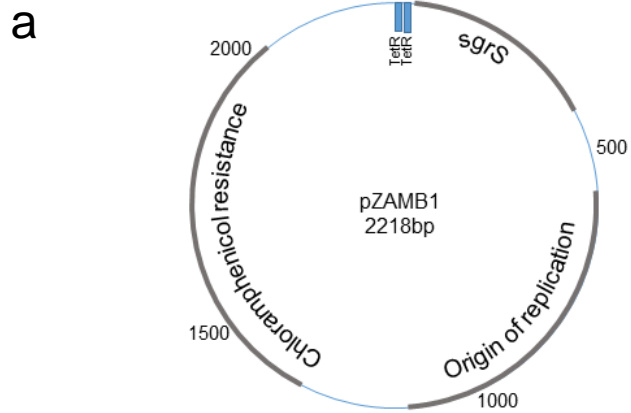
30 **Supplementary Note 1**

31 **References**

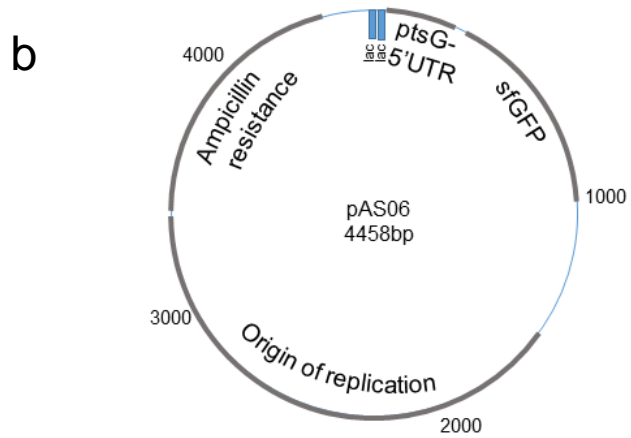
32

33

34 **Supplementary Figures**



35

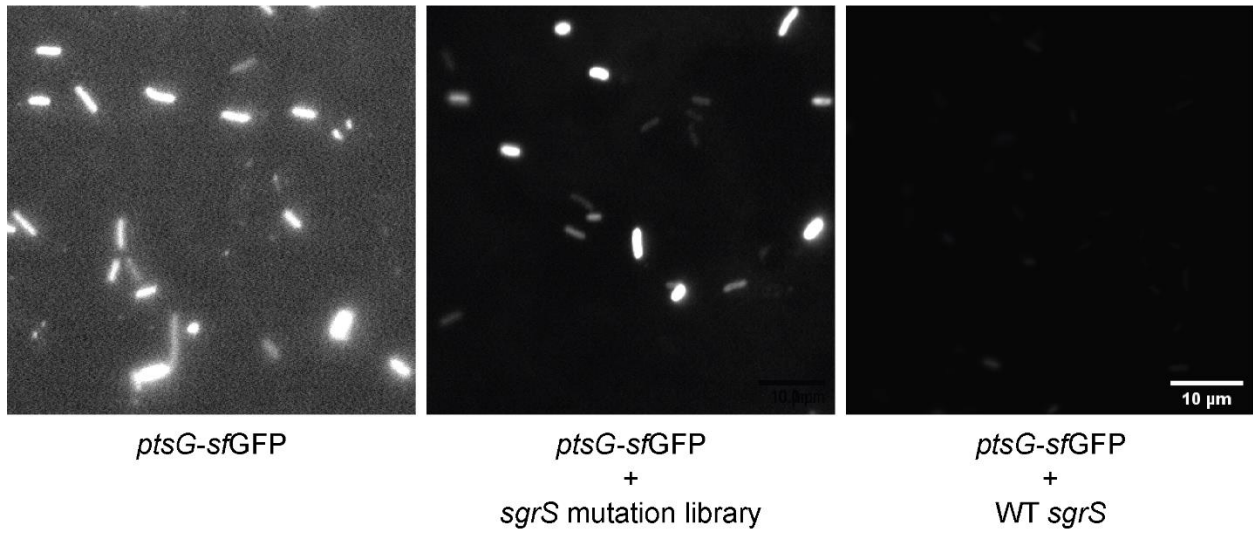


36

37 **Supplementary Figure 1. Plasmids used for Sort-Seq.** (a) pZAMB1 plasmid containing wild-
38 type *sgrS* sequence, (b) pAS06 plasmid containing *ptsG* 5' UTR fused to superfolder GFP
39 (sfGFP).

40

41



42

43

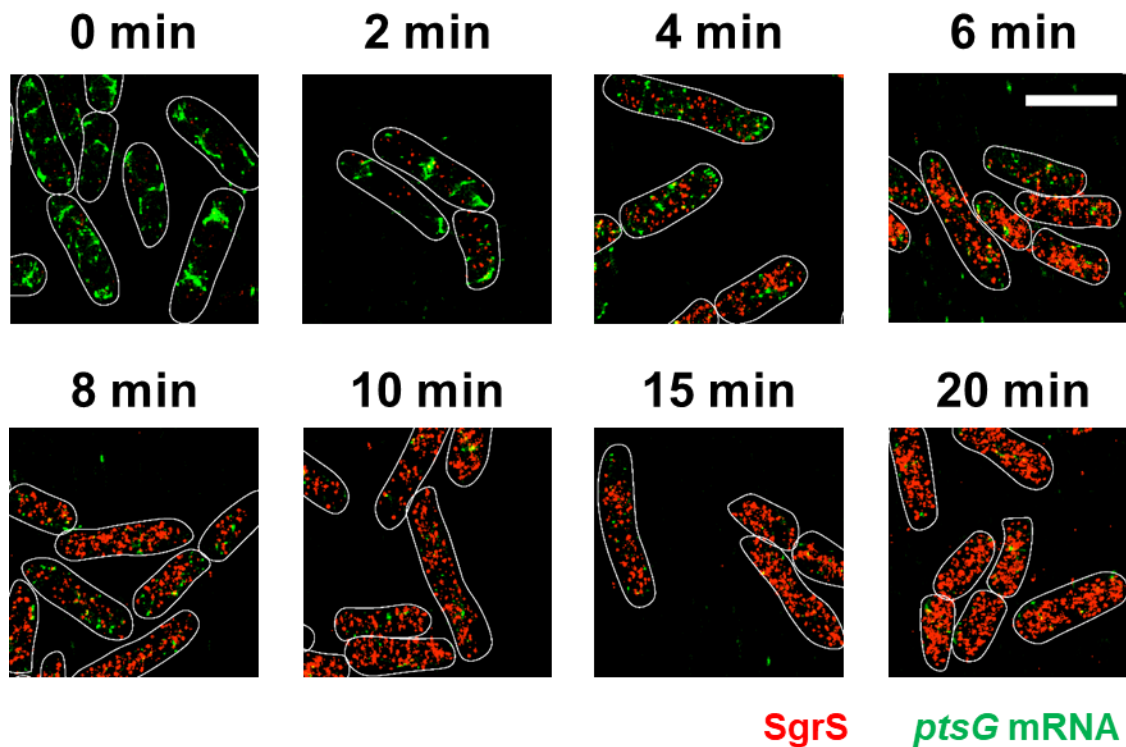
44 **Supplementary Figure 2. Verification of target-reporter system.** Epifluorescence imaging of

45 cells expressing only *ptsG-sfGFP*, *ptsG-sfGFP* with WT *sgrS* and *ptsG-sfGFP* with *sgrS* mutation

46 library. Each experiment was performed independently 2 times. Scale bar is 10 μm and applies to

47 all the panels.

48

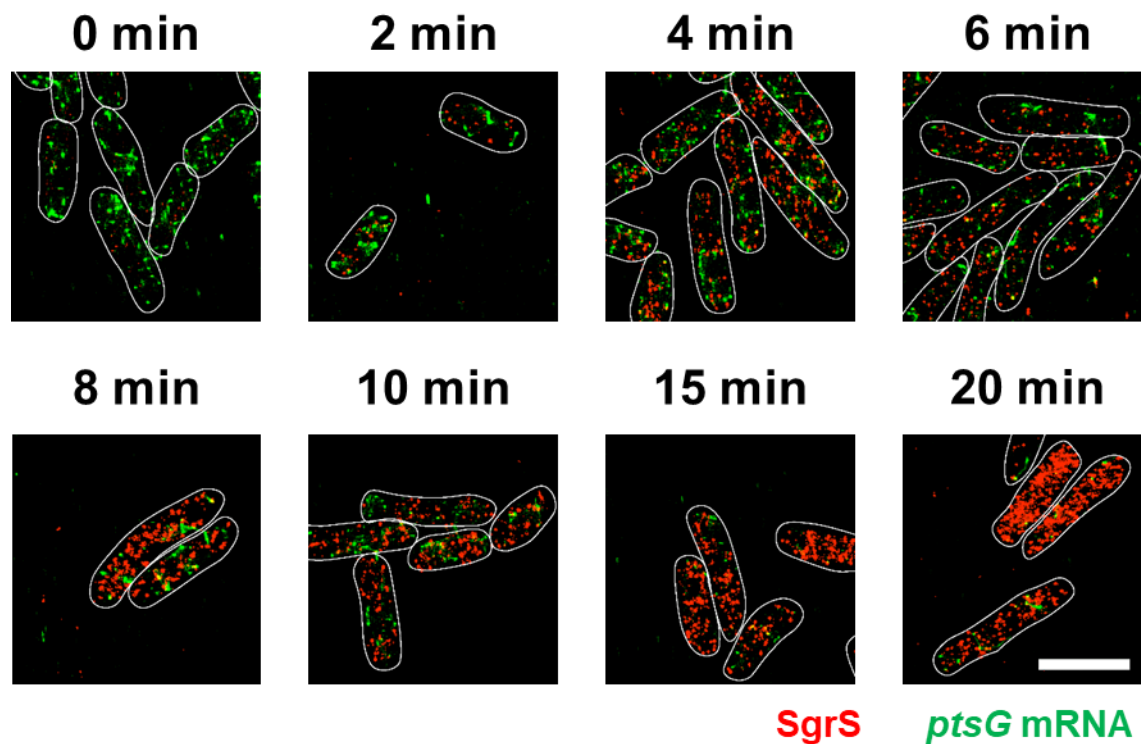


49

50 **Supplementary Figure 3. 3D super-resolution images of SgrS (red) and *ptsG* mRNA (green)**
 51 **in the wild-type SgrS strain projected on 2D planes.** The panels show the multi-color images
 52 of WT SgrS cells before (0 min) and 2, 4, 6, 8, 10, 15, 20 min after α MG (non-metabolizable
 53 sugar analog) induction. Each experiment was performed independently 2 times. White lines
 54 denote cell boundaries. Scale bar is 2 μ m and applies to all the panels.

55

56



57

58 **Supplementary Figure 4. 3D super-resolution images of SgrS (red) and *ptsG* mRNA (green)**

59 **in the SgrS A177U mutant strain projected on 2D planes.** The panels show the multi-color

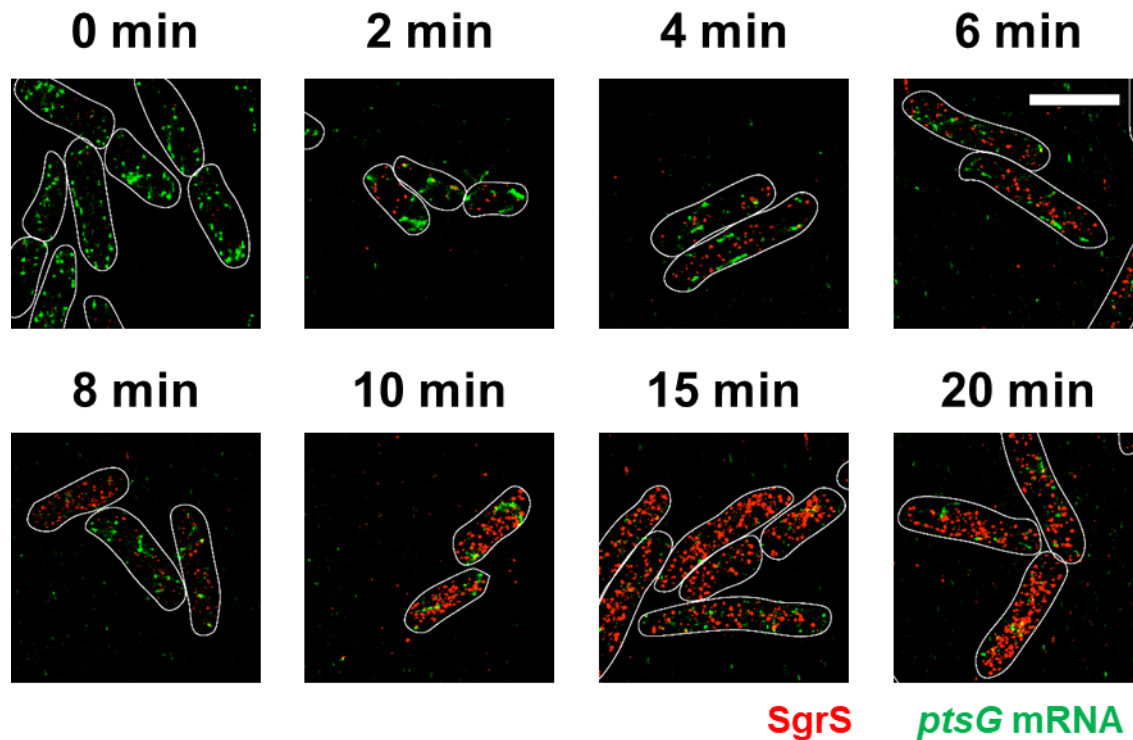
60 images of SgrS A177U cells before (0 min) and 2, 4, 6, 8, 10, 15, 20 min after α MG (non-

61 metabolizable sugar analog) induction. Each experiment was performed independently 2 times.

62 White lines denote cell boundaries. Scale bar is 2 μ m and applies to all the panels.

63

64

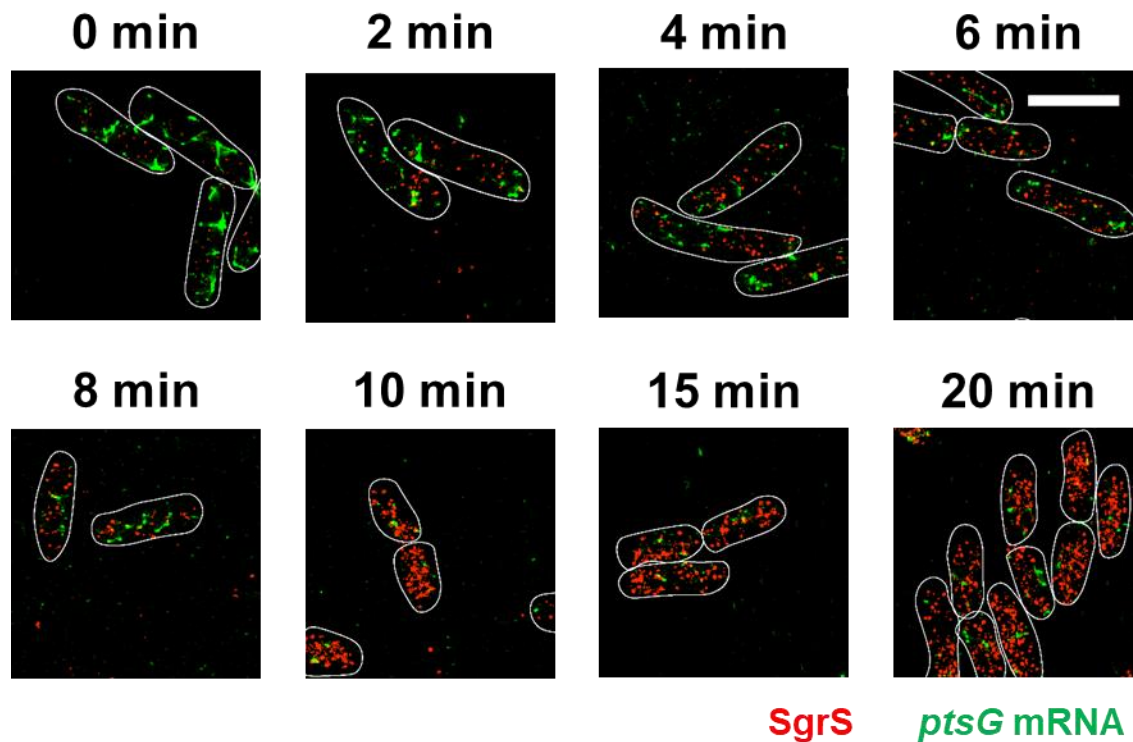


65

66 **Supplementary Figure 5. 3D super-resolution images of SgrS (red) and *ptsG* mRNA (green)**
 67 **in the SgrS G178A mutant strain projected on 2D planes.** The panels show the multi-color
 68 images of SgrS G178A cells before (0 min) and 2, 4, 6, 8, 10, 15, 20 min after α MG (non-
 69 metabolizable sugar analog) induction. Each experiment was performed independently 2 times.
 70 White lines denote cell boundaries. Scale bar is 2 μ m and applies to all the panels.

71

72



73

74 **Supplementary Figure 6. 3D super-resolution images of SgrS (red) and *ptsG* mRNA (green)**

75 **in the SgrS G178U mutant strain projected on 2D planes.** The panels show the multi-color

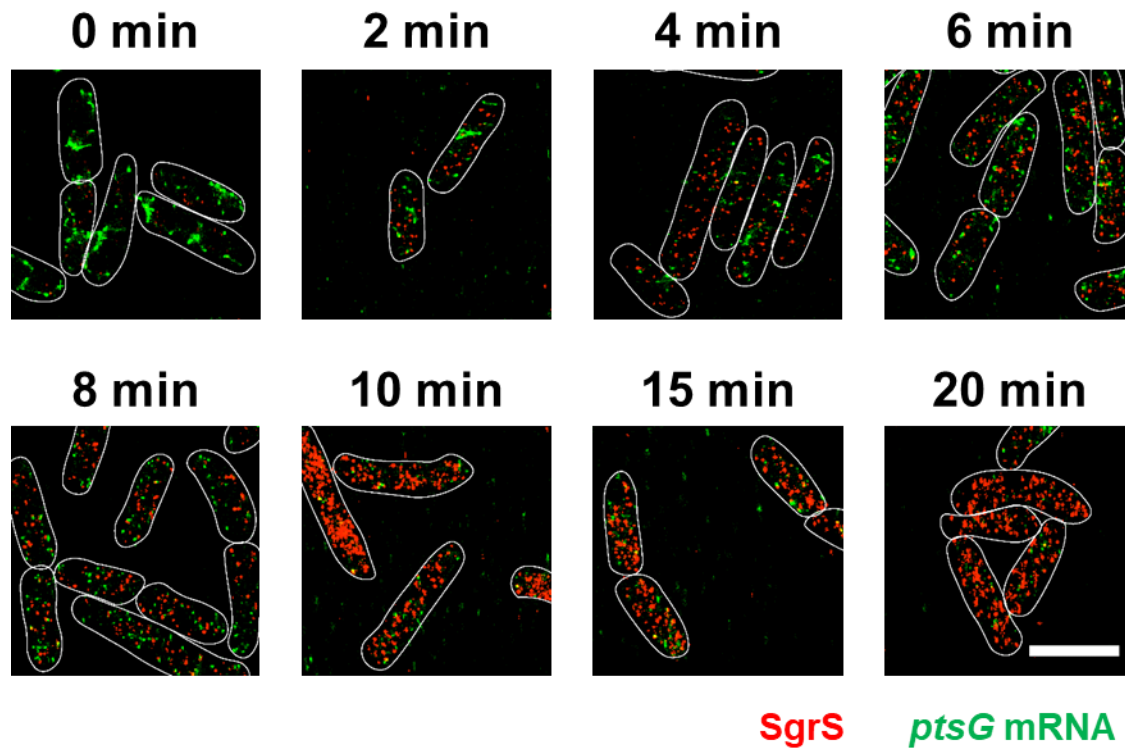
76 images of SgrS G178U cells before (0 min) and 2, 4, 6, 8, 10, 15, 20 min after α MG (non-

77 metabolizable sugar analog) induction. Each experiment was performed independently 2 times.

78 White lines denote cell boundaries. Scale bar is 2 μ m and applies to all the panels.

79

80



81

82 **Supplementary Figure 7. 3D super-resolution images of SgrS (red) and *ptsG* mRNA (green)**

83 **in the SgrS U181A mutant strain projected on 2D planes.** The panels show the multi-color

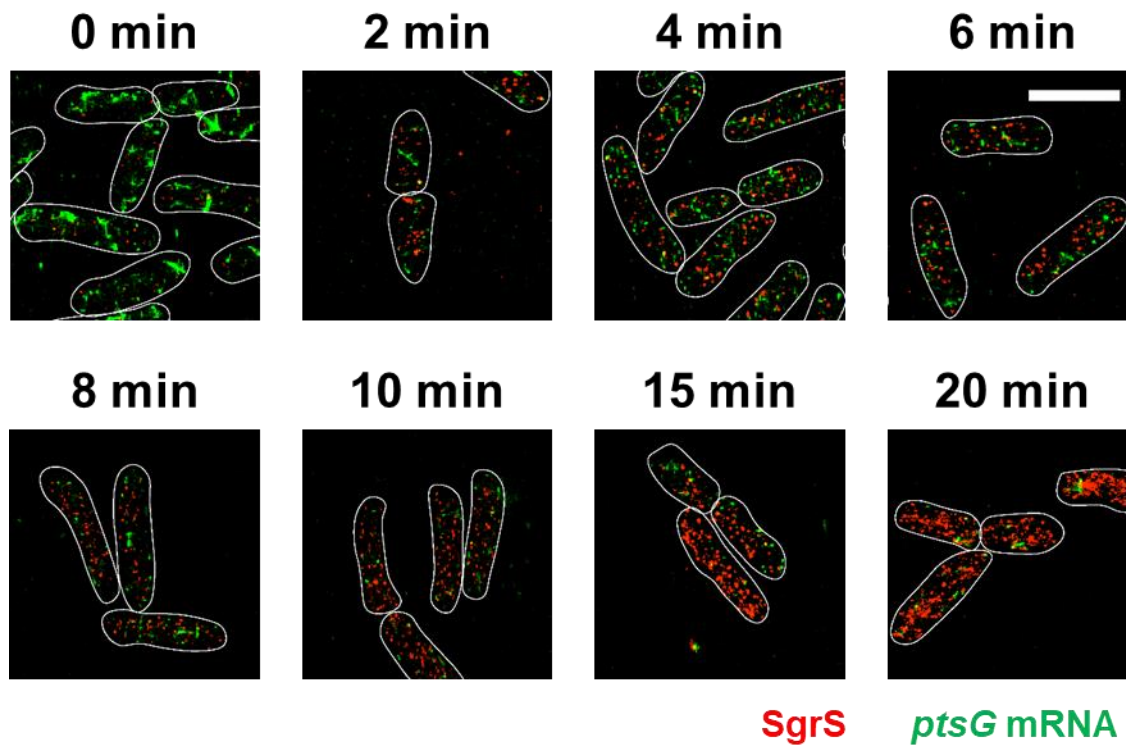
84 images of SgrS U181A cells before (0 min) and 2, 4, 6, 8, 10, 15, 20 min after α MG (non-

85 metabolizable sugar analog) induction. Each experiment was performed independently 2 times.

86 White lines denote cell boundaries. Scale bar is 2 μ m and applies to all the panels.

87

88



89

90 **Supplementary Figure 8. 3D super-resolution images of SgrS (red) and *ptsG* mRNA (green)**

91 **in the SgrS U182A mutant strain projected on 2D planes.** The panels show the multi-color

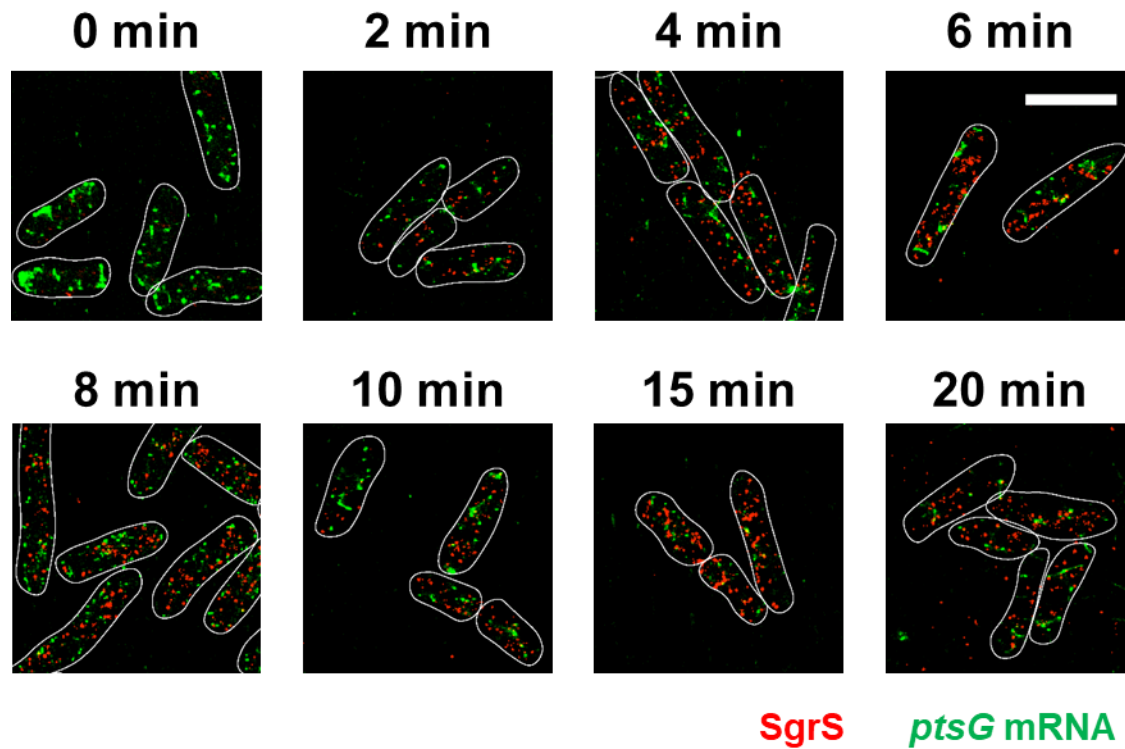
92 images of SgrS U182A cells before (0 min) and 2, 4, 6, 8, 10, 15, 20 min after α MG (non-

93 metabolizable sugar analog) induction. Each experiment was performed independently 2 times.

94 White lines denote cell boundaries. Scale bar is 2 μ m and applies to all the panels.

95

96



97

98 **Supplementary Figure 9. 3D super-resolution images of SgrS (red) and *ptsG* mRNA (green)**

99 **in the SgrS G184A mutant strain projected on 2D planes.** The panels show the multi-color

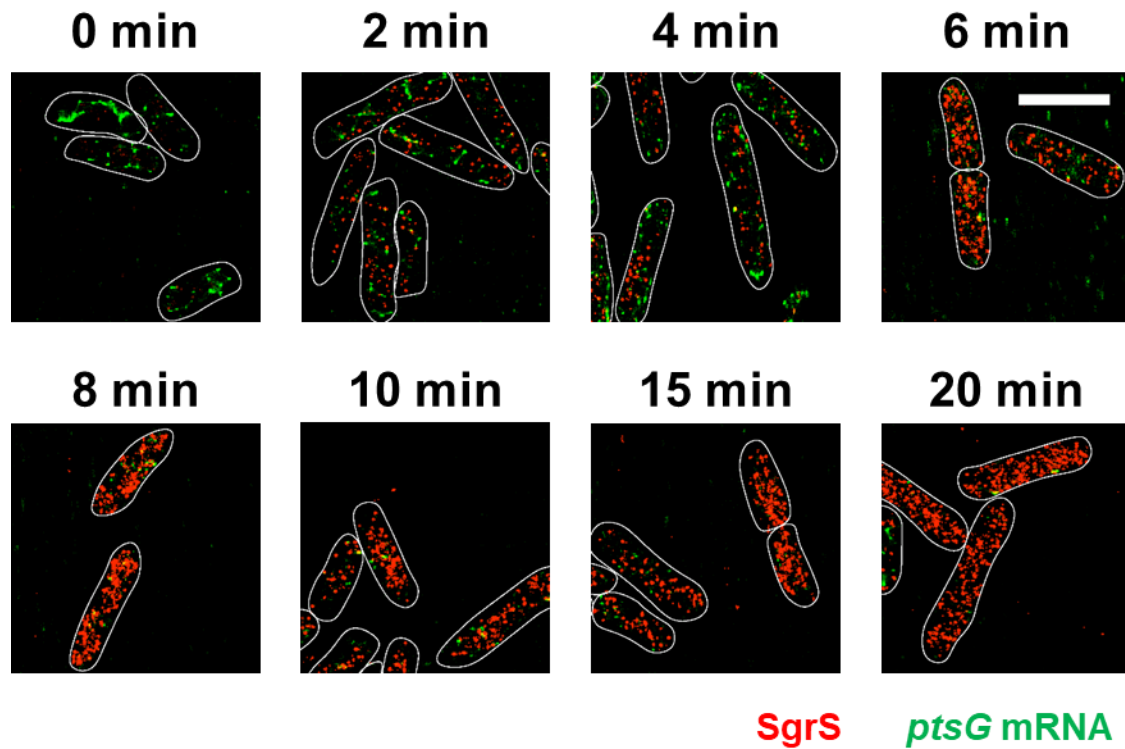
100 images of SgrS G184A cells before (0 min) and 2, 4, 6, 8, 10, 15, 20 min after α MG (non-

101 metabolizable sugar analog) induction. Each experiment was performed independently 2 times.

102 White lines denote cell boundaries. Scale bar is 2 μ m and applies to all the panels.

103

104

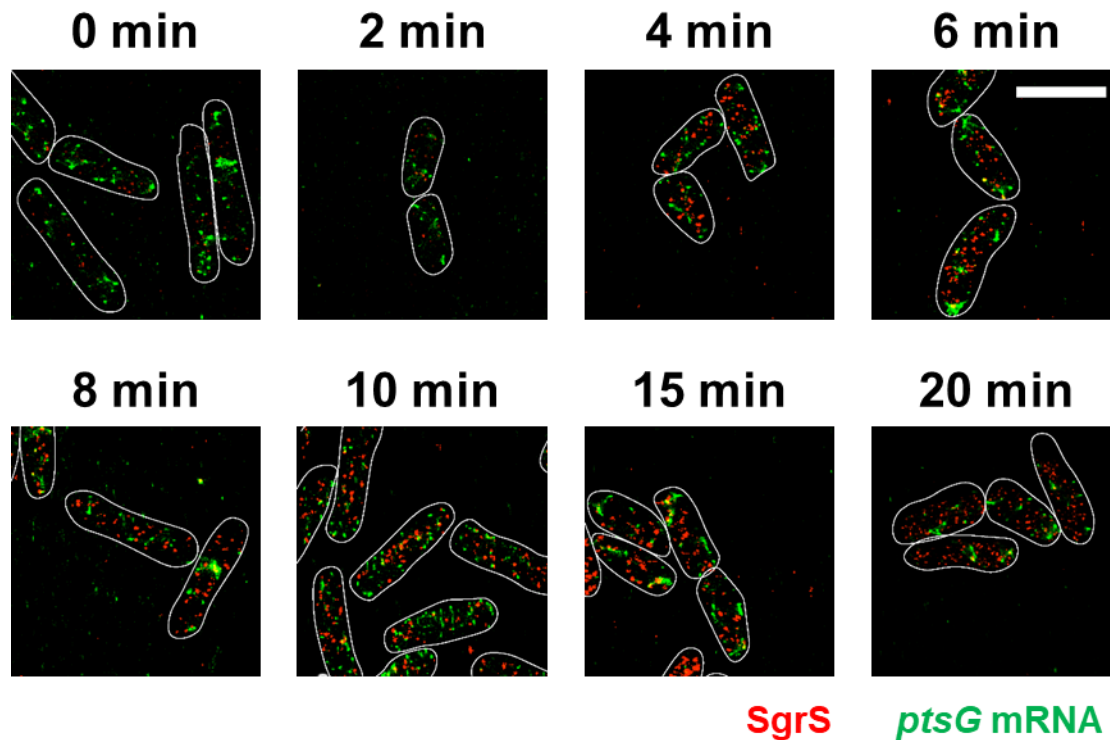


105

106 **Supplementary Figure 10. 3D super-resolution images of SgrS (red) and *ptsG* mRNA**
 107 **(green) in the SgrS G184A-C195U mutant strain projected on 2D planes.** The panels show
 108 the multi-color images of SgrS G184A-C195U cells before (0 min) and 2, 4, 6, 8, 10, 15, 20 min
 109 after α MG (non-metabolizable sugar analog) induction. Each experiment was performed
 110 independently 2 times. White lines denote cell boundaries. Scale bar is 2 μ m and applies to all
 111 the panels.

112

113



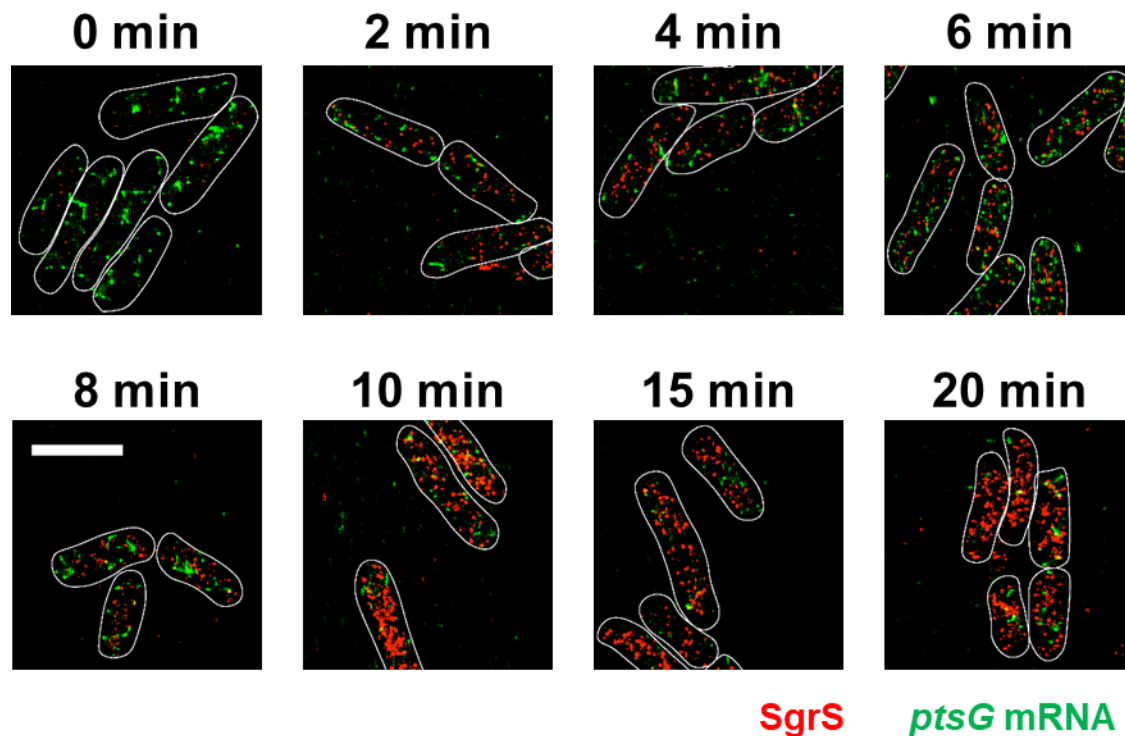
114

115 **Supplementary Figure 11. 3D super-resolution images of SgrS (red) and *ptsG* mRNA**
 116 **(green) in the SgrS G215A mutant strain projected on 2D planes.** The panels show the multi-
 117 color images of SgrS G215A cells before (0 min) and 2, 4, 6, 8, 10, 15, 20 min after α MG (non-
 118 metabolizable sugar analog) induction. Each experiment was performed independently 2 times.
 119 White lines denote cell boundaries. Scale bar is 2 μ m and applies to all the panels.

120

121

122

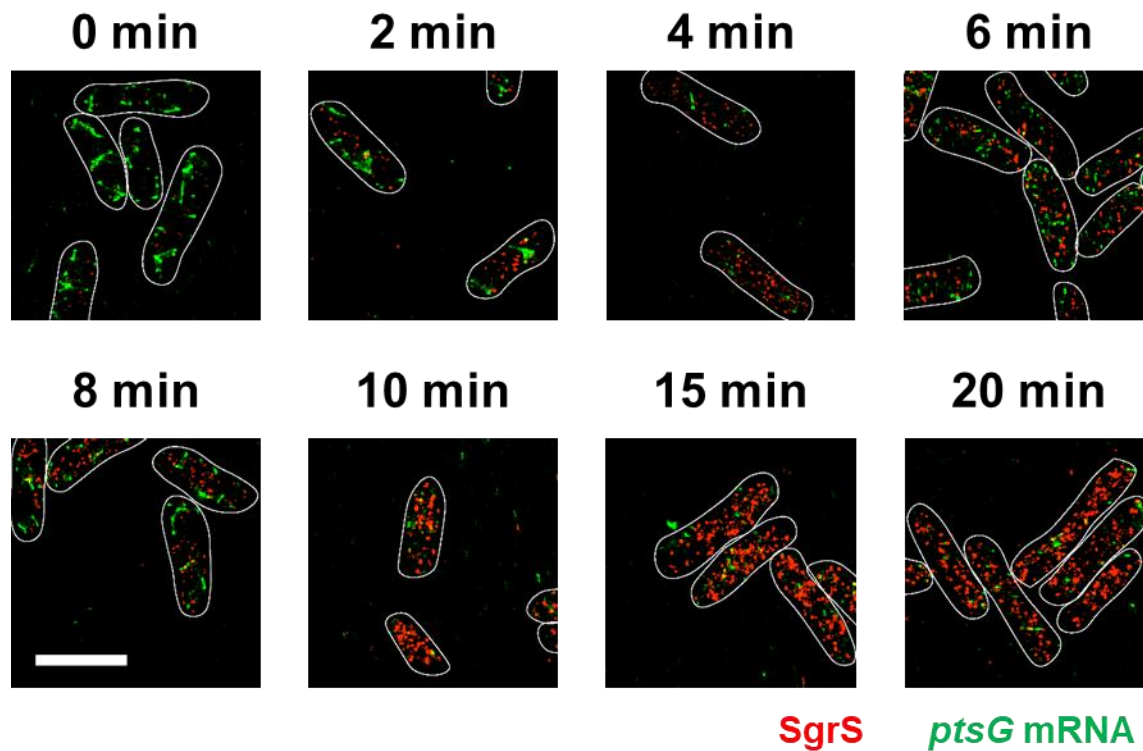


123

124 **Supplementary Figure 12. 3D super-resolution images of SgrS (red) and *ptsG* mRNA**
 125 **(green) in the SgrS U224A mutant strain projected on 2D planes.** The panels show the multi-
 126 color images of SgrS U224A cells before (0 min) and 2, 4, 6, 8, 10, 15, 20 min after α MG (non-
 127 metabolizable sugar analog) induction. Each experiment was performed independently 2 times.
 128 White lines denote cell boundaries. Scale bar is 2 μ m and applies to all the panels.

129

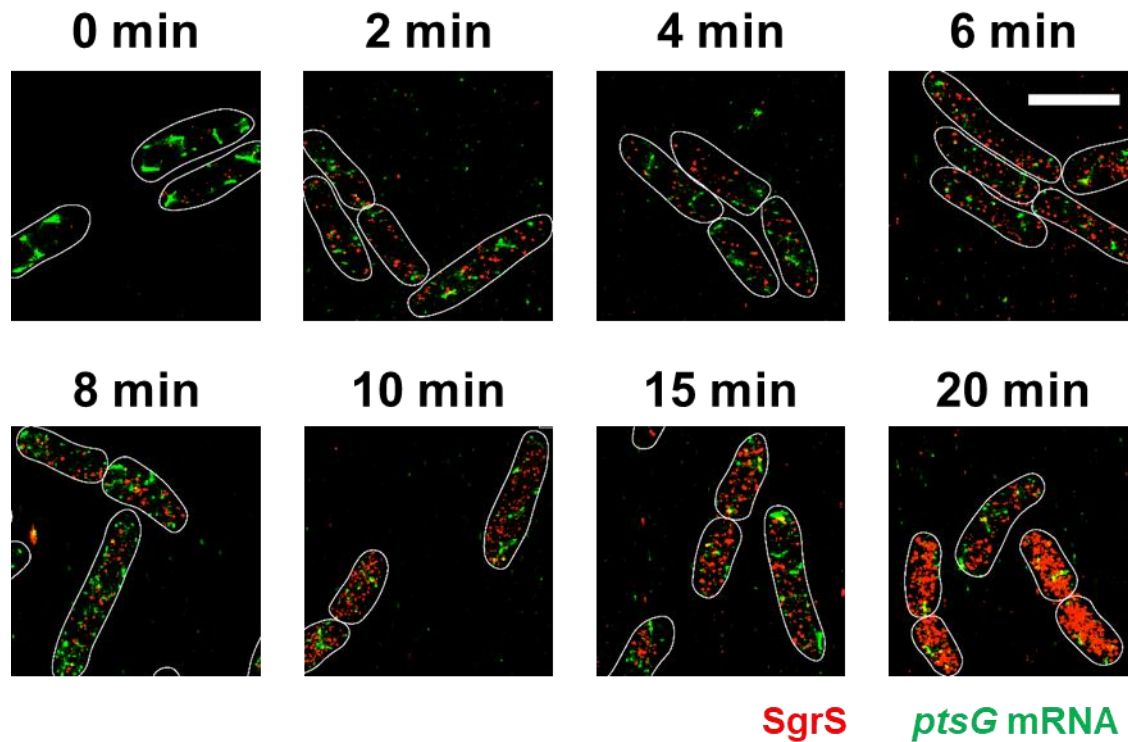
130



131

132 **Supplementary Figure 13. 3D super-resolution images of SgrS (red) and *ptsG* mRNA**
 133 **(green) in the SgrS U224G mutant strain projected on 2D planes.** The panels show the multi-
 134 color images of SgrS U224G cells before (0 min) and 2, 4, 6, 8, 10, 15, 20 min after α MG (non-
 135 metabolizable sugar analog) induction. Each experiment was performed independently 2 times.
 136 White lines denote cell boundaries. Scale bar is 2 μ m and applies to all the panels.

137

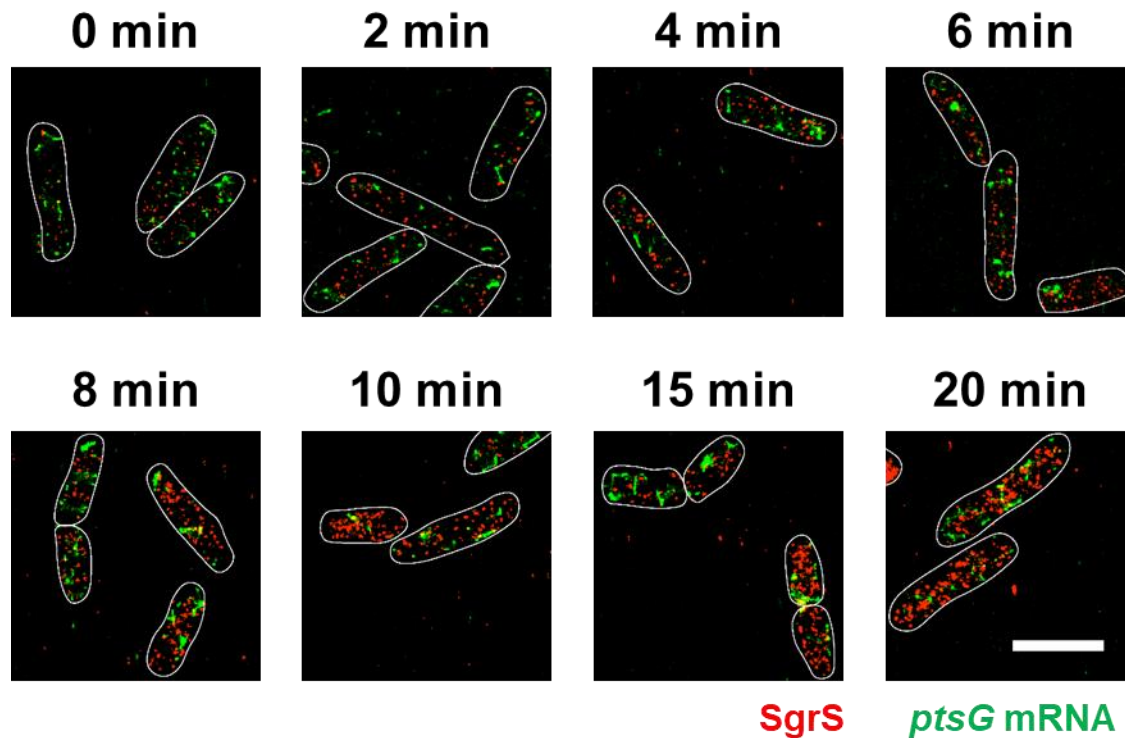


138

139 **Supplementary Figure 14. 3D super-resolution images of SgrS (red) and *ptsG* mRNA**
 140 **(green) in the wild-type SgrS RNase E mutant strain projected on 2D planes.** The panels
 141 show the multi-color images of WT SgrS RNase E mutant cells before (0 min) and 2, 4, 6, 8, 10,
 142 15, 20 min after α MG (non-metabolizable sugar analog) induction. Each experiment was
 143 performed independently 2 times. White lines denote cell boundaries. Scale bar is 2 μ m and
 144 applies to all the panels.

145

146

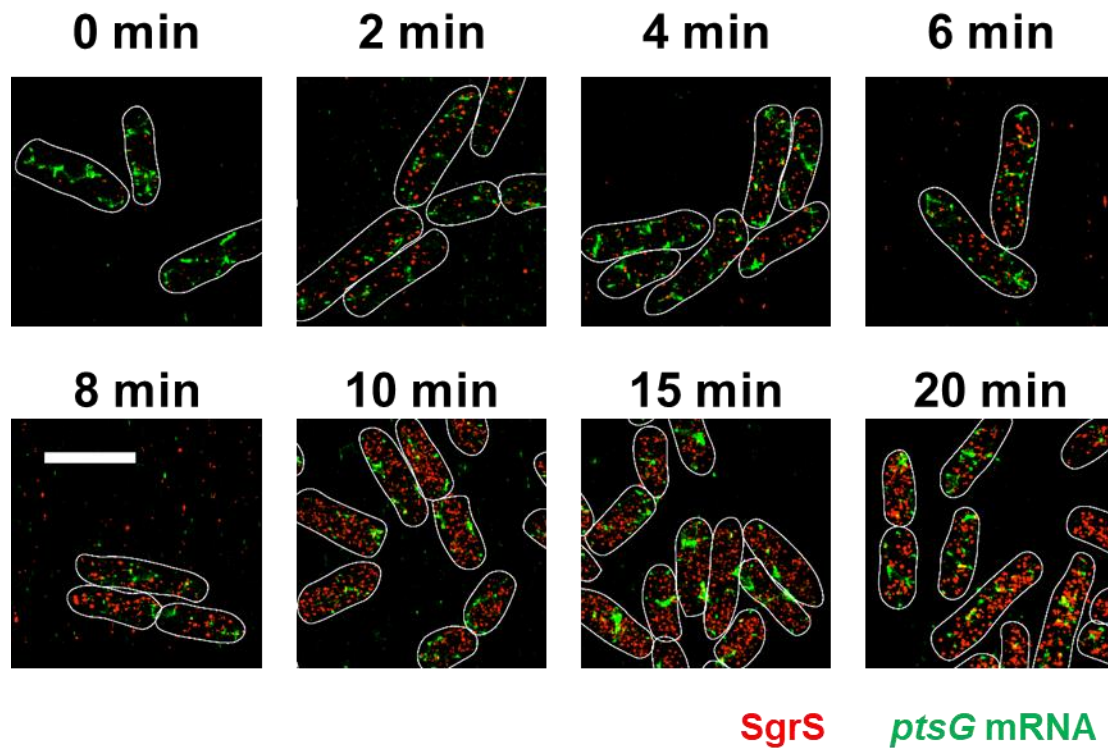


147

148 **Supplementary Figure 15. 3D super-resolution images of SgrS (red) and *ptsG* mRNA**
 149 **(green) in the SgrS A177U RNase E mutant strain projected on 2D planes.** The panels show
 150 the multi-color images of SgrS A177U RNase E mutant cells before (0 min) and 2, 4, 6, 8, 10,
 151 15, 20 min after α MG (non-metabolizable sugar analog) induction. Each experiment was
 152 performed independently 2 times. White lines denote cell boundaries. Scale bar is 2 μ m and
 153 applies to all the panels.

154

155

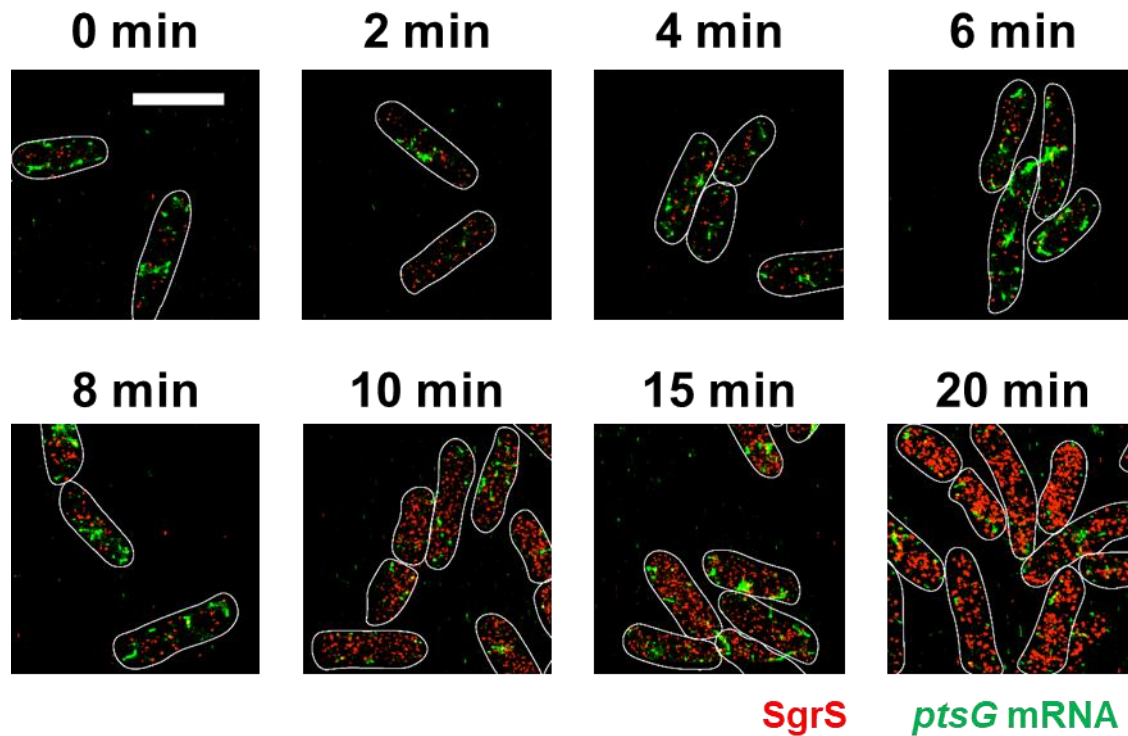


156

157 **Supplementary Figure 16. 3D super-resolution images of SgrS (red) and *ptsG* mRNA**
 158 **(green) in the SgrS G178A RNase E mutant strain projected on 2D planes.** The panels show
 159 the multi-color images of SgrS G178A RNase E mutant cells before (0 min) and 2, 4, 6, 8, 10,
 160 15, 20 min after α MG (non-metabolizable sugar analog) induction. Each experiment was
 161 performed independently 2 times. White lines denote cell boundaries. Scale bar is 2 μ m and
 162 applies to all the panels.

163

164

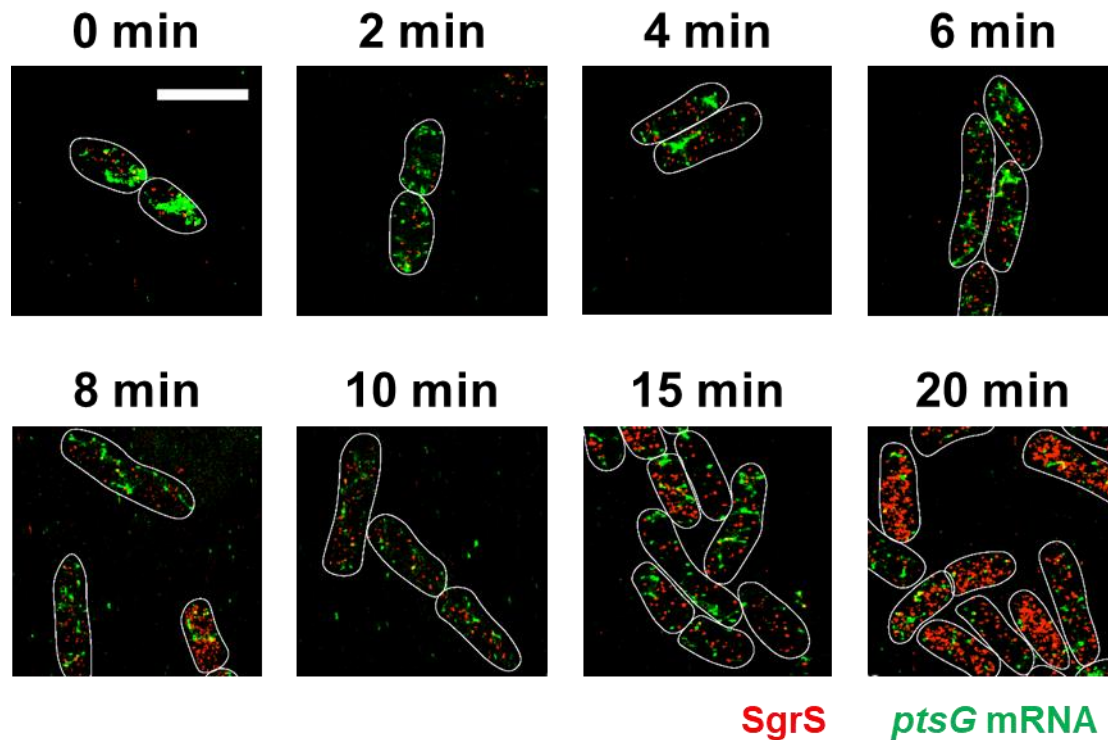


165

166 **Supplementary Figure 17. 3D super-resolution images of SgrS (red) and *ptsG* mRNA**
 167 **(green) in the SgrS G178U RNase E mutant strain projected on 2D planes.** The panels show
 168 the multi-color images of SgrS G178U RNase E mutant cells before (0 min) and 2, 4, 6, 8, 10,
 169 15, 20 min after α MG (non-metabolizable sugar analog) induction. Each experiment was
 170 performed independently 2 times. White lines denote cell boundaries. Scale bar is 2 μ m and
 171 applies to all the panels.

172

173

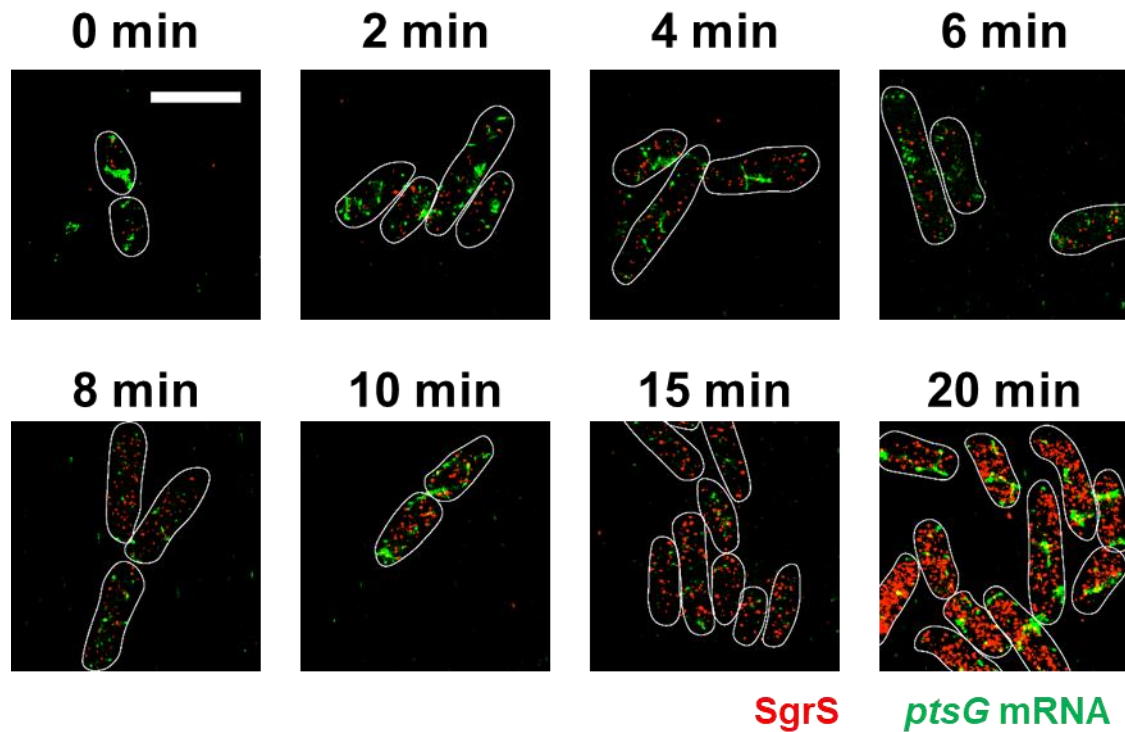


174

175 **Supplementary Figure 18. 3D super-resolution images of SgrS (red) and *ptsG* mRNA**
 176 **(green) in the SgrS U181A RNase E mutant strain projected on 2D planes.** The panels show
 177 the multi-color images of SgrS U181A RNase E mutant cells before (0 min) and 2, 4, 6, 8, 10,
 178 15, 20 min after α MG (non-metabolizable sugar analog) induction. Each experiment was
 179 performed independently 2 times. White lines denote cell boundaries. Scale bar is 2 μ m and
 180 applies to all the panels.

181

182

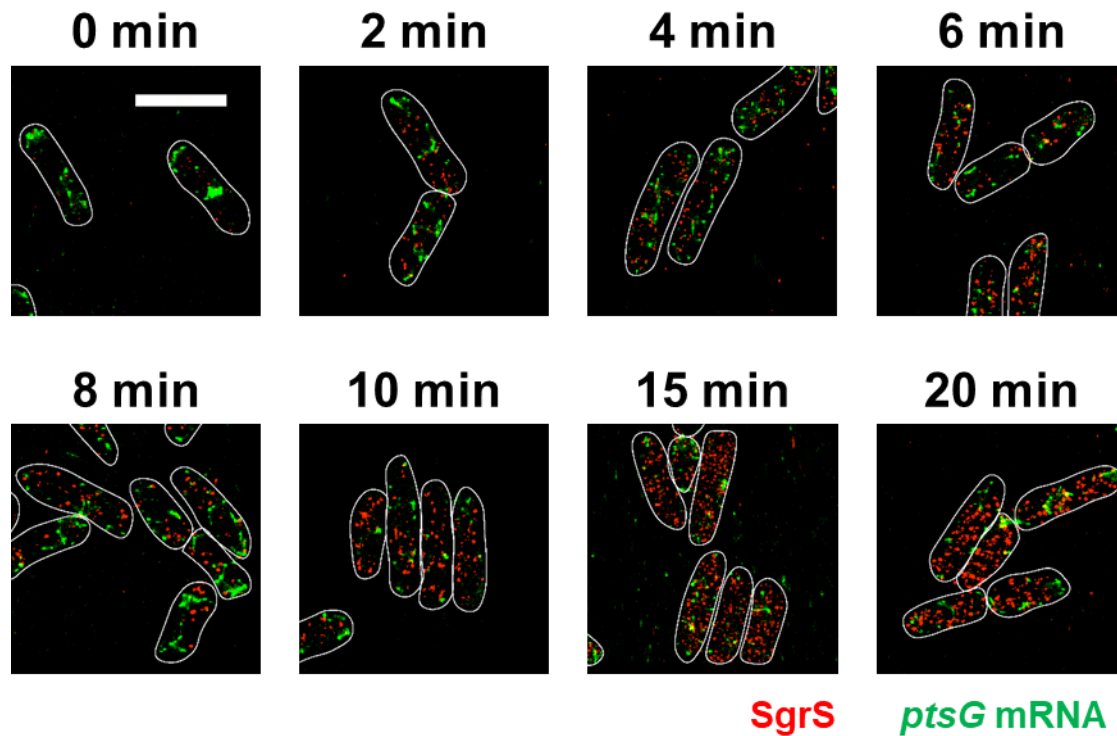


183

184 **Supplementary Figure 19. 3D super-resolution images of SgrS (red) and *ptsG* mRNA**
 185 **(green) in the SgrS U182A RNase E mutant strain projected on 2D planes.** The panels show
 186 the multi-color images of SgrS U182A RNase E mutant cells before (0 min) and 2, 4, 6, 8, 10,
 187 15, 20 min after α MG (non-metabolizable sugar analog) induction. Each experiment was
 188 performed independently 2 times. White lines denote cell boundaries. Scale bar is 2 μ m and
 189 applies to all the panels.

190

191

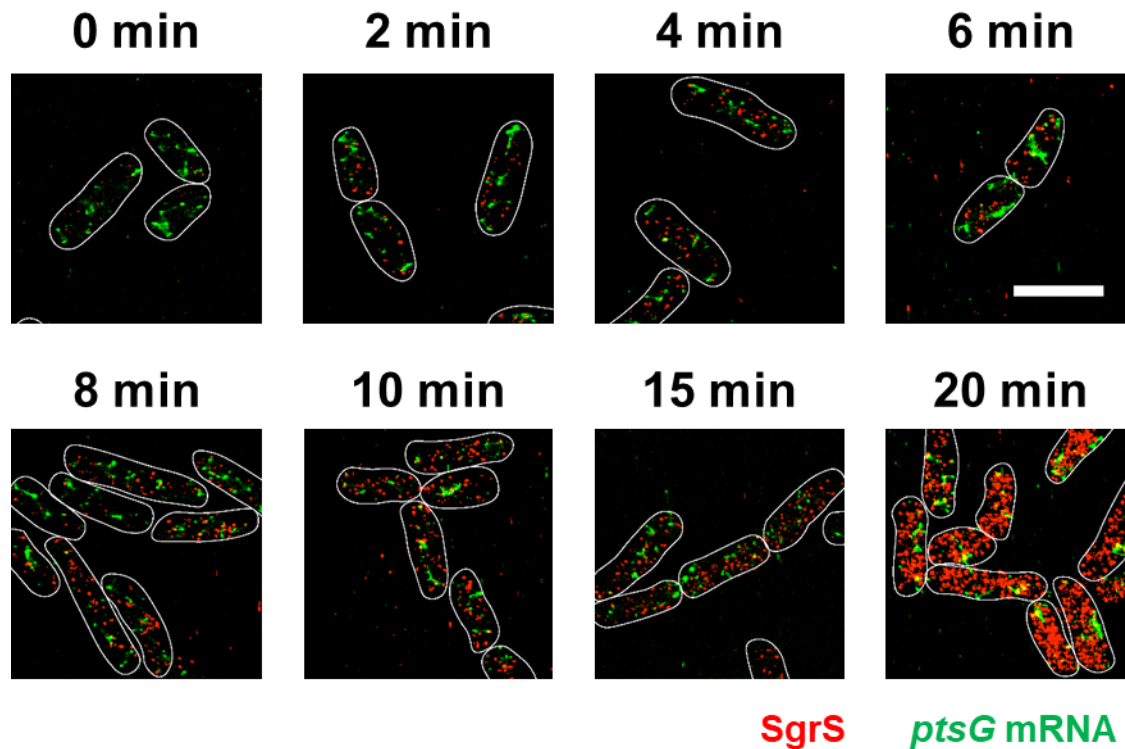


192

193 **Supplementary Figure 20. 3D super-resolution images of SgrS (red) and *ptsG* mRNA**
 194 **(green) in the SgrS G184A RNase E mutant strain projected on 2D planes.** The panels show
 195 the multi-color images of SgrS G184A RNase E mutant cells before (0 min) and 2, 4, 6, 8, 10,
 196 15, 20 min after α MG (non-metabolizable sugar analog) induction. Each experiment was
 197 performed independently 2 times. White lines denote cell boundaries. Scale bar is 2 μ m and
 198 applies to all the panels.

199

200

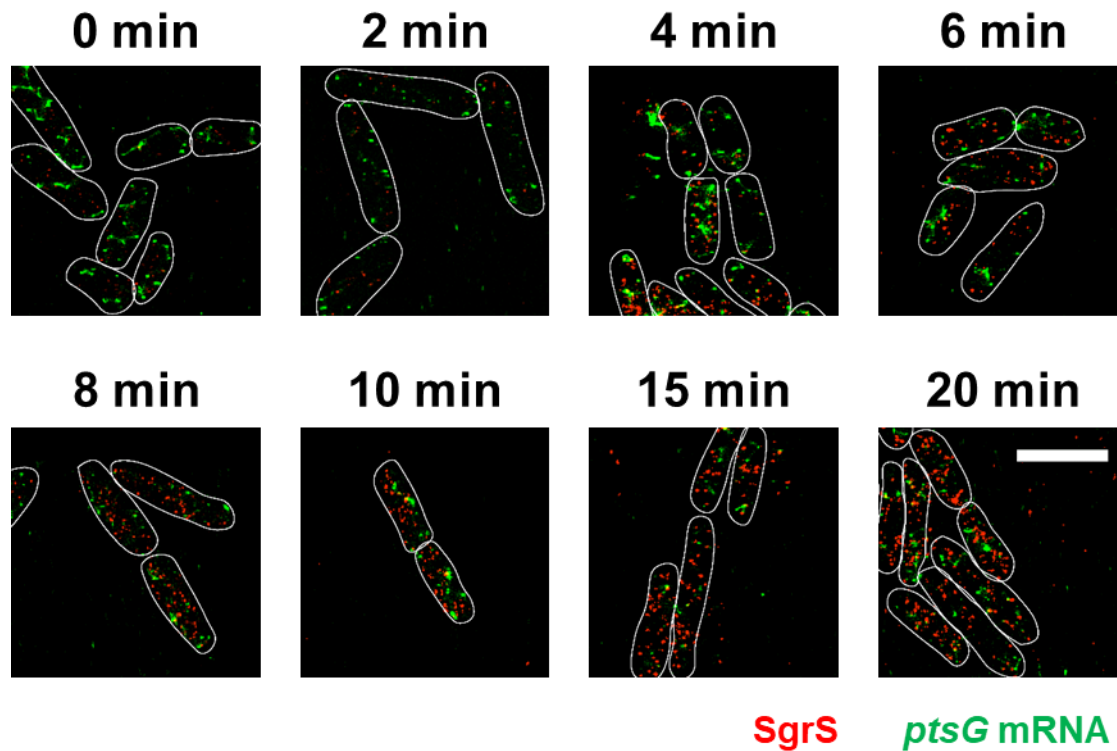


201

202 **Supplementary Figure 21. 3D super-resolution images of SgrS (red) and *ptsG* mRNA**
 203 **(green) in the SgrS G184A-C195U RNase E mutant strain projected on 2D planes.** The
 204 panels show the multi-color images of SgrS G184A-C195U RNase E mutant cells before (0 min)
 205 and 2, 4, 6, 8, 10, 15, 20 min after α MG (non-metabolizable sugar analog) induction. Each
 206 experiment was performed independently 2 times. White lines denote cell boundaries. Scale bar
 207 is 2 μ m and applies to all the panels.

208

209

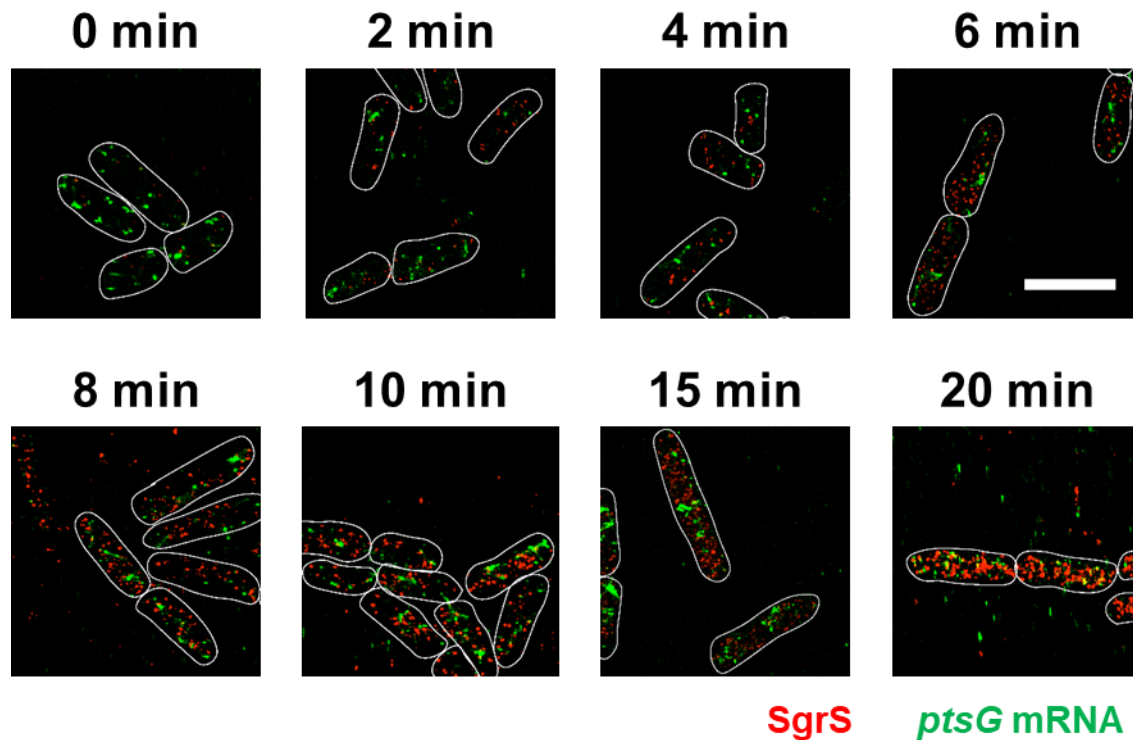


210

211 **Supplementary Figure 22. 3D super-resolution images of SgrS (red) and *ptsG* mRNA**
 212 **(green) in the SgrS G215A RNase E mutant strain projected on 2D planes.** The panels show
 213 the multi-color images of SgrS G215A RNase E mutant cells before (0 min) and 2, 4, 6, 8, 10,
 214 15, 20 min after α MG (non-metabolizable sugar analog) induction. Each experiment was
 215 performed independently 2 times. White lines denote cell boundaries. Scale bar is 2 μ m and
 216 applies to all the panels.

217

218

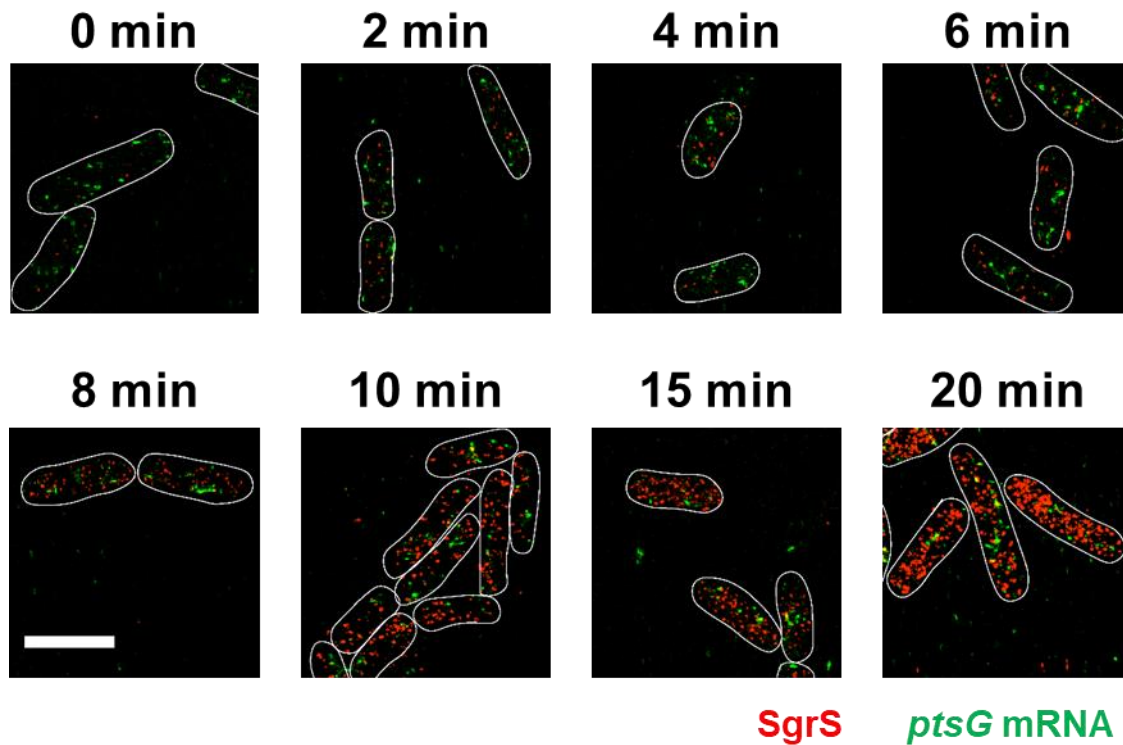


219

220 **Supplementary Figure 23. 3D super-resolution images of SgrS (red) and *ptsG* mRNA**
 221 **(green) in the SgrS U224A RNase E mutant strain projected on 2D planes.** The panels show
 222 the multi-color images of SgrS U224A RNase E mutant cells before (0 min) and 2, 4, 6, 8, 10,
 223 15, 20 min after α MG (non-metabolizable sugar analog) induction. Each experiment was
 224 performed independently 2 times. White lines denote cell boundaries. Scale bar is 2 μ m and
 225 applies to all the panels.

226

227

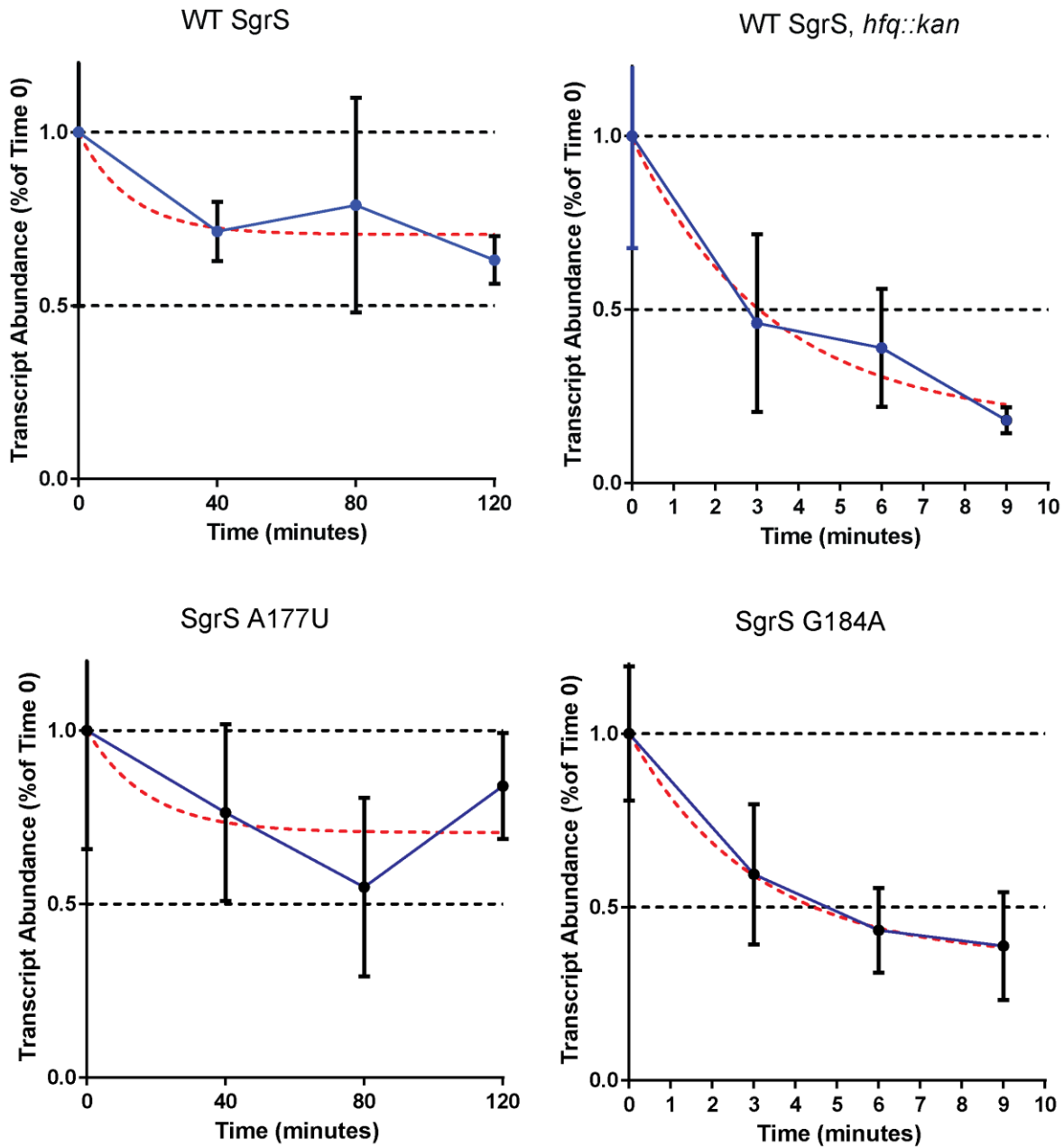


228

229 **Supplementary Figure 24. 3D super-resolution images of SgrS (red) and *ptsG* mRNA**
 230 **(green) in the SgrS U224G RNase E mutant strain projected on 2D planes.** The panels show
 231 the multi-color images of SgrS U224G RNase E mutant cells before (0 min) and 2, 4, 6, 8, 10,
 232 15, 20 min after α MG (non-metabolizable sugar analog) induction. Each experiment was
 233 performed independently 2 times. White lines denote cell boundaries. Scale bar is 2 μ m and
 234 applies to all the panels.

235

236

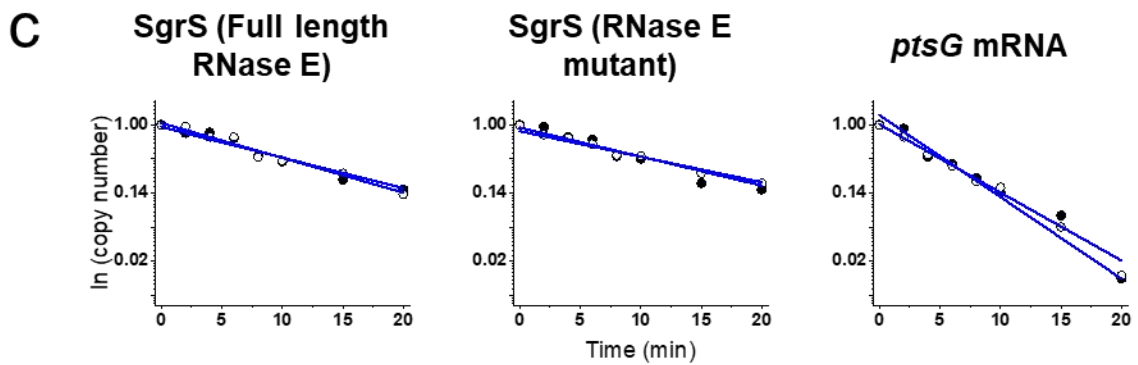
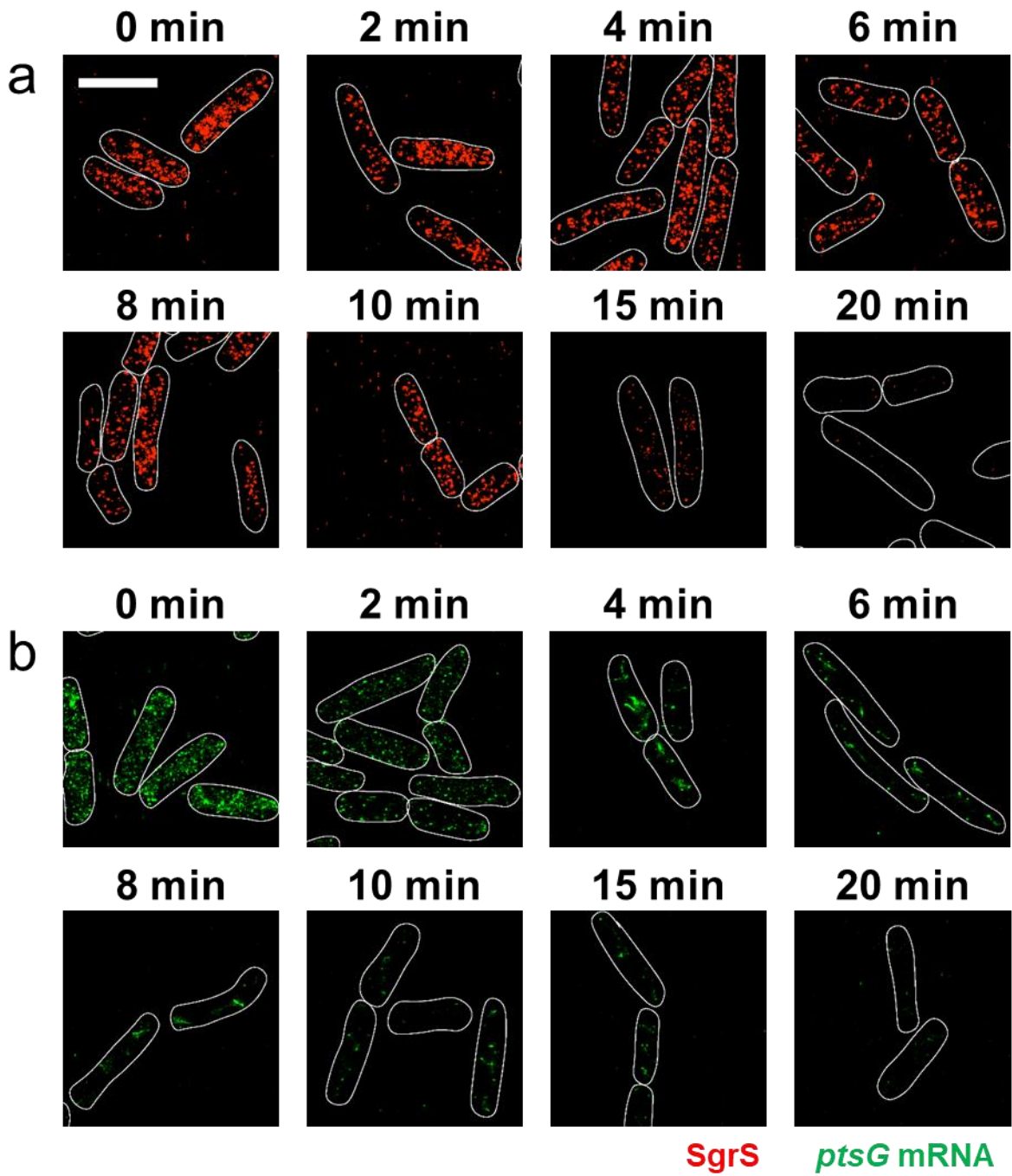


237

238 **Supplementary Figure 25. Stability of SgrS transcripts in different strains, (a) wild-type**
 239 **SgrS, (b) Δhfq wild-type strain, (c) SgrS A177U strain, (d) SgrS G184A strain.** Rifampicin was
 240 added to the SgrS induced culture to inhibit the synthesis of all cellular transcripts (including
 241 SgrS and all its targets). To measure target independent half-life of SgrS, the starting time point
 242 was set 5 minutes after the addition of rifampicin. The cells were harvested for total RNA

243 extraction at the indicated time points, and mRNA levels were measured with RT-PCR. The
244 relative transcript concentration was determined using $\Delta\Delta Cq$ method normalized to 16S
245 ribosome gene (*rrsA*) transcripts and was expressed as fractions of abundance in time point 0
246 samples. The transcript turnover rates were calculated based on the non-linear fit one phase
247 exponential decay curves using GraphPad software (red dotted lines). Data was obtained from
248 n=3 biological replicates and presented as mean values +/- SD. Source data are provided as a
249 Source Data file.

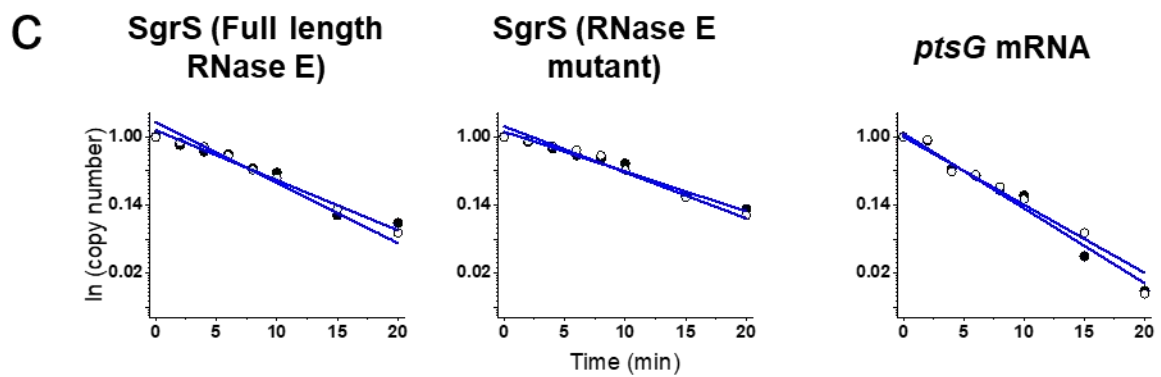
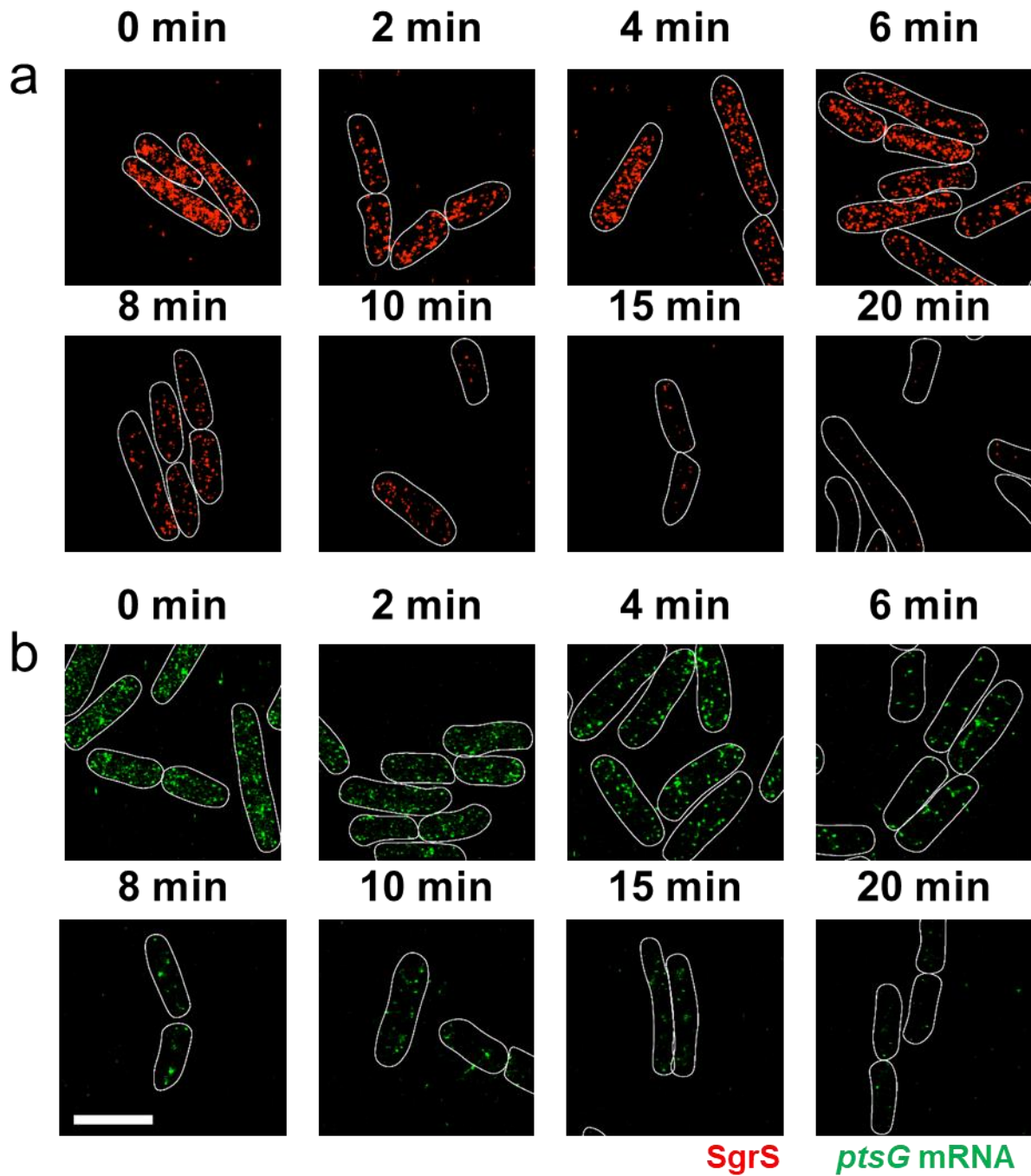
250



252 **Supplementary Figure 26. RNA lifetime measurements for the wild-type strain. (a)** SgrS
253 degradation in the wild-type strain. Each experiment was performed independently 2 times. **(b)**
254 *ptsG* mRNA degradation in the wild-type strain. Each experiment was performed independently
255 2 times. **(c)** Calculation of RNA lifetime. Filled and open circles are two independent
256 measurements with mean value from ~80 cells in each case. The copy numbers have been
257 normalized to time $t=0$ in each case. The degradation rates calculated from the lifetimes are
258 shown in Fig. 6a, Supplementary Fig. 37 and Supplementary Table 3. Scale bar is 2 μm and
259 applies to all the panels. Source data are provided as a Source Data file.

260

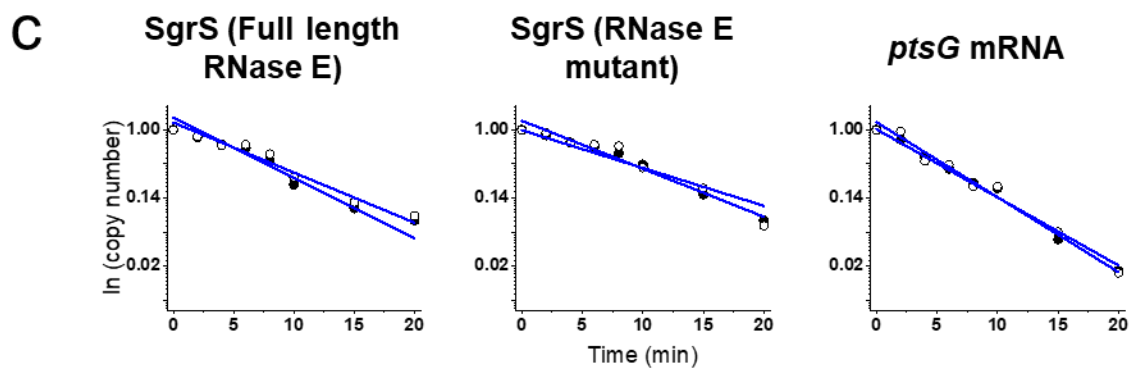
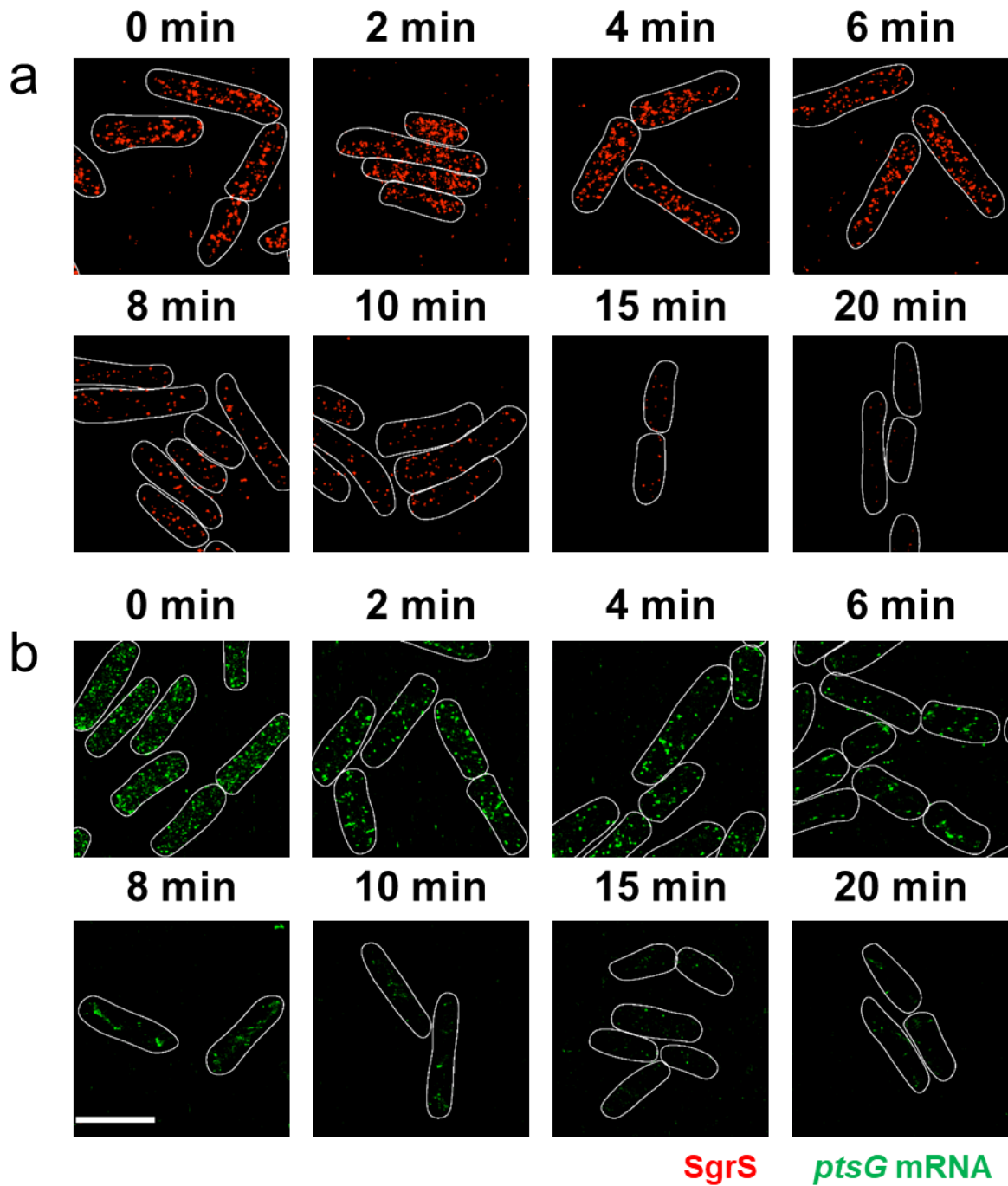
261



263 **Supplementary Figure 27. RNA lifetime measurements for the A177U strain. (a)** SgrS
264 degradation in the A177U strain. Each experiment was performed independently 2 times. **(b)**
265 *ptsG* mRNA degradation in the A177U strain. Each experiment was performed independently 2
266 times. **(c)** Calculation of RNA lifetime. Filled and open circles are two independent
267 measurements with mean value from ~80 cells in each case. The copy numbers have been
268 normalized to time $t=0$ in each case. The degradation rates calculated from the lifetimes are
269 shown in Fig. 6a, Supplementary Fig. 37 and Supplementary Table 3. Scale bar is 2 μm and
270 applies to all the panels. Source data are provided as a Source Data file.

271

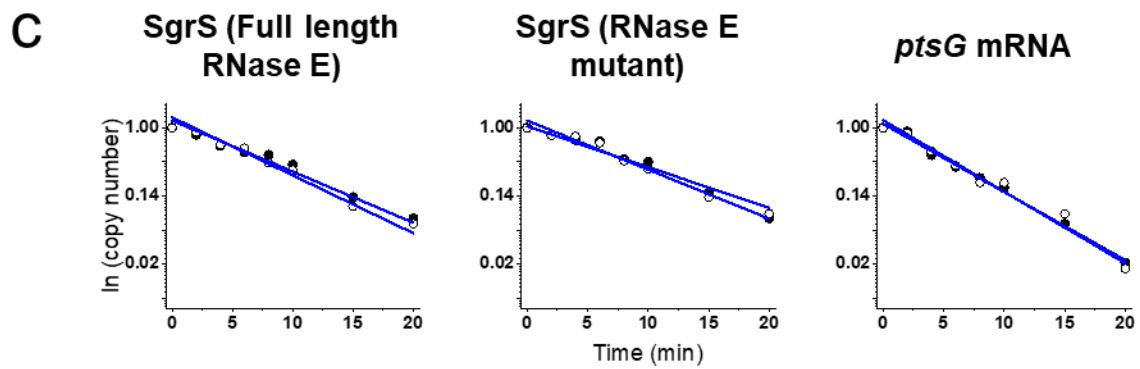
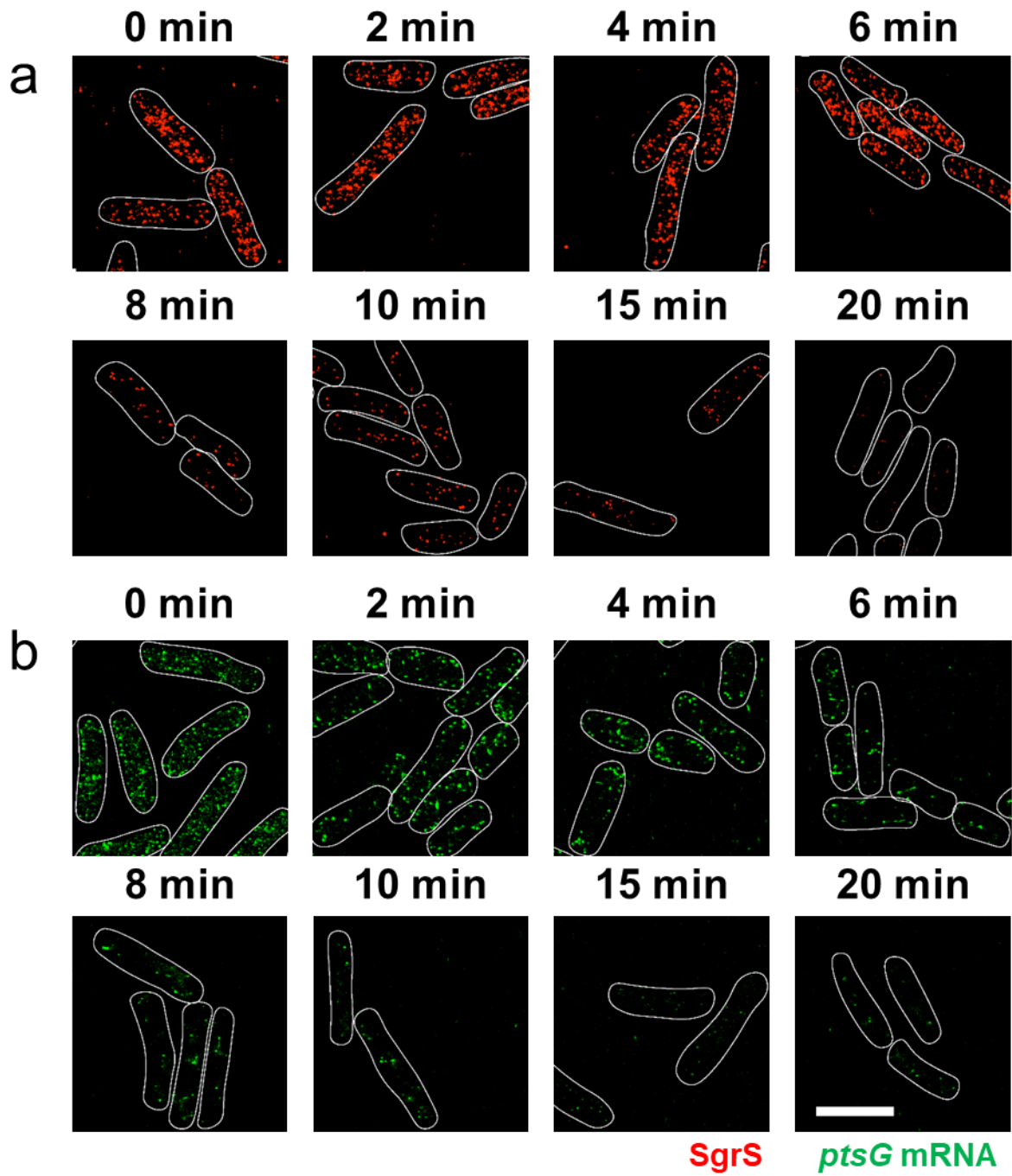
272



274 **Supplementary Figure 28. RNA lifetime measurements for the G178A strain. (a)** SgrS
275 degradation in the G178A strain. Each experiment was performed independently 2 times. **(b)**
276 *ptsG* mRNA degradation in the G178A strain. Each experiment was performed independently 2
277 times. **(c)** Calculation of RNA lifetime. Filled and open circles are two independent
278 measurements with mean value from ~80 cells in each case. The copy numbers have been
279 normalized to time t=0 in each case. The degradation rates calculated from the lifetimes are
280 shown in Fig. 6a, Supplementary Fig. 37 and Supplementary Table 3. Scale bar is 2 μm and
281 applies to all the panels. Source data are provided as a Source Data file.

282

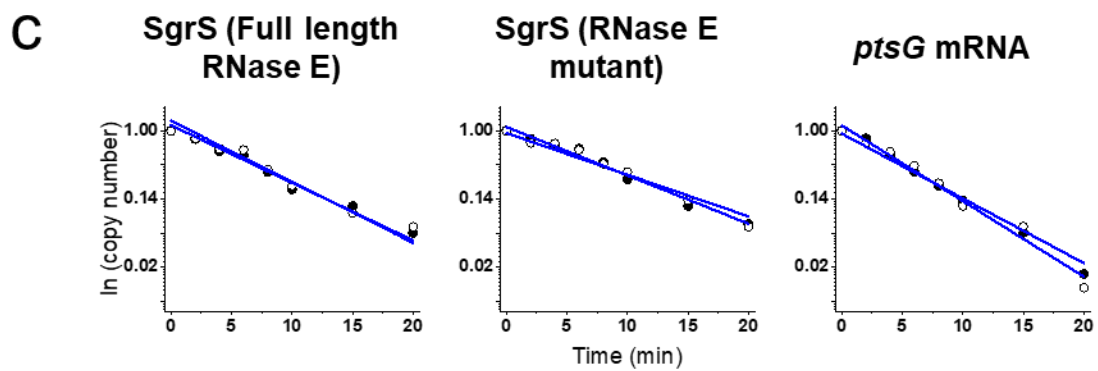
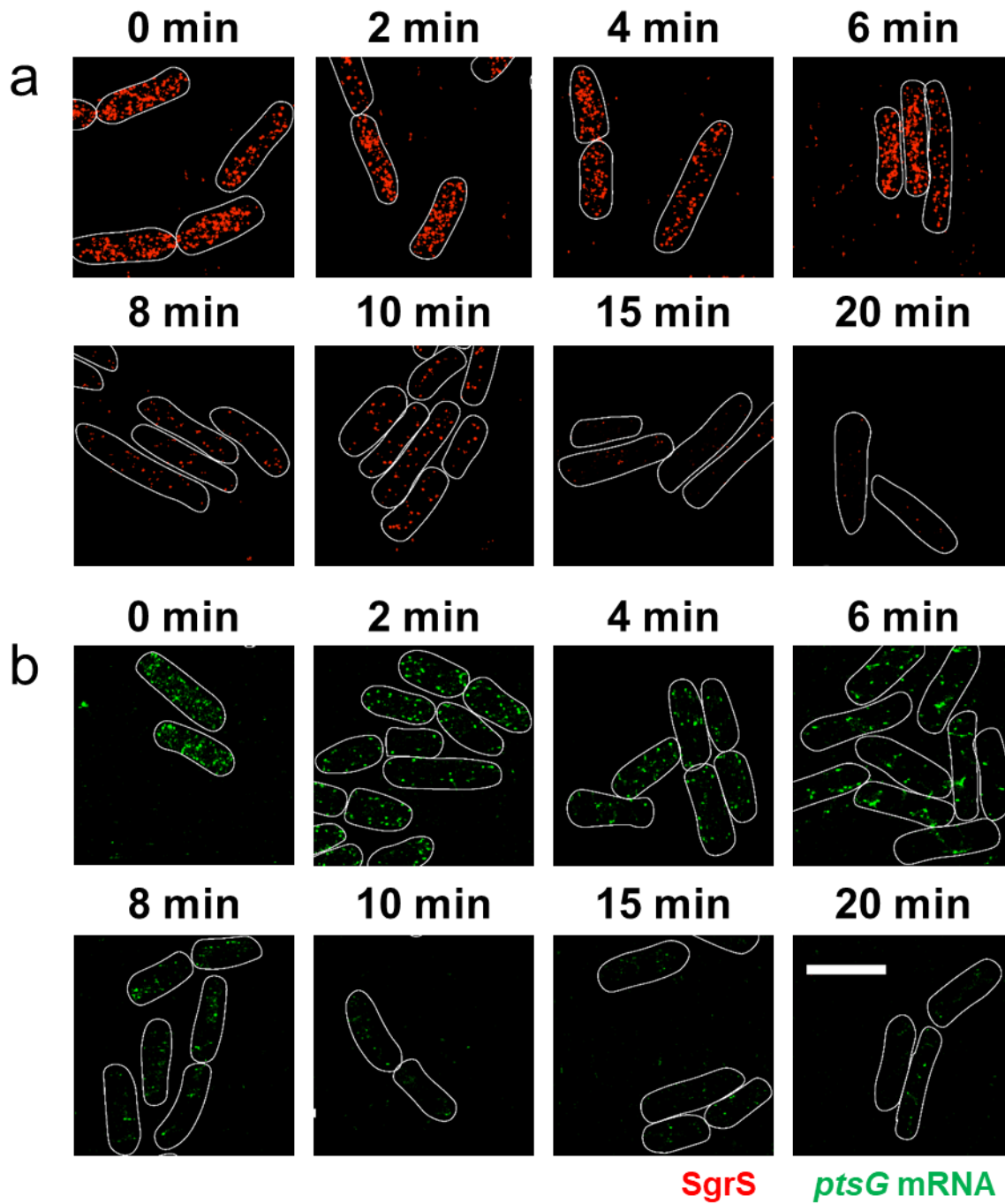
283



285 **Supplementary Figure 29. RNA lifetime measurements for the G178U strain. (a)** SgrS
286 degradation in the G178U strain. Each experiment was performed independently 2 times. **(b)**
287 *ptsG* mRNA degradation in the G178U strain. Each experiment was performed independently 2
288 times. **(c)** Calculation of RNA lifetime. Filled and open circles are two independent
289 measurements with mean value from ~80 cells in each case. The copy numbers have been
290 normalized to time t=0 in each case. The degradation rates calculated from the lifetimes are
291 shown in Fig. 6a, Supplementary Fig. 37 and Supplementary Table 3. Scale bar is 2 μm and
292 applies to all the panels. Source data are provided as a Source Data file.

293

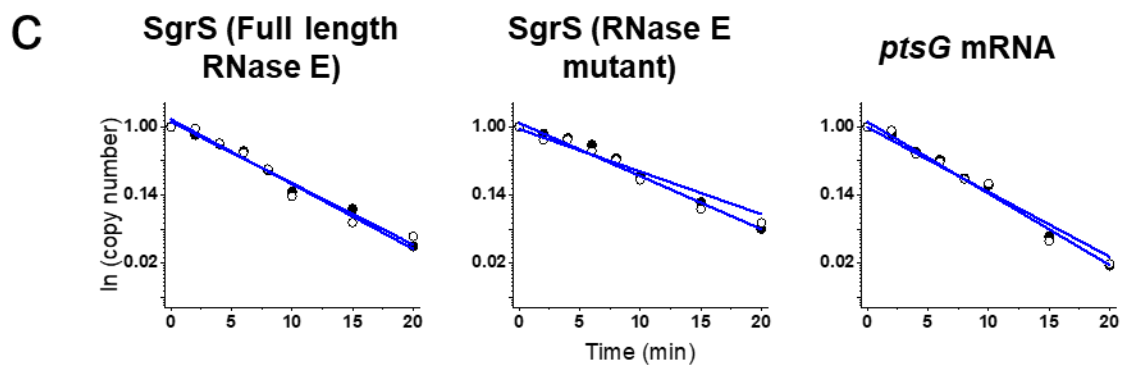
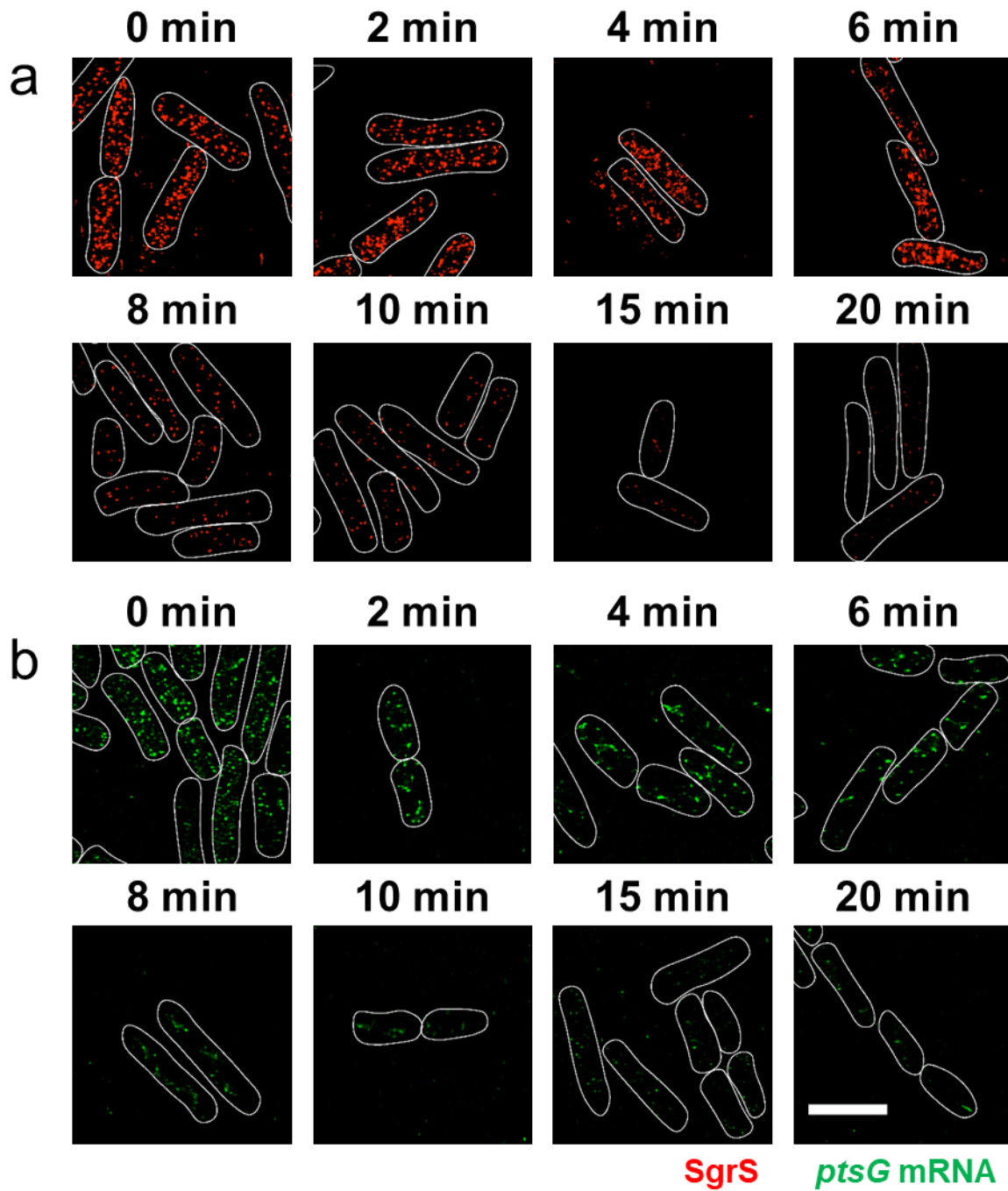
294



296 **Supplementary Figure 30. RNA lifetime measurements for the U181A strain. (a)** SgrS
297 degradation in the U181A strain. Each experiment was performed independently 2 times. **(b)**
298 *ptsG* mRNA degradation in the U181A strain. Each experiment was performed independently 2
299 times. **(c)** Calculation of RNA lifetime. Filled and open circles are two independent
300 measurements with mean value from ~80 cells in each case. The copy numbers have been
301 normalized to time $t=0$ in each case. The degradation rates calculated from the lifetimes are
302 shown in Fig. 6a, Supplementary Fig. 37 and Supplementary Table 3. Scale bar is 2 μm and
303 applies to all the panels. Source data are provided as a Source Data file.

304

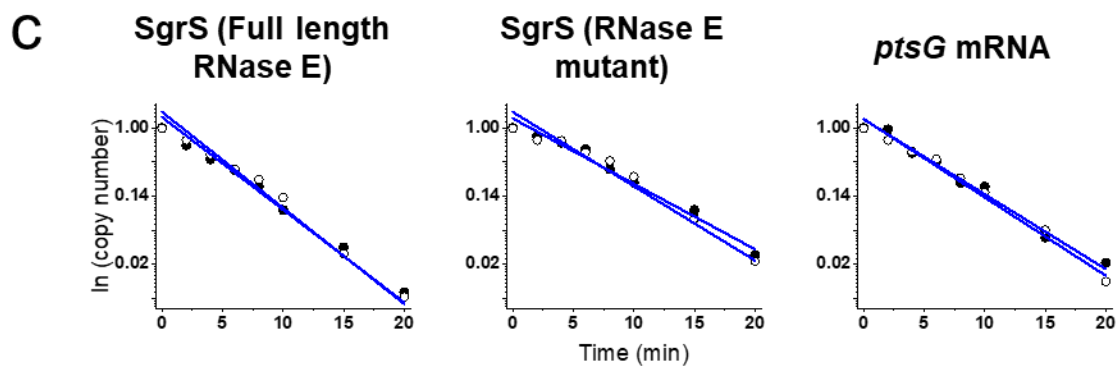
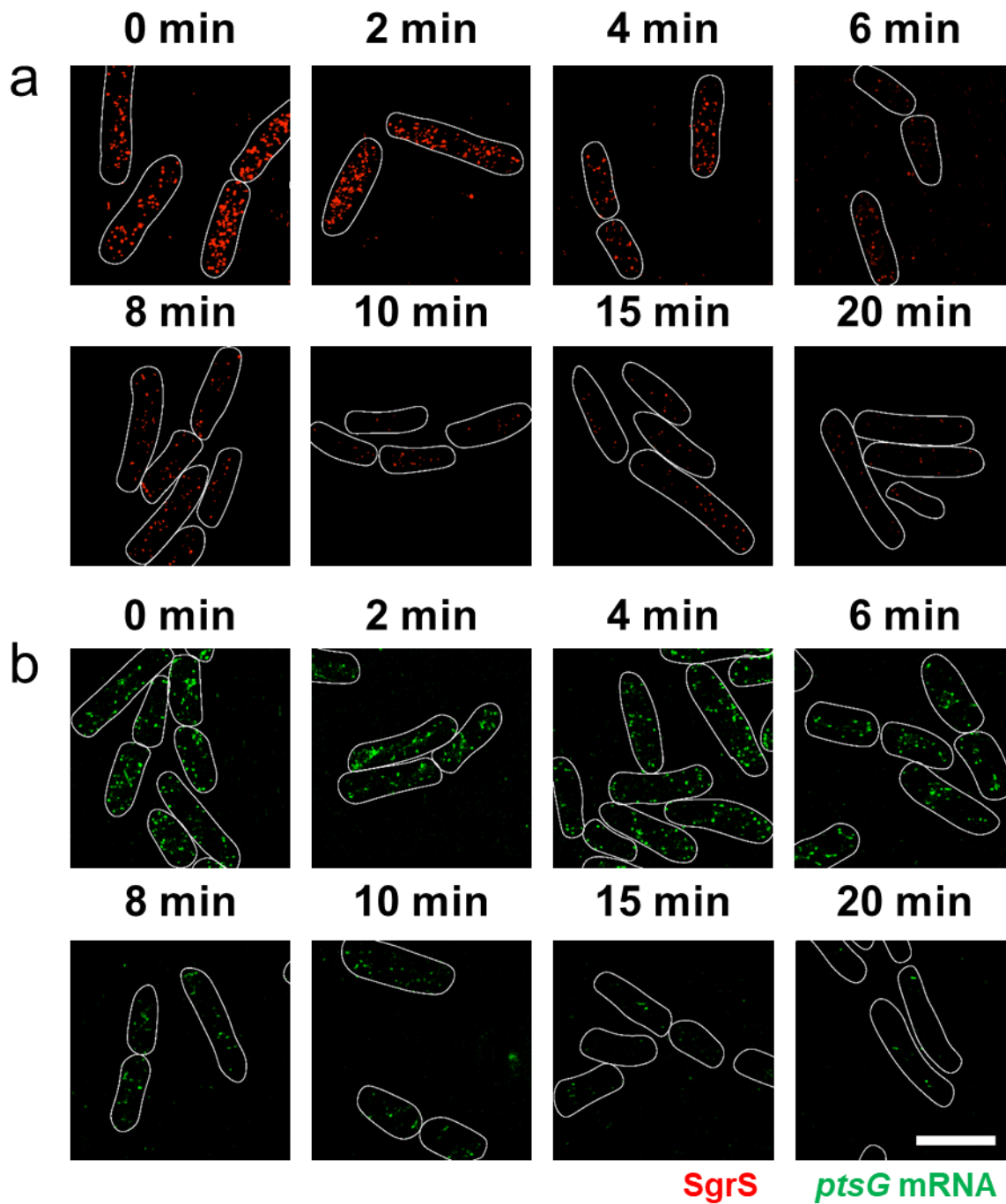
305



307 **Supplementary Figure 31. RNA lifetime measurements for the U182A strain. (a)** SgrS
308 degradation in the U182A strain. Each experiment was performed independently 2 times. **(b)**
309 *ptsG* mRNA degradation in the U182A strain. Each experiment was performed independently 2
310 times. **(c)** Calculation of RNA lifetime. Filled and open circles are two independent
311 measurements with mean value from ~80 cells in each case. The copy numbers have been
312 normalized to time $t=0$ in each case. The degradation rates calculated from the lifetimes are
313 shown in Fig. 6a, Supplementary Fig. 37 and Supplementary Table 3. Scale bar is 2 μm and
314 applies to all the panels. Source data are provided as a Source Data file.

315

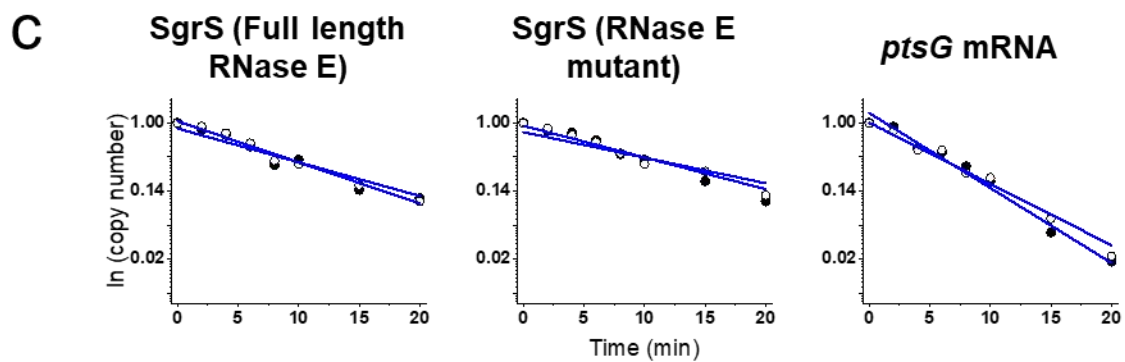
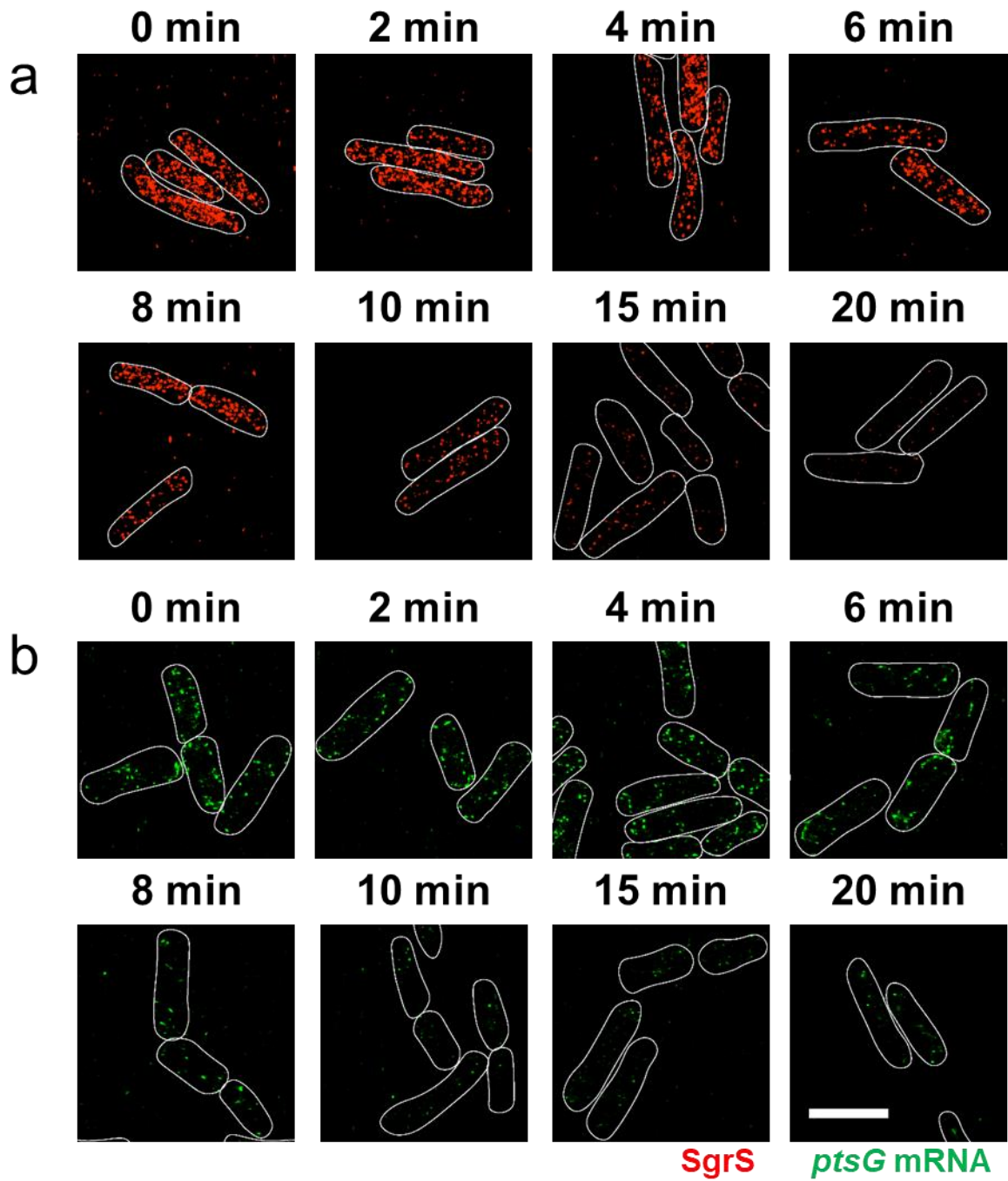
316



318 **Supplementary Figure 32. RNA lifetime measurements for the G184A strain.** (a) SgrS
319 degradation in the G184A strain. Each experiment was performed independently 2 times. (b)
320 *ptsG* mRNA degradation in the G184A strain. Each experiment was performed independently 2
321 times. (c) Calculation of RNA lifetime. Filled and open circles are two independent
322 measurements with mean value from ~80 cells in each case. The copy numbers have been
323 normalized to time $t=0$ in each case. The degradation rates calculated from the lifetimes are
324 shown in Fig. 6a, Supplementary Fig. 37 and Supplementary Table 3. Scale bar is 2 μm and
325 applies to all the panels. Source data are provided as a Source Data file.

326

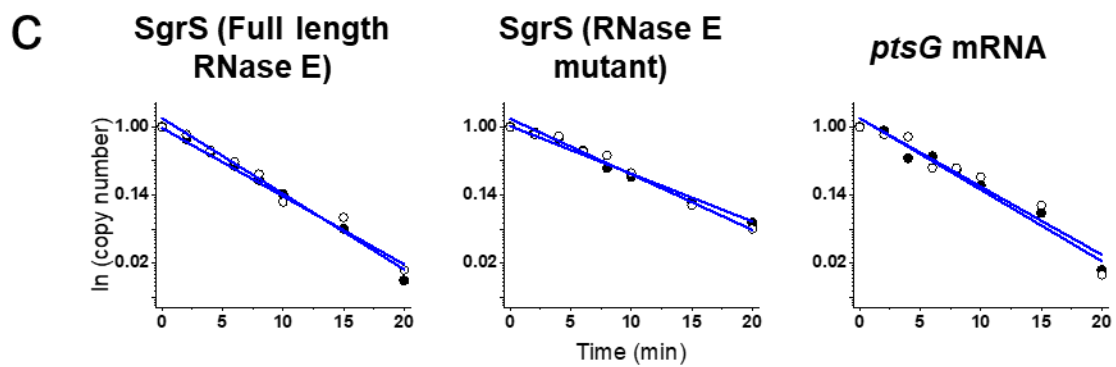
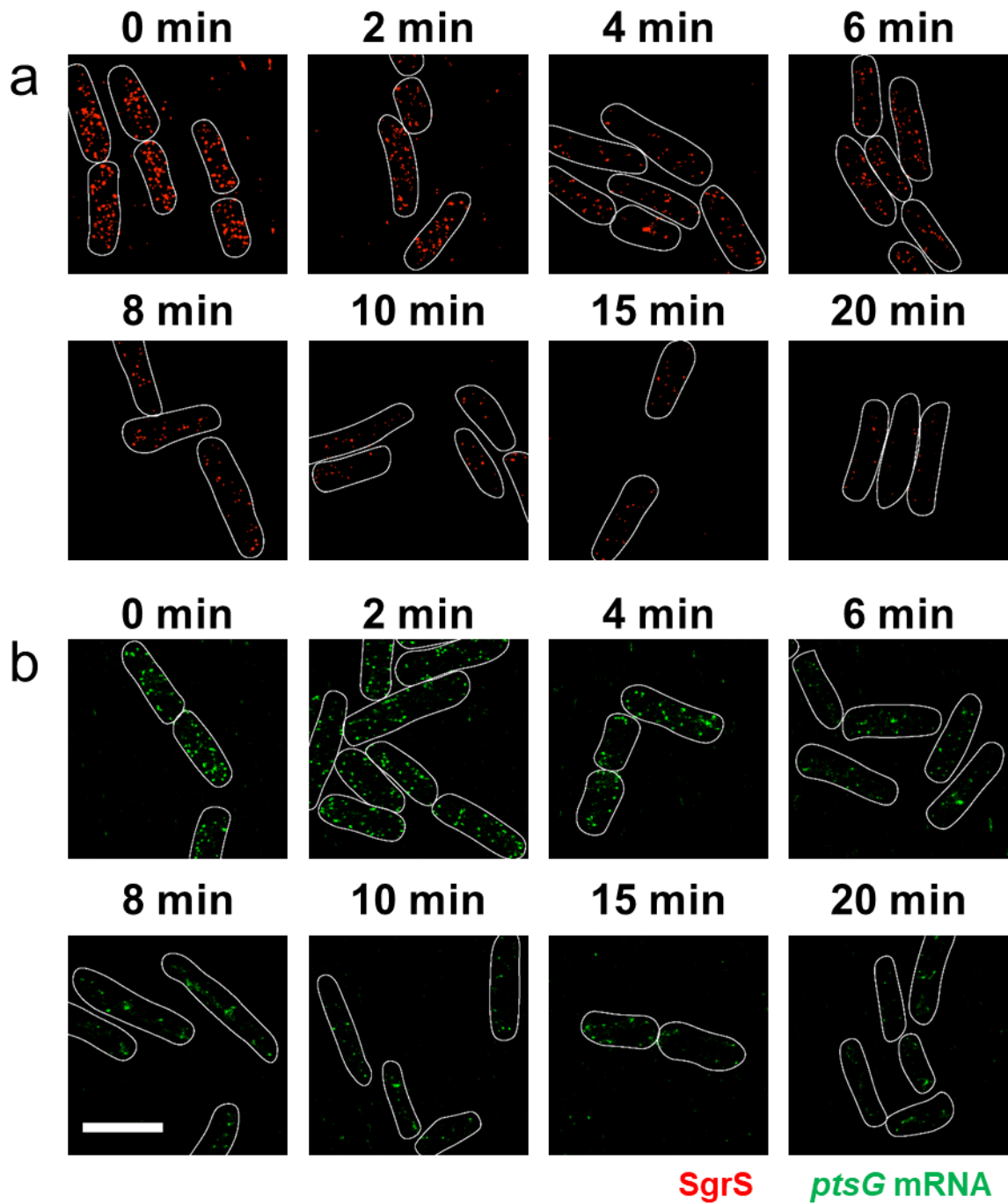
327



329 **Supplementary Figure 33. RNA lifetime measurements for the G184A-C195U strain. (a)**
330 SgrS degradation in the G184A-C195U strain. Each experiment was performed independently 2
331 times. **(b)** *ptsG* mRNA degradation in the G184A-C195U strain. Each experiment was performed
332 independently 2 times. **(c)** Calculation of RNA lifetime. Filled and open circles are two
333 independent measurements with mean value from ~80 cells in each case. The copy numbers have
334 been normalized to time $t=0$ in each case. The degradation rates calculated from the lifetimes are
335 shown in Fig. 6a, Supplementary Fig. 37 and Supplementary Table 3. Scale bar is 2 μm and
336 applies to all the panels. Source data are provided as a Source Data file.

337

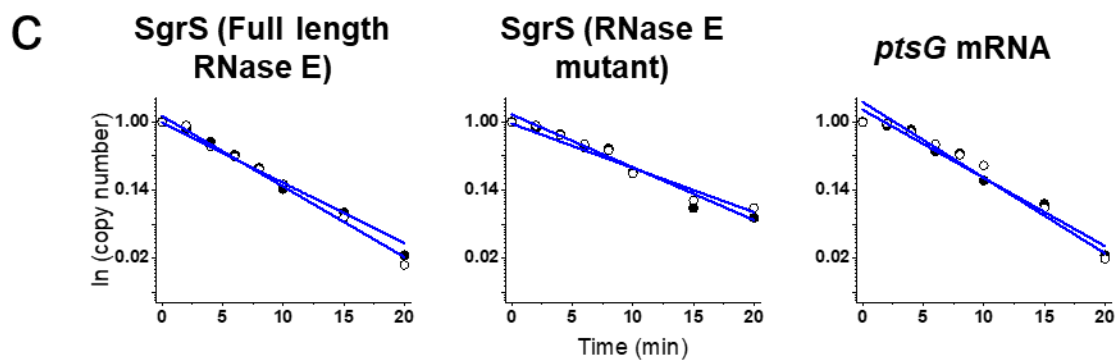
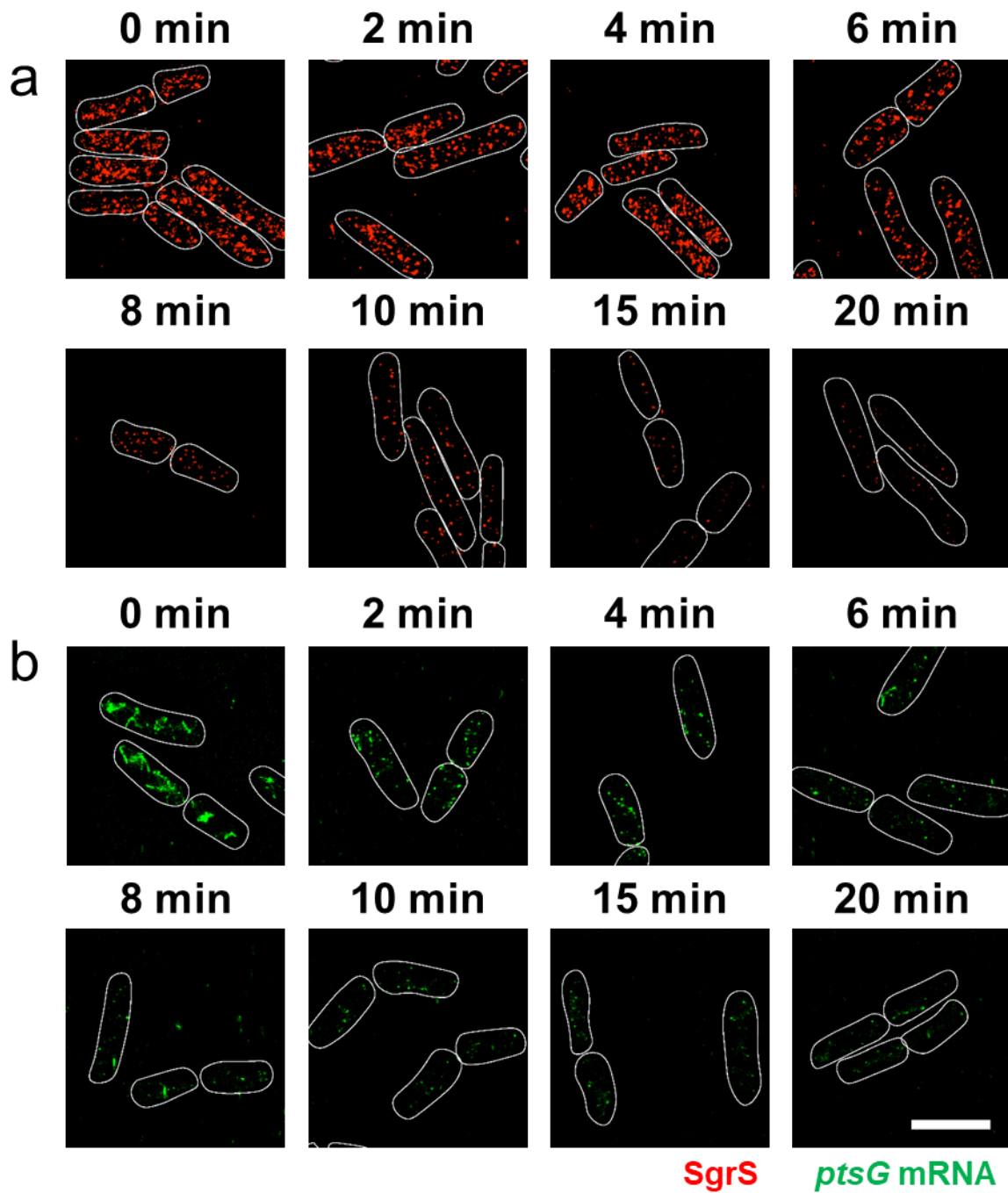
338



340 **Supplementary Figure 34. RNA lifetime measurements for the G215A strain. (a)** SgrS
341 degradation in the G215A strain. Each experiment was performed independently 2 times. **(b)**
342 *ptsG* mRNA degradation in the G215A strain. Each experiment was performed independently 2
343 times. **(c)** Calculation of RNA lifetime. Filled and open circles are two independent
344 measurements with mean value from ~80 cells in each case. The copy numbers have been
345 normalized to time $t=0$ in each case. The degradation rates calculated from the lifetimes are
346 shown in Fig. 6a, Supplementary Fig. 37 and Supplementary Table 3. Scale bar is 2 μm and
347 applies to all the panels. Source data are provided as a Source Data file.

348

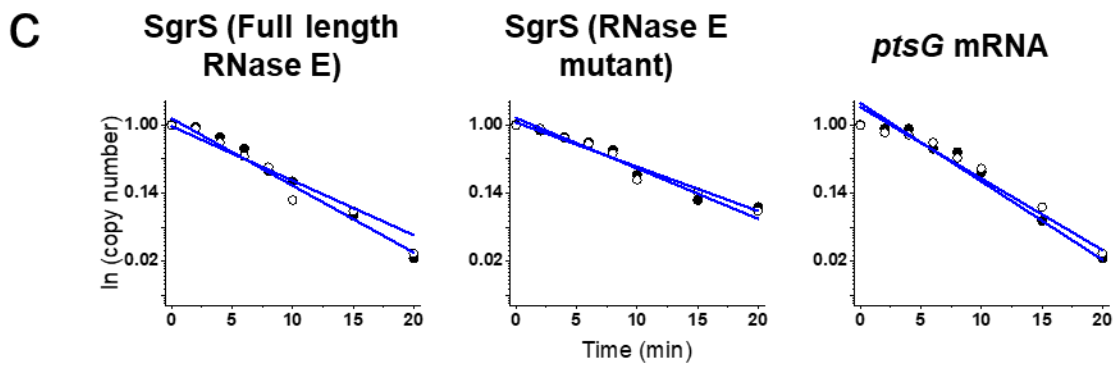
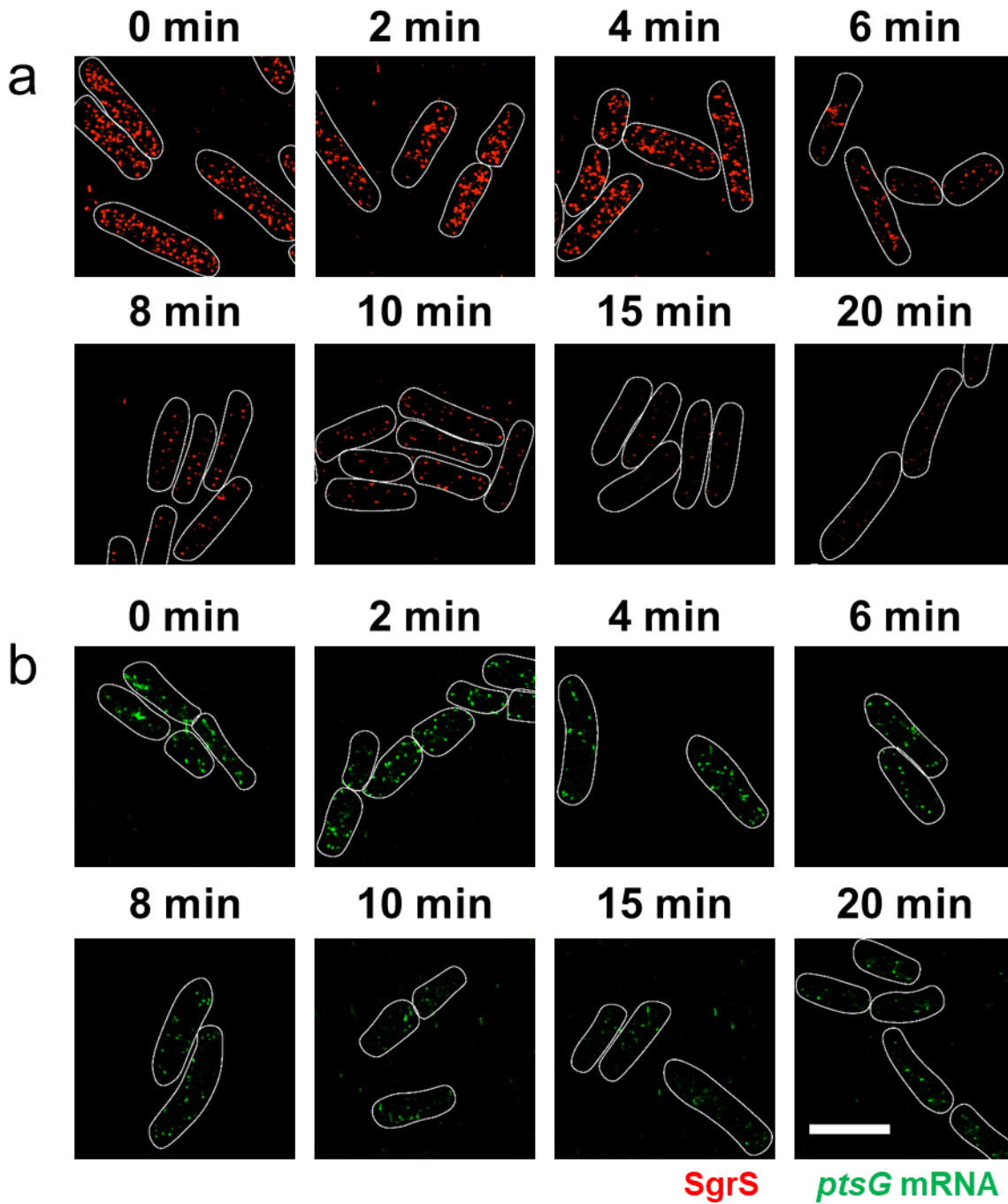
349



351 **Supplementary Figure 35. RNA lifetime measurements for the U224A strain. (a)** SgrS
352 degradation in the U224A strain. Each experiment was performed independently 2 times. **(b)**
353 *ptsG* mRNA degradation in the U224A strain. Each experiment was performed independently 2
354 times. **(c)** Calculation of RNA lifetime. Filled and open circles are two independent
355 measurements with mean value from ~80 cells in each case. The copy numbers have been
356 normalized to time $t=0$ in each case. The degradation rates calculated from the lifetimes are
357 shown in Fig. 6a, Supplementary Fig. 37 and Supplementary Table 3. Scale bar is 2 μm and
358 applies to all the panels. Source data are provided as a Source Data file.

359

360

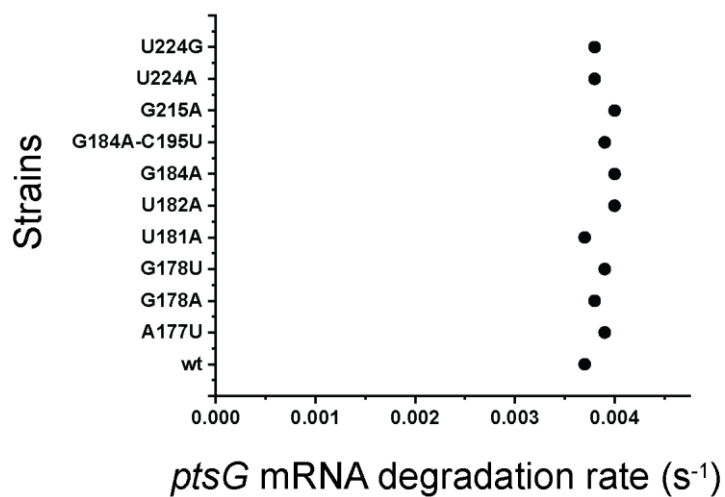


362 **Supplementary Figure 36. RNA lifetime measurements for the U224G strain. (a)** SgrS
363 degradation in the U224G strain. Each experiment was performed independently 2 times. **(b)**
364 *ptsG* mRNA degradation in the U224G strain. Each experiment was performed independently 2
365 times. **(c)** Calculation of RNA lifetime. Filled and open circles are two independent
366 measurements with mean value from ~80 cells in each case. The copy numbers have been
367 normalized to time $t=0$ in each case. The degradation rates calculated from the lifetimes are
368 shown in Fig. 6a, Supplementary Fig. 37 and Supplementary Table 3. Scale bar is 2 μm and
369 applies to all the panels. Source data are provided as a Source Data file.

370

371

372



373

374

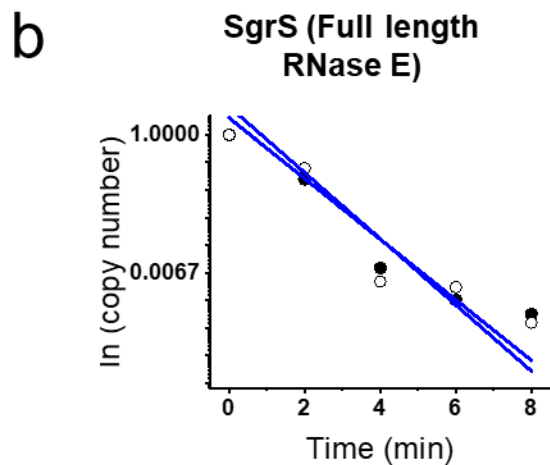
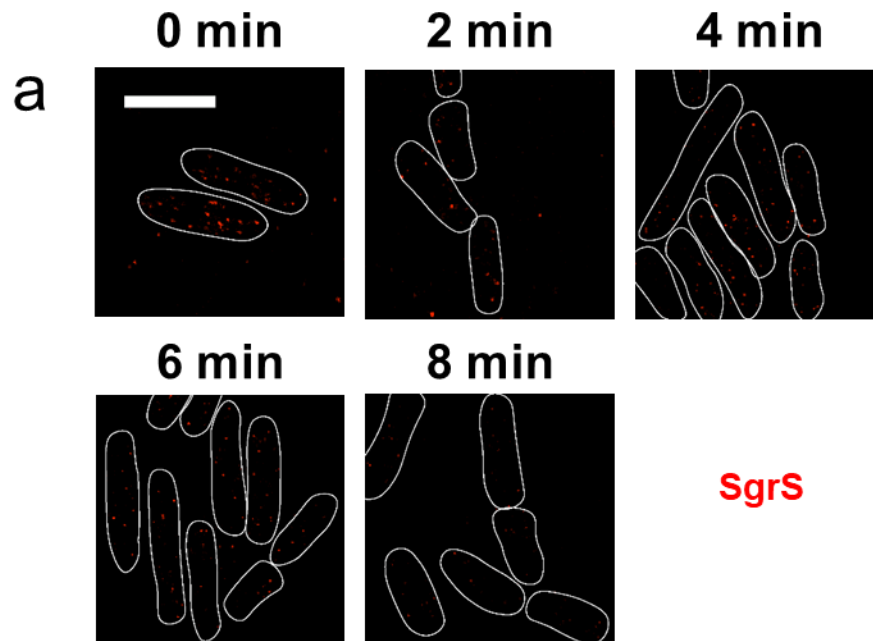
375 **Supplementary Figure 37. Degradation rates of *ptsG* mRNA in wild-type and the mutant**

376 **strains.** Degradation rates of *ptsG* mRNA in wild-type and the strains A177U, G178A, G178U,

377 U181A, U182A, G184A, G184A-C195U, G215A, U224A and U224G. The plot shows mean

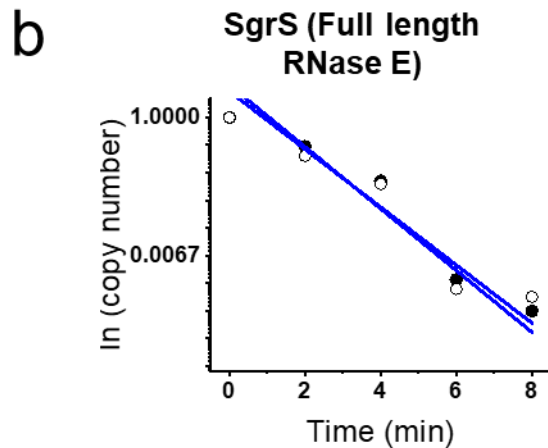
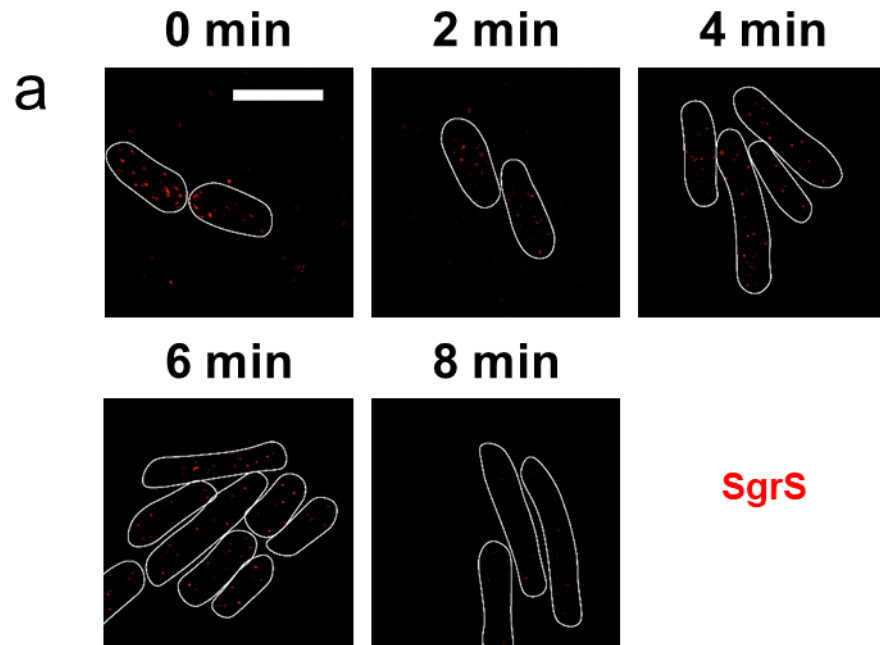
378 values obtained from two experimental replicates. Source data are provided as a Source Data file.

379



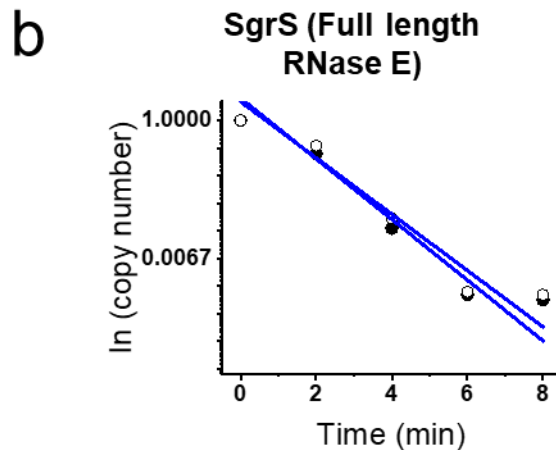
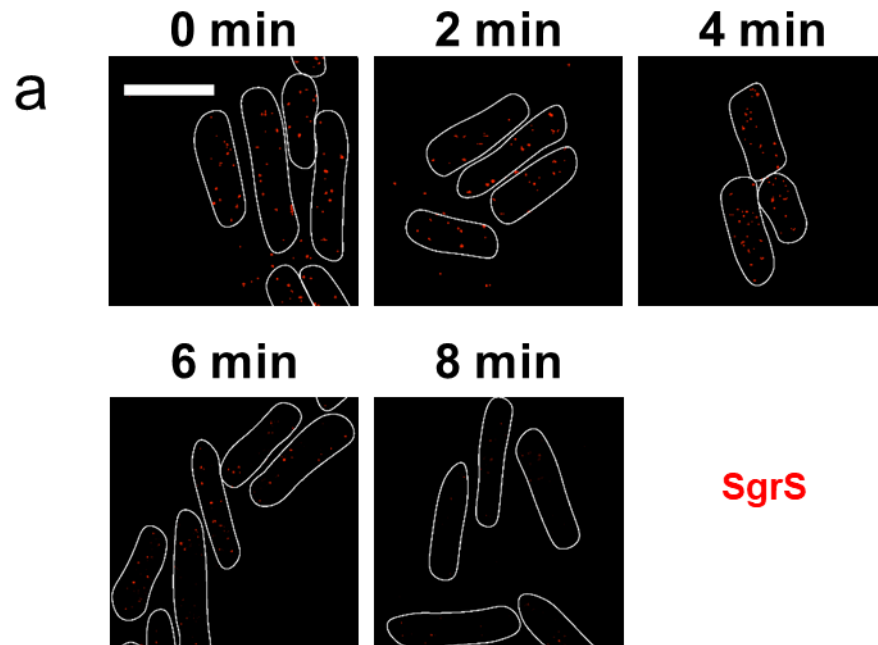
380

381 **Supplementary Figure 38. RNA lifetime measurements for the Δhfq wild-type strain. (a)**
 382 SgrS degradation in the Δhfq wild-type strain. Each experiment was performed independently 2
 383 times. Scale bar is 2 μm and applies to all the panels. **(b)** Calculation of RNA lifetime. Filled and
 384 open circles are two independent measurements with mean value from ~ 70 cells in each case.
 385 The copy numbers have been normalized to time $t=0$ in each case. The degradation rates
 386 calculated from the lifetimes are shown in Fig 6a. Source data are provided as a Source Data file.



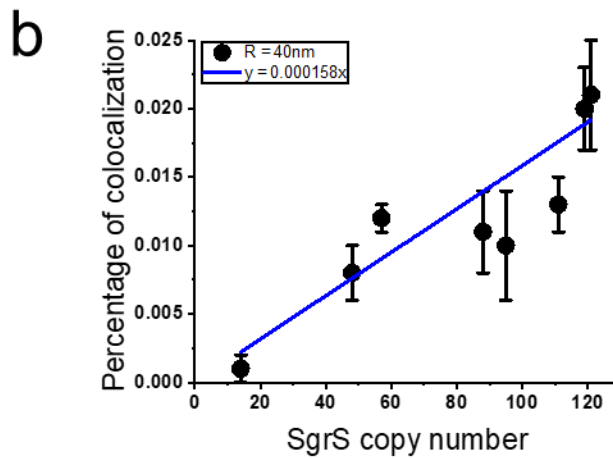
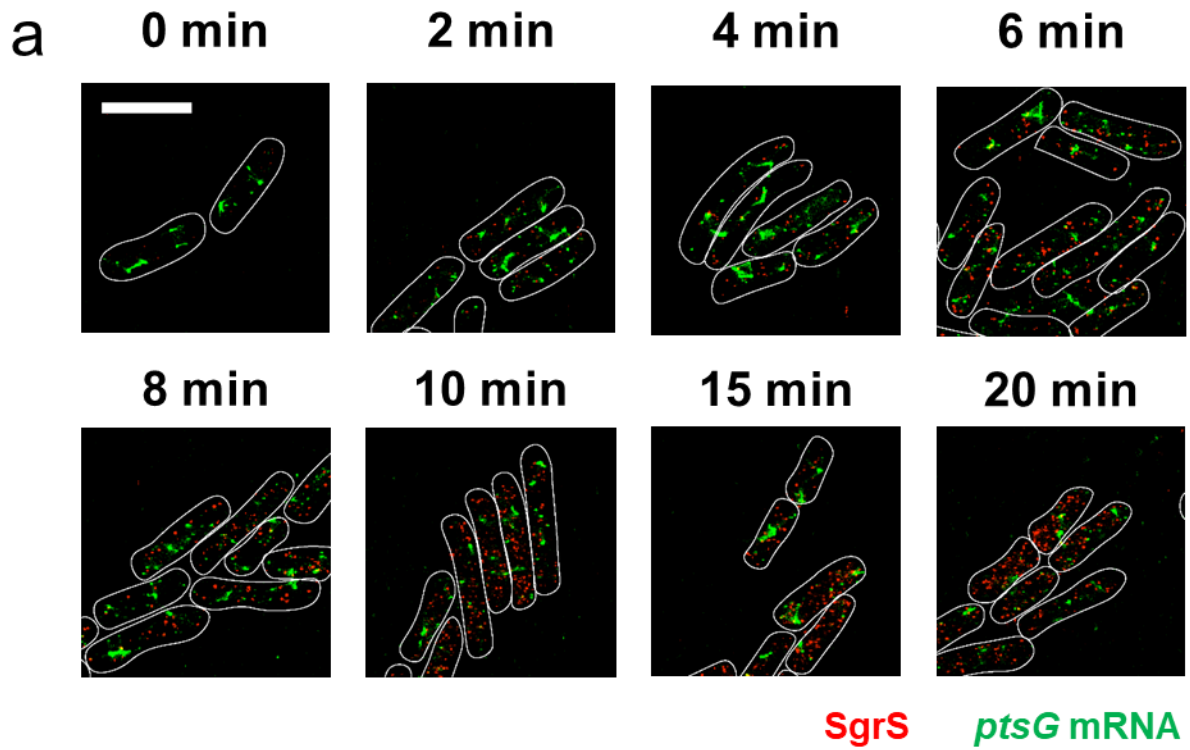
387

388 **Supplementary Figure 39. RNA lifetime measurements for the Δhfq A177U strain.** (a) SgrS
 389 degradation in the Δhfq A177U strain. Each experiment was performed independently 2 times.
 390 Scale bar is 2 μm and applies to all the panels. (b) Calculation of RNA lifetime. Filled and open
 391 circles are two independent measurements with mean value from ~ 70 cells in each case. The
 392 copy numbers have been normalized to time $t=0$ in each case. The degradation rates calculated
 393 from the lifetimes are shown in Fig 6a. Source data are provided as a Source Data file.



394

395 **Supplementary Figure 40. RNA lifetime measurements for the Δhfq G184A strain.** (a) SgrS
 396 degradation in the Δhfq G184A strain. Each experiment was performed independently 2 times.
 397 Scale bar is 2 μm and applies to all the panels. (b) Calculation of RNA lifetime. Filled and open
 398 circles are two independent measurements with mean value from ~ 70 cells in each case. The
 399 copy numbers have been normalized to time $t=0$ in each case. The degradation rates calculated
 400 from the lifetimes are shown in Fig 6a. Source data are provided as a Source Data file.



401

402 **Supplementary Figure 41. Colocalization analysis for base-pairing mutant strain.** (a) 3D
 403 super-resolution images of SgrS (red) and *ptsG* mRNA (green) in the base-pairing mutant strain
 404 projected on 2D planes. The panels show the multi-color images of cells before (0 min) and 2, 4,

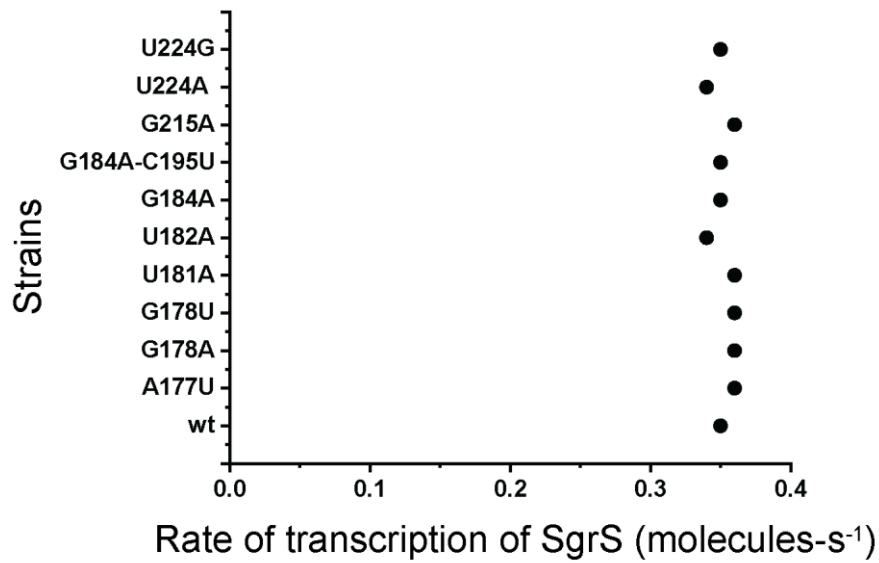
405 6, 8, 10, 15, 20 min after α MG (non-metabolizable sugar analog) induction. Each experiment
406 was performed independently 2 times. White lines denote cell boundaries. Scale bar is 2 μ m and
407 applies to all the panels. (b) The percentage of colocalization in the base-pairing mutant strain
408 with R=40 nm as a function of mean SgrS copy number. The plot is fit with a linear function for
409 correction of colocalization by chance. Data are presented as mean values +/-SD from n=3, 5, 4,
410 3, 6, 5, 4, 3 images for 0, 2, 4, 6, 8, 10, 15, 20 min after α MG induction. Source data are
411 provided as a Source Data file.

412

413

414

415



416

417

418 **Supplementary Figure 42. Rates of transcription of SgrS for wild-type and the mutant**

419 **strains.** Rates of transcription of SgrS for wild-type and the strains A177U, G178A, G178U,

420 U181A, U182A, G184A, G184A-C195U, G215A, U224A and U224G calculated from the time

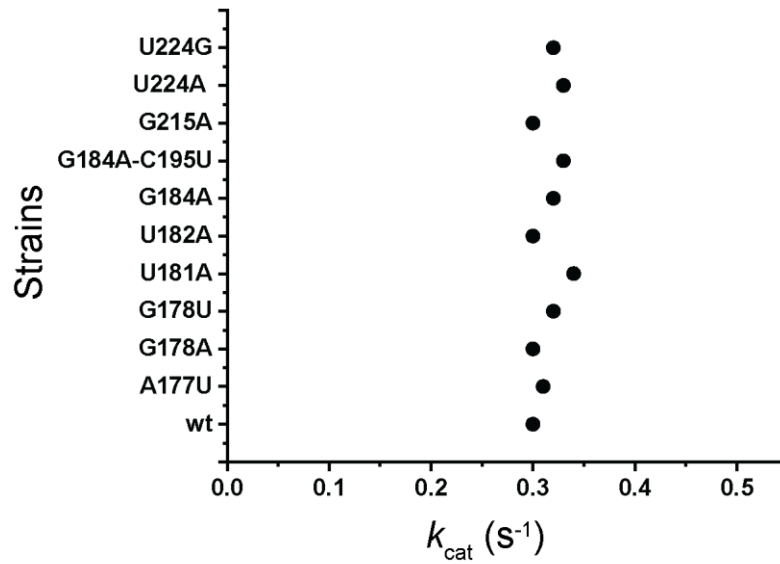
421 dependent modeling curves of the SgrS, *ptsG* mRNA and SgrS-*ptsG* mRNA complexes. These

422 were determined simultaneously in the wild-type and the RNase E mutants. The plot shows mean

423 values from the independent fitting of two replicates. Source data are provided as a Source Data

424 file.

425



426

427 **Supplementary Figure 43. Co-degradation rate of SgrS-*ptsG* mRNA complex for wild-type**

428 **and the mutants.** k_{cat} measured from the time dependent modeling curves of the SgrS, *ptsG*

429 mRNA and SgrS-*ptsG* mRNA complexes for the wild-type and strains A177U, G178A, G178U,

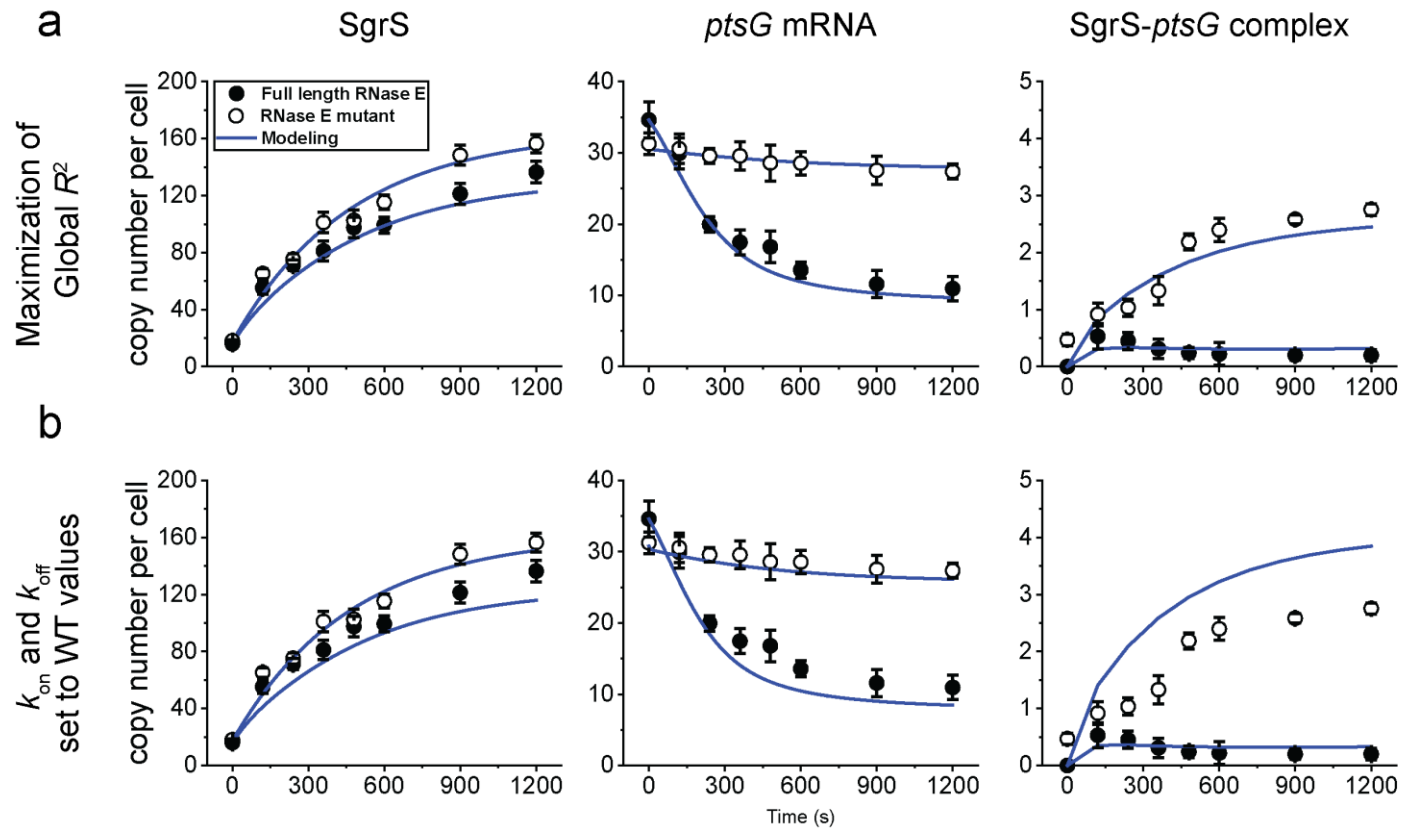
430 U181A, U182A, G184A, G184A-C195U, G215A, U224A, U224G. These were determined

431 simultaneously in the wild-type and RNase E mutants. The plot shows mean values from the

432 independent fitting on two replicates. Source data are provided as a Source Data file.

433

434



435

436 **Supplementary Figure 44. Change in the copy numbers of SgrS and *ptsG* mRNA over time**

437 **for SgrS A177U mutant strain.** Time course changes from 0 min (0 s) to 20 min (1200 s) after

438 the induction of glucose-phosphate stress using α MG (non-metabolizable sugar analog) and the

439 corresponding modeling curves for SgrS, *ptsG* mRNA and SgrS-*ptsG* complexes for SgrS

440 A177U strain by (a) maximization of global R^2 and (b) setting k_{on} and k_{off} to WT values. The

441 average copy numbers per cell are plotted over time in each case. Rate constants obtained from

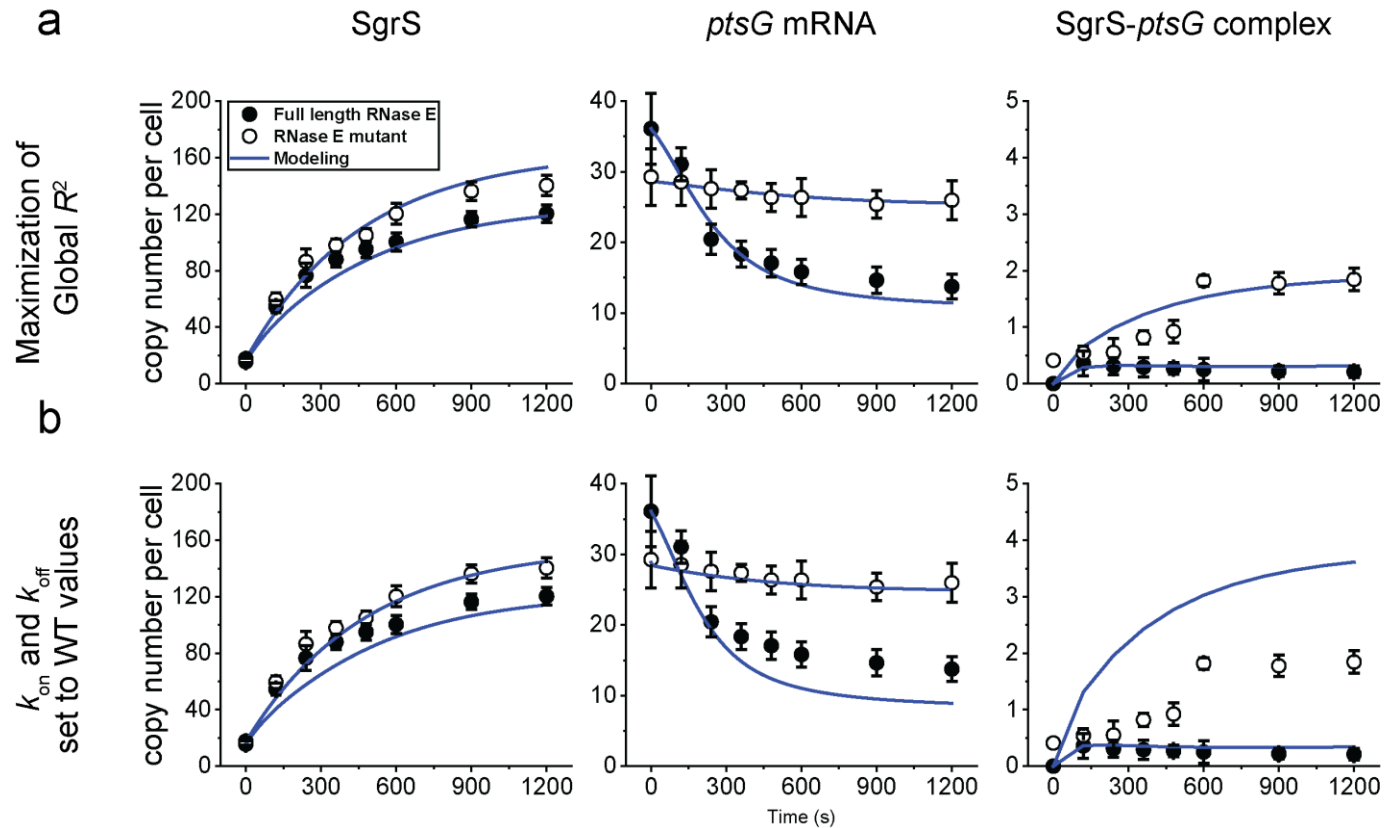
442 (a) are shown in Fig. 6b, c, d and in Supplementary Table 3. Weighted R^2 's for the modeling

443 curves are reported in Supplementary Table 4. Data are presented as mean values +/- SEM in (a),

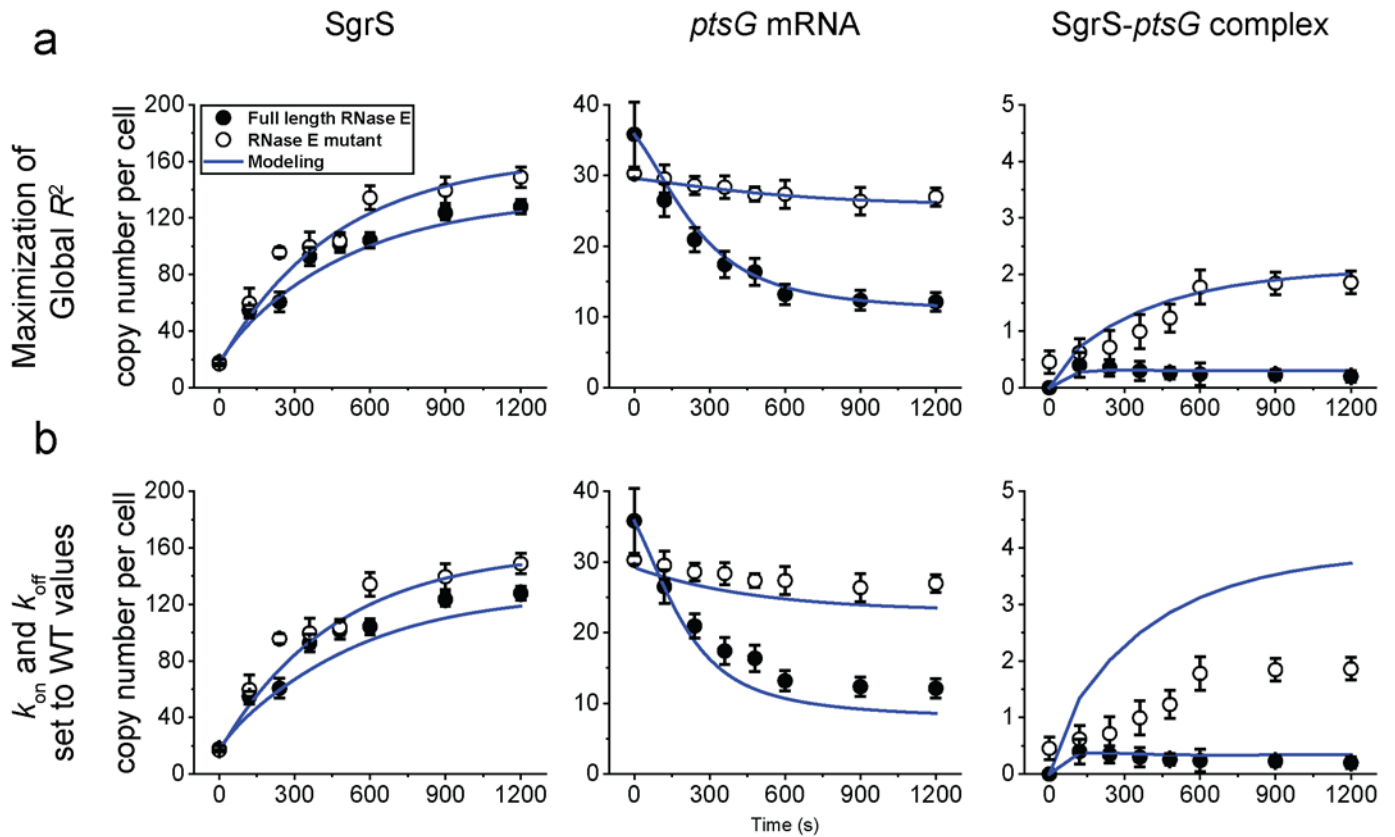
444 (b) from n=132, 81, 88, 80, 85, 88, 86, 80 cells examined over 2 independent experiments after

445 0, 2, 4, 6, 8, 10, 15, 20 minutes induction respectively. Source data are provided as a Source Data

446 file.



447
 448 **Supplementary Figure 45. Change in the copy numbers of SgrS and *ptsG* mRNA over time**
 449 **for SgrS G178A mutant strain.** Time course changes from 0 min (0 s) to 20 min (1200 s) after
 450 the induction of glucose-phosphate stress using α MG (non-metabolizable sugar analog) and the
 451 corresponding modeling curves for SgrS, *ptsG* mRNA and SgrS-*ptsG* complexes for SgrS
 452 G178A strain by (a) maximization of global R^2 and (b) setting k_{on} and k_{off} to WT values. The
 453 average copy numbers per cell are plotted over time in each case. Rate constants obtained from
 454 (a) are shown in Fig. 6b, c, d and in Supplementary Table 3. Weighted R^2 's for the modeling
 455 curves are reported in Supplementary Table 4. Data are presented as mean values +/- SEM in(a),
 456 (b) from n=81, 86, 89, 82, 87, 80, 83, 82 cells examined over 2 independent experiments after 0,
 457 2, 4, 6, 8, 10, 15, 20 minutes induction respectively. Source data are provided as a Source Data
 458 file.



459

460 **Supplementary Figure 46. Change in the copy numbers of SgrS and *ptsG* mRNA over time**

461 **for SgrS G178U mutant strain.** Time course changes from 0 min (0 s) to 20 min (1200 s) after

462 the induction of glucose-phosphate stress using α MG (non-metabolizable sugar analog) and the

463 corresponding modeling curves for SgrS, *ptsG* mRNA and SgrS-*ptsG* complexes for SgrS

464 G178U strain by (a) maximization of global R^2 and (b) setting k_{on} and k_{off} to WT values. The

465 average copy numbers per cell are plotted over time in each case. Rate constants obtained from

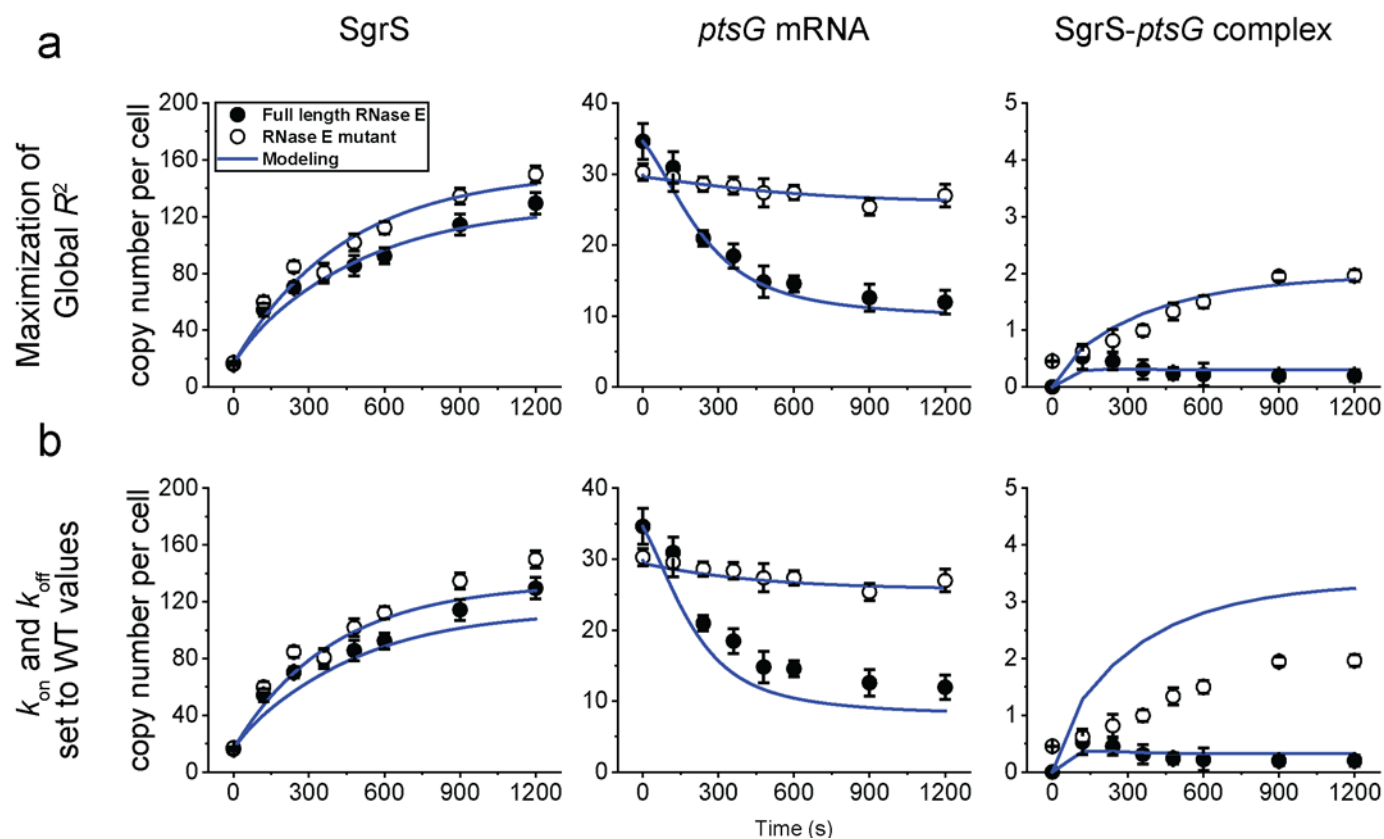
466 (a) are shown in Fig. 6b, c, d and in Supplementary Table 3. Weighted R^2 's for the modeling

467 curves are reported in Supplementary Table 4. Data are presented as mean values \pm SEM in (a),

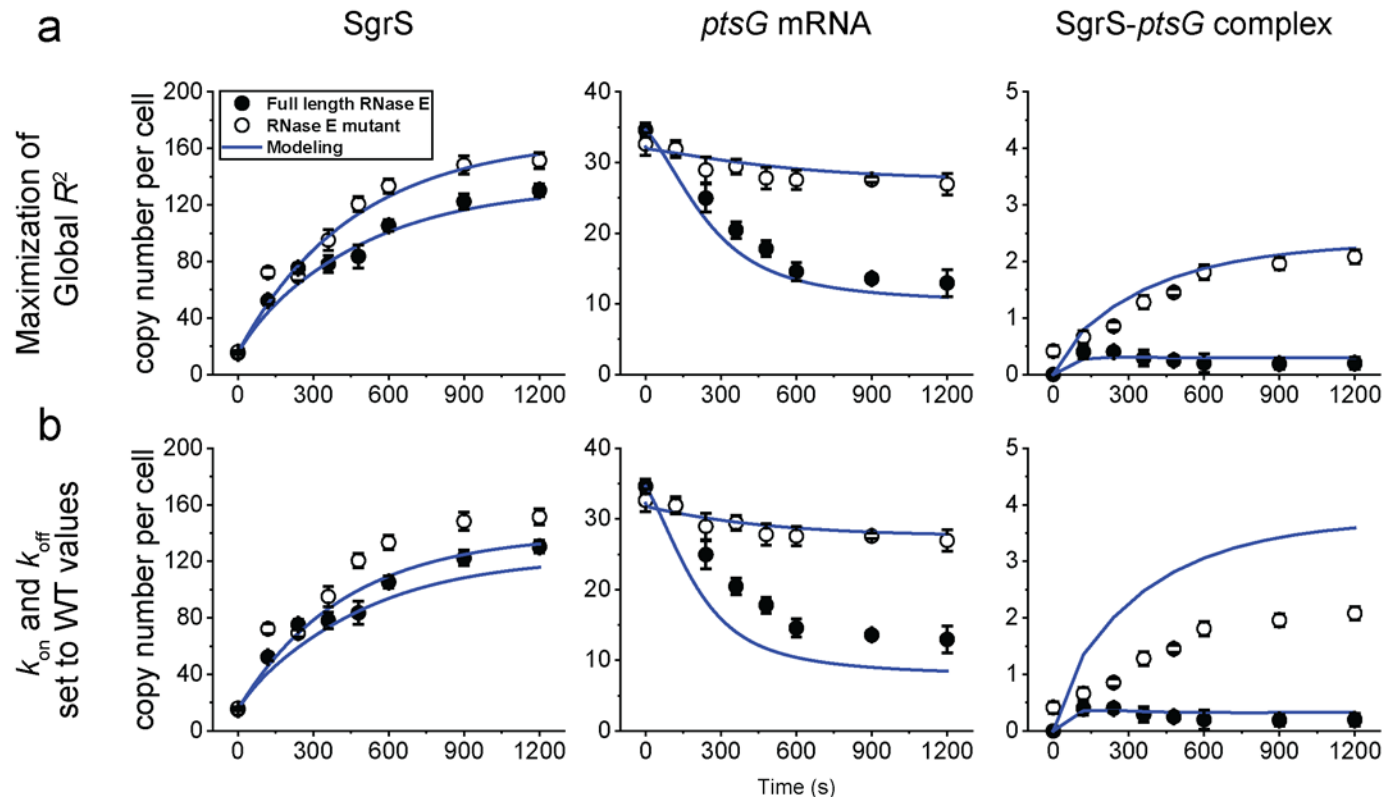
468 (b) from n=88, 83, 97, 88, 90, 85, 86, 83 cells examined over 2 independent experiments after 0,

469 2, 4, 6, 8, 10, 15, 20 minutes induction respectively. Source data are provided as a Source Data

470 file.



471
 472 **Supplementary Figure 47. Change in the copy numbers of SgrS and *ptsG* mRNA over time**
 473 **for SgrS U181A mutant strain.** Time course changes from 0 min (0 s) to 20 min (1200 s) after
 474 the induction of glucose-phosphate stress using α MG (non-metabolizable sugar analog) and the
 475 corresponding modeling curves for SgrS, *ptsG* mRNA and SgrS-*ptsG* complexes for SgrS
 476 U181A strain by (a) maximization of global R^2 and (b) setting k_{on} and k_{off} to WT values. The
 477 average copy numbers per cell are plotted over time in each case. Rate constants obtained from
 478 (a) are shown in Fig. 6b, c, d and in Supplementary Table 3. Weighted R^2 's for the modeling
 479 curves are reported in Supplementary Table 4. Data are presented as mean values \pm SEM in (a),
 480 (b) from $n=91, 101, 85, 86, 90, 107, 95, 97$ cells examined over 2 independent experiments after
 481 0, 2, 4, 6, 8, 10, 15, 20 minutes induction respectively. Source data are provided as a Source Data
 482 file.



483

484 **Supplementary Figure 48. Change in the copy numbers of SgrS and *ptsG* mRNA over time**

485 **for SgrS U182A mutant strain.** Time course changes from 0 min (0 s) to 20 min (1200 s) after

486 the induction of glucose-phosphate stress using α MG (non-metabolizable sugar analog) and the

487 corresponding modeling curves for SgrS, *ptsG* mRNA and SgrS-*ptsG* complexes for SgrS

488 U182A strain by (a) maximization of global R^2 and (b) setting k_{on} and k_{off} to WT values. The

489 average copy numbers per cell are plotted over time in each case. Rate constants obtained from

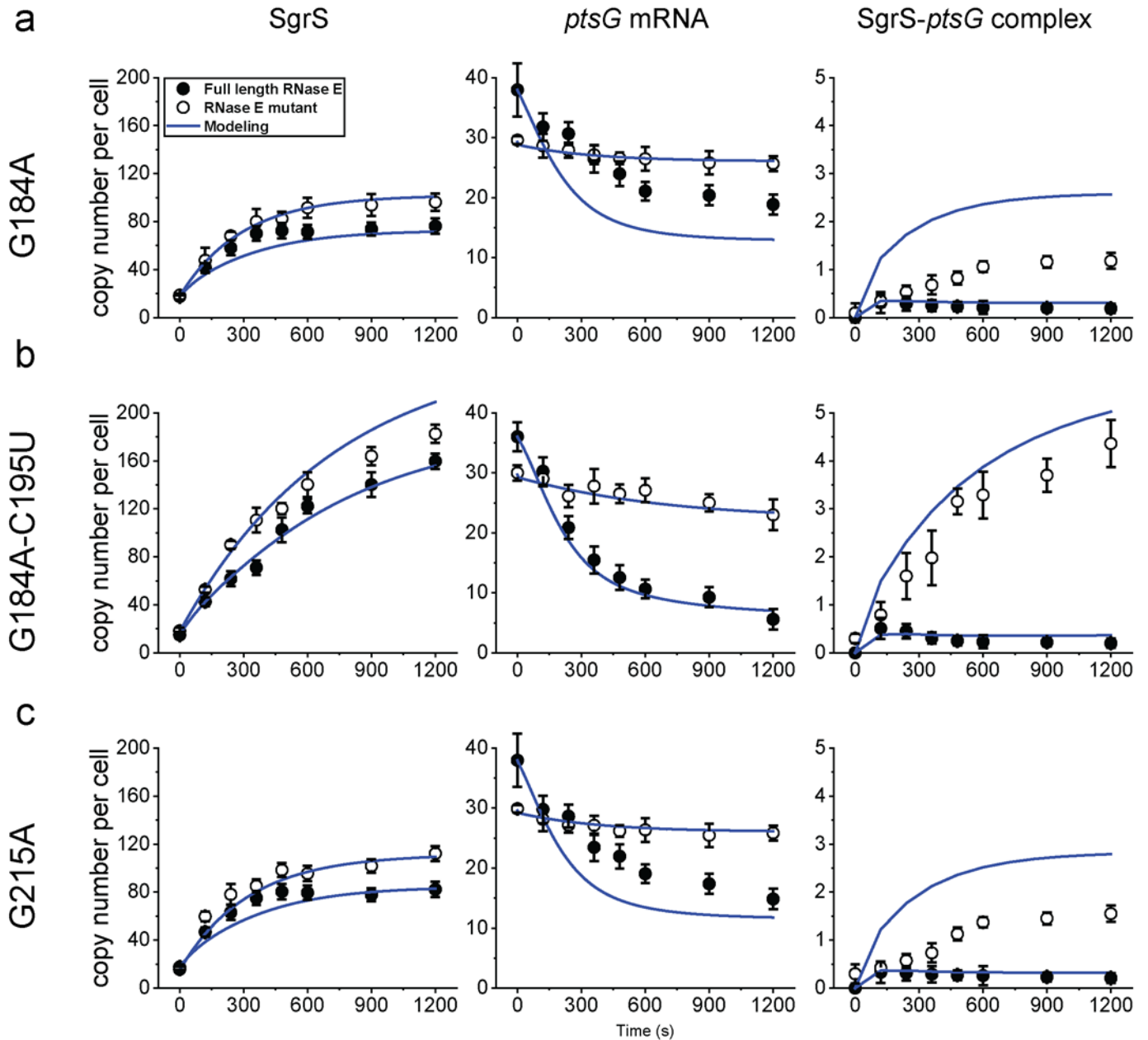
490 (a) are shown in Fig. 6b, c, d and in Supplementary Table 3. Weighted R^2 's for the modeling

491 curves are reported in Supplementary Table 4. Data are presented as mean values \pm SEM in (a),

492 (b) from n=101, 84, 87, 90, 112, 107, 82, 94 cells examined over 2 independent experiments

493 after 0, 2, 4, 6, 8, 10, 15, 20 minutes induction respectively. Source data are provided as a Source

494 Data file.



495

496 **Supplementary Figure 49. Change in the copy numbers of SgrS and *ptsG* mRNA over time**

497 **for SgrS mutant strains.** Time course changes from 0 min (0 s) to 20 min (1200 s) after the

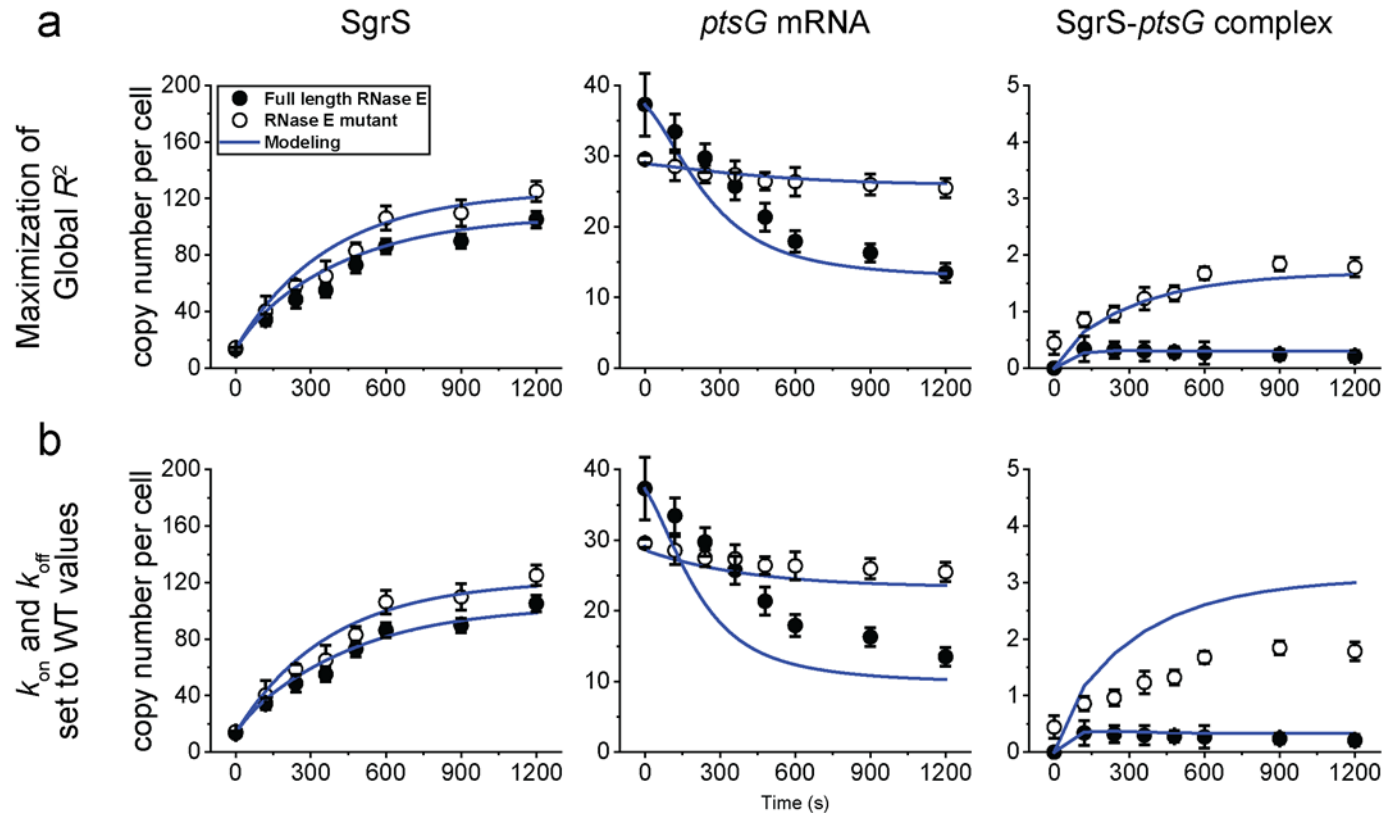
498 induction of glucose-phosphate stress using α MG (non-metabolizable sugar analog) and the

499 corresponding modeling curves for SgrS, *ptsG* mRNA and SgrS-*ptsG* complexes for (a) SgrS

500 G184A strain, (b) SgrS G184A-C195U strain, (c) SgrS G215A strain by setting k_{on} and k_{off} to

501 WT values. The average copy numbers per cell are plotted over time in each case. Weighted R^2 's

502 for the modeling curves are reported in Supplementary Table 4. Data are presented as mean
503 values +/- SEM in (a), (b), (c) from n=84, 84, 94, 99, 94, 90, 87, 88 cells examined over 2
504 independent experiments after 0, 2, 4, 6, 8, 10, 15, 20 minutes induction respectively for G184A
505 mutant strain; for n=117, 101, 115, 111, 102, 110, 104, 104 cells examined over 2 independent
506 experiments after 0, 2, 4, 6, 8, 10, 15, 20 minutes induction respectively for G184A-C195U
507 mutant strain and for n=82, 88, 94, 104, 94, 90, 89, 88 cells examined over 2 independent
508 experiments after 0, 2, 4, 6, 8, 10, 15, 20 minutes induction respectively for G215A mutant
509 strain. Source data are provided as a Source Data file.



510

511 **Supplementary Figure 50. Change in the copy numbers of SgrS and *ptsG* mRNA over time**

512 **for SgrS U224A mutant strain.** Time course changes from 0 min (0 s) to 20 min (1200 s) after

513 the induction of glucose-phosphate stress using α MG (non-metabolizable sugar analog) and the

514 corresponding modeling curves for SgrS, *ptsG* mRNA and SgrS-*ptsG* complexes for SgrS

515 U224A strain by (a) maximization of global R^2 and (b) setting k_{on} and k_{off} to WT values. The

516 average copy numbers per cell are plotted over time in each case. Rate constants obtained from

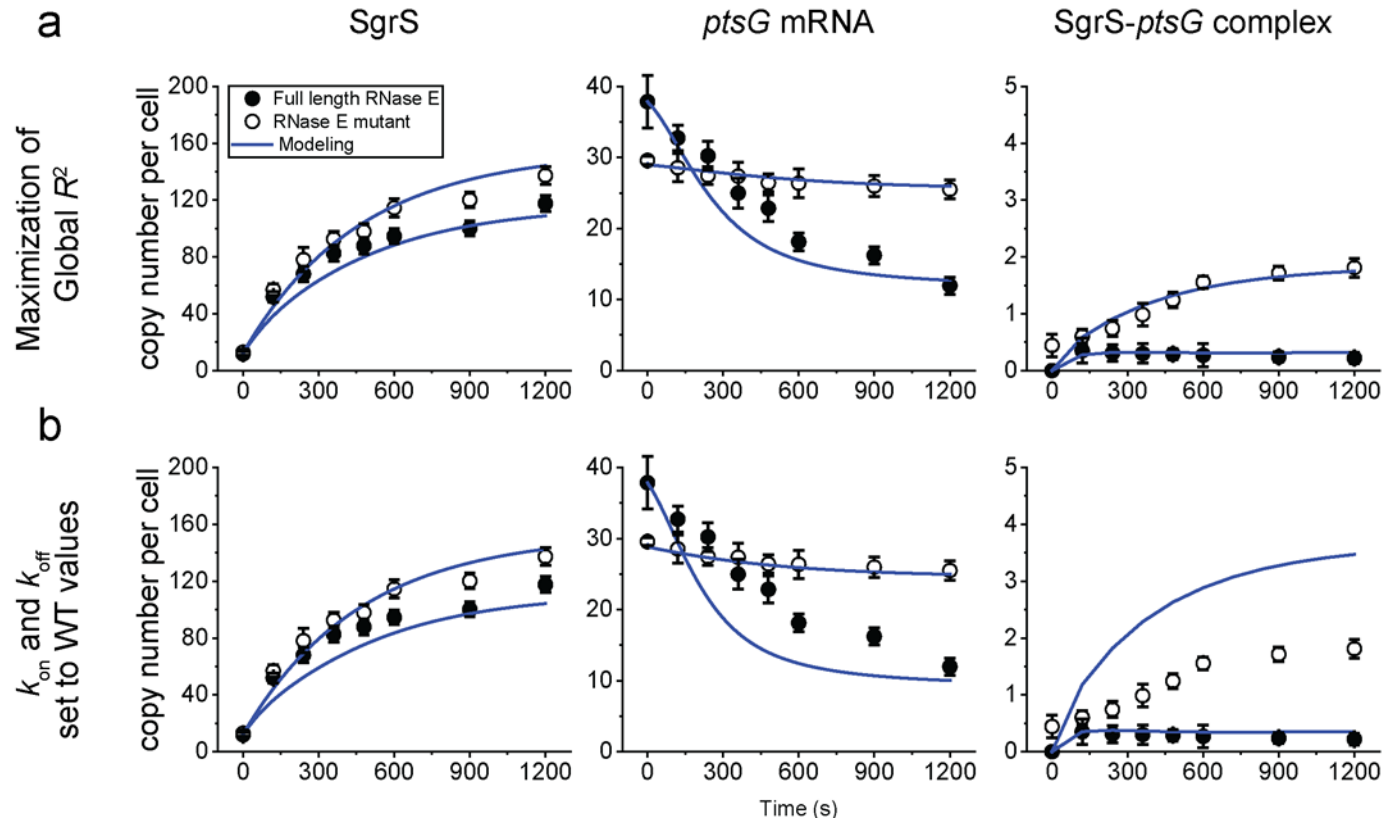
517 (a) are shown in Fig. 6b, c, d and in Supplementary Table 3. Weighted R^2 's for the modeling

518 curves are reported in Supplementary Table 4. Data are presented as mean values \pm SEM in (a),

519 (b) from n=90, 99, 99, 82, 83, 81, 81, 84 cells examined over 2 independent experiments after 0,

520 2, 4, 6, 8, 10, 15, 20 minutes induction respectively. Source data are provided as a Source Data

521 file.



522

523 **Supplementary Figure 51. Change in the copy numbers of SgrS and *ptsG* mRNA over time**

524 **for SgrS U224G mutant strain.** Time course changes from 0 min (0 s) to 20 min (1200 s) after

525 the induction of glucose-phosphate stress using α MG (non-metabolizable sugar analog) and the

526 corresponding modeling curves for SgrS, *ptsG* mRNA and SgrS-*ptsG* complexes for SgrS

527 U224G strain by (a) maximization of global R^2 and (b) setting k_{on} and k_{off} to WT values. The

528 average copy numbers per cell are plotted over time in each case. Rate constants obtained from

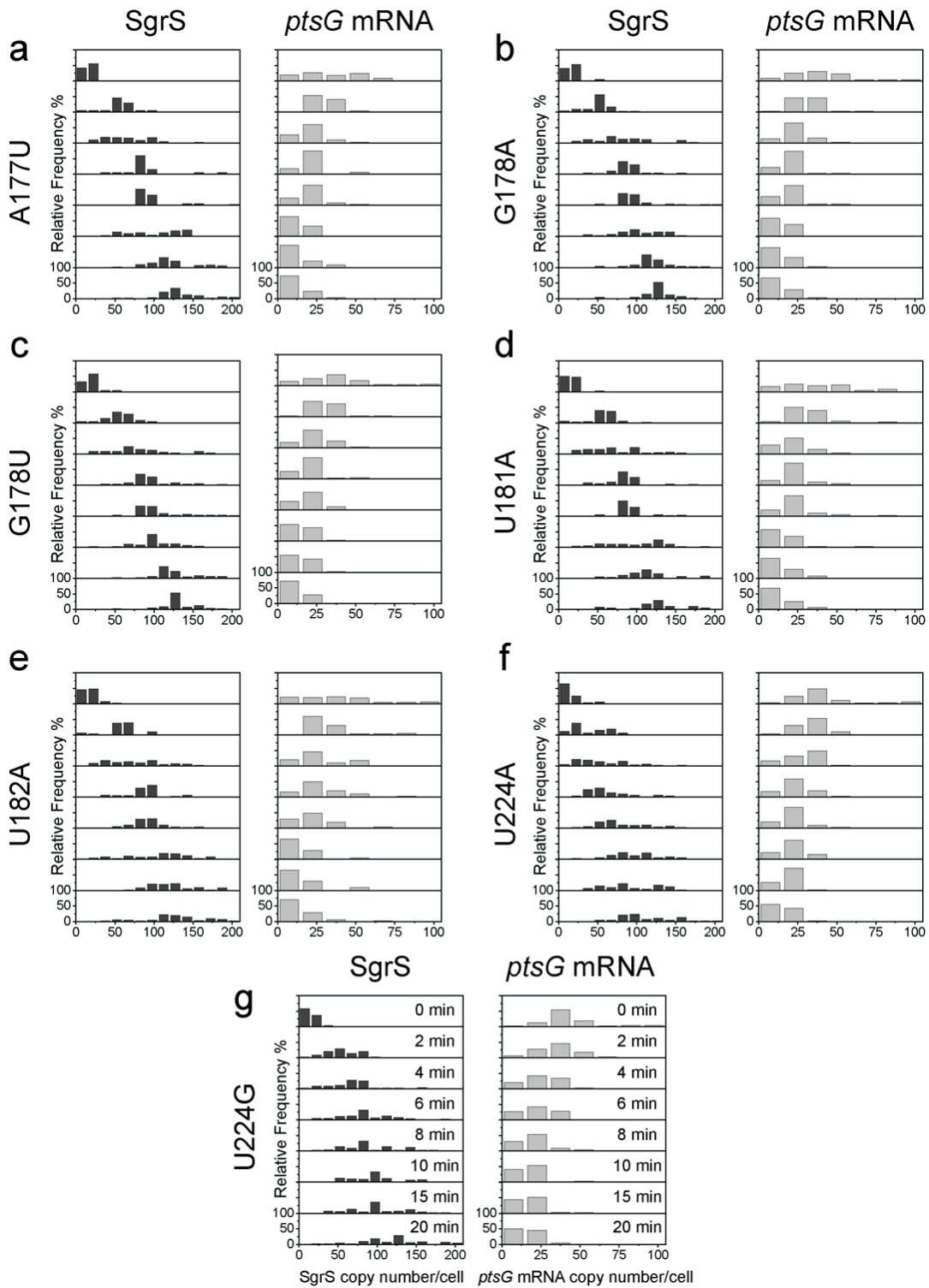
529 (a) are shown in Fig. 6b, c, d and in Supplementary Table 3. Weighted R^2 's for the modeling

530 curves are reported in Supplementary Table 4. Data are presented as mean values \pm SEM in (a),

531 (b) from n=92, 102, 105, 108, 83, 91, 94, 100 cells examined over 2 independent experiments

532 after 0, 2, 4, 6, 8, 10, 15, 20 minutes induction respectively. Source data are provided as a Source

533 Data file.



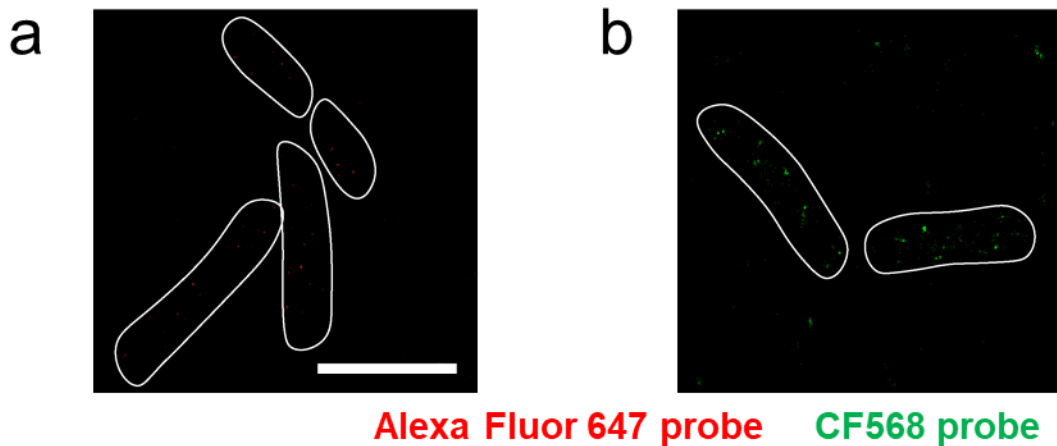
534

535

536 **Supplementary Figure 52. Time dependent changes in the copy numbers of SgrS and ptsG**

537 **mRNA. Histograms showing the change in distribution of SgrS and ptsG mRNA copy numbers**

538 for (a) n=132, 81, 88, 80, 85, 88, 86, 80 cells examined over 2 independent experiments after 0,
539 2, 4, 6, 8, 10, 15, 20 minutes induction respectively for SgrS A177U mutant strain, (b) n=81, 86,
540 89, 82, 87, 80, 83, 82 cells examined over 2 independent experiments after 0, 2, 4, 6, 8, 10, 15,
541 20 minutes induction respectively for G178A mutant strain, (c) n=88, 83, 97, 88, 90, 85, 86, 83
542 cells examined over 2 independent experiments after 0, 2, 4, 6, 8, 10, 15, 20 minutes induction
543 respectively for G178U mutant strain, (d) n=91, 101, 85, 86, 90, 107, 95, 97 cells examined over
544 2 independent experiments after 0, 2, 4, 6, 8, 10, 15, 20 minutes induction respectively for
545 U181A mutant strain, (e) n=101, 84, 87, 90, 112, 107, 82, 94 cells examined over 2 independent
546 experiments after 0, 2, 4, 6, 8, 10, 15, 20 minutes induction respectively for U182A mutant
547 strain, (f) n=90, 99, 99, 82, 83, 81, 81, 84 cells examined over 2 independent experiments after 0,
548 2, 4, 6, 8, 10, 15, 20 minutes induction respectively for U224A mutant strain, (g) n=92, 102, 105,
549 108, 83, 91, 94, 100 cells examined over 2 independent experiments after 0, 2, 4, 6, 8, 10, 15, 20
550 minutes induction respectively for U224G mutant strain. Source data are provided as a Source
551 Data file.



552

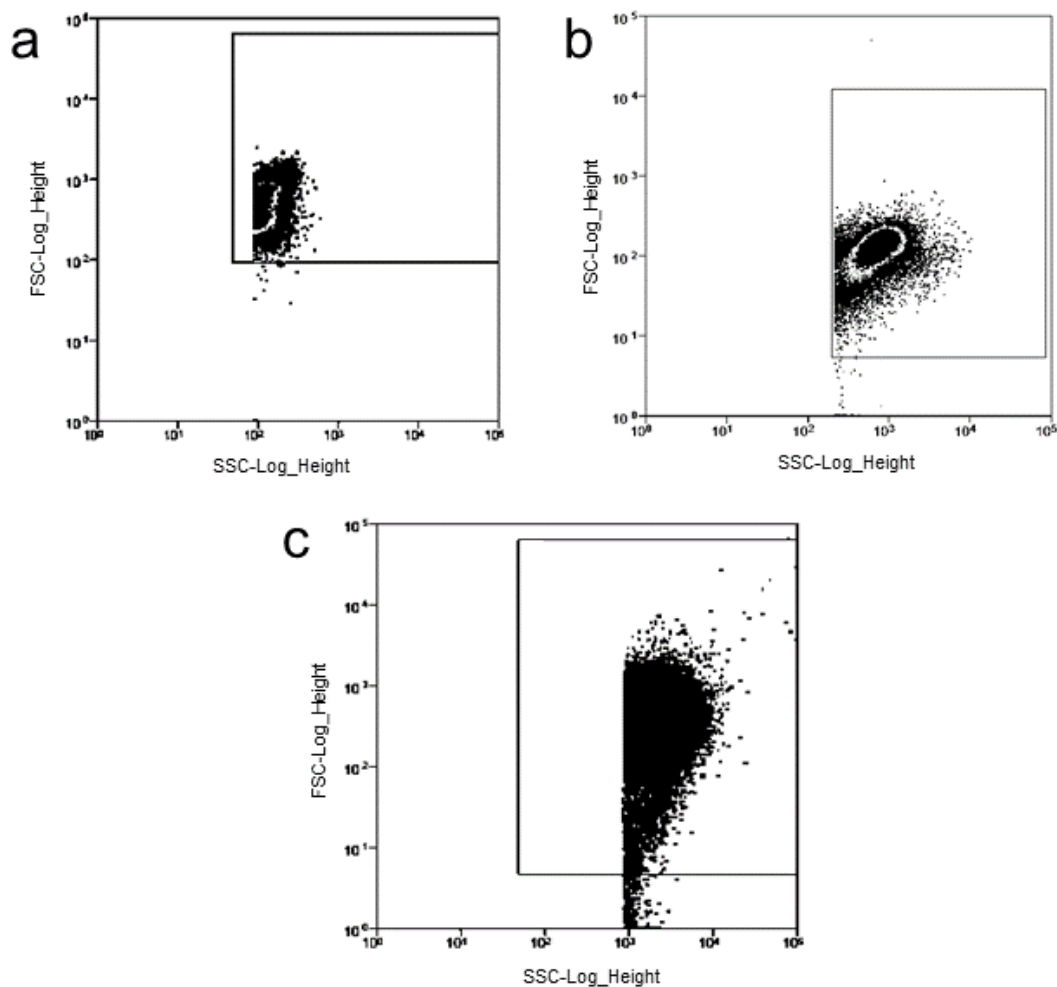
553

554 **Supplementary Figure 53. Negative control for copy number calculation.** (a) Background
555 due to the non-specific binding of Alexa Fluor 647-labeled probes against SgrS in $\Delta sgrS$ strain.
556 This experiment was performed independently 2 times. (b) Background due to the non-specific
557 binding of CF568-labeled probes against *ptsG* mRNA in $\Delta ptsG$ strain. This experiment was
558 performed independently 2 times. Scale bar is 2 μm and applies to all the panels.

559

560

561



562
 563 **Supplementary Figure 54. FACS gating strategies used for cell sorting.** (a) Gating strategy
 564 used for *E. coli* cells with target (*ptsG*)-only (green curve) shown in Fig. 2b. This experiment
 565 was performed independently 2 times. (b) Gating strategy used for *E. coli* cells with wild-type
 566 SgrS along with target (*ptsG*) (black curve) shown in Fig. 2b. This experiment was performed
 567 independently 2 times. (c) Gating strategy used for *E. coli* cells with SgrS library along with
 568 target (*ptsG*) (blue curve) shown in Fig. 2b. These cells were sorted into 5 evenly spaced (log
 569 scale) fluorescence bins and those details are presented in Fig. 2b itself. This experiment was
 570 performed independently 2 times.

571 **Supplementary Tables**572 **Supplementary Table 1. Plasmids and strains used in this study.**

Plasmid	Background	Source or Reference
pSIM6	<i>P_L-gam-bet-exo</i> genes under the control of CI857 repressor, Amp ^R (Ts)	Don Court
pZAMB1	<i>P_{Ltet0-1}-sgrS</i>	3
pZEMB8	<i>P_{Llac0-1}-ptsG-gfpsf</i>	3
pZAMB1A177T	<i>P_{Ltet0-1}-sgrS</i> A177T	This work
pZAMB1G178T	<i>P_{Ltet0-1}-sgrS</i> G178T	This work
pZAMB1G178A	<i>P_{Ltet0-1}-sgrS</i> G178A	This work
pZAMB1G184A	<i>P_{Ltet0-1}-sgrS</i> G184A	This work
pZAMB1C215A	<i>P_{Ltet0-1}-sgrS</i> C215A	This work
pZAMB1T224G	<i>P_{Ltet0-1}-sgrS</i> T224G	This work
pZAMB1T224A	<i>P_{Ltet0-1}-sgrS</i> T224A	This work
Strain	Background	Source or Reference
DJ480	MG1655 Δ <i>lac</i> X74	D. Jin, NCI
CV104	DJ480 Δ <i>lac</i> X74, <i>mal::lacI^q</i> , Δ <i>sgrS::kan^R</i>	C. K. Vanderpool, S. Gottesman, 2004
DB166	MG1655 Δ X74 <i>lac</i> , <i>lacI^q-tetR-spec^R</i>	Divya Balasubramanian
MB1	Δ <i>ptsG</i> , Δ <i>sgrS</i> , <i>lacI^q-tetR-spec^R</i>	This work
MB130	<i>lacI^q::P_{BAD}-ptsG'-lacZ</i> , <i>lattB::lacI^q-PN25tetR-spec^R</i> , <i>miniλte^R</i> , Δ <i>araBAD</i> <i>araC⁺</i> , <i>mal::lacI^q</i>	This work
MB205	Δ <i>sgrS::cat-sacB</i> , <i>lacI^q-tetR-spec^R</i>	This work
MB206	<i>sgrS</i> A177T, <i>lacI^q-tetR-spec^R</i>	This work

MB207	<i>sgrS</i> G178T, <i>lacI^q-tetR-spec^R</i>	This work
MB208	<i>sgrS</i> G178A, <i>lacI^q-tetR-spec^R</i>	This work
MB209	<i>sgrS</i> G184A, <i>lacI^q-tetR-spec^R</i>	This work
SA1701	<i>sgrS</i> G215A, <i>lacI^q-tetR-spec^R</i>	This work
XM180	<i>sgrS</i> G184A-C195T, <i>lacI^q-tetR-spec^R</i>	This work
XM181	<i>sgrS</i> T181A, <i>lacI^q-tetR-spec^R</i>	This work
XM182	<i>sgrS</i> T182A, <i>lacI^q-tetR-spec^R</i>	This work
SA1708	<i>sgrS</i> T224A, <i>lacI^q-tetR-spec^R</i>	This work
SA1709	<i>sgrS</i> T224G, <i>lacI^q-tetR-spec^R</i>	This work
TM528	<i>rne701-FLAG-cat</i>	4
SA1740	<i>sgrS</i> A177T, <i>lacI^q-tetR-spec^R</i> , <i>rne131::kan^R</i>	This work
SA1741	<i>sgrS</i> A178T, <i>lacI^q-tetR-spec^R</i> , <i>rne131::kan^R</i>	This work
SA1742	<i>sgrS</i> A178A, <i>lacI^q-tetR-spec^R</i> , <i>rne131::kan^R</i>	This work
SA1743	<i>sgrS</i> A184A, <i>lacI^q-tetR-spec^R</i> , <i>rne131::kan^R</i>	This work
SA1744	<i>sgrS</i> G215A, <i>lacI^q-tetR-spec^R</i> , <i>rne131::kan^R</i>	This work
SA1745	<i>sgrS</i> T224G, <i>lacI^q-tetR-spec^R</i> , <i>rne131::kan^R</i>	This work
SA1746	<i>sgrS</i> T224A, <i>lacI^q-tetR-spec^R</i> , <i>rne131::kan^R</i>	This work
SA1908	<i>sgrS</i> G184A-C195T, <i>lacI^q-tetR-spec^R</i> , <i>rne131::kan^R</i>	This work
SA1909	<i>sgrS</i> T181A, <i>lacI^q-tetR-spec^R</i> , <i>rne131::kan^R</i>	This work
SA1910	<i>sgrS</i> T182A, <i>lacI^q-tetR-spec^R</i> , <i>rne131::kan^R</i>	This work
XM199	<i>lacI^q-tetR-spec^R</i> , <i>Δhfq::kan^R</i>	This work
XM200	<i>sgrS</i> A177T, <i>lacI^q-tetR-spec^R</i> , <i>Δhfq::kan^R</i>	This work

XM201	<i>sgrS</i> G184A, <i>lacI^q-tetR-spec^R</i> , <i>Δhfq::kan^R</i>	This work
CS196	<i>ΔptsG::tet^R</i>	5
CS123	<i>DJ480</i> strain carrying <i>G178C/G176C</i> mutations on <i>sgrS</i>	6,7

573

574

575 **Supplementary Table 2. Oligonucleotides used in this study.**

Oligo	Description	Sequence 5'-3'
1	Forward Primer for mutagenesis PCR of SgrS	CTATCAGTGATAGAGATACTGAGCACATATG
2	Reverse Primer for mutagenesis PCR of SgrS	GAGCCTTTCGTTTTATTTGATGGATCC
3	Forward primer for sequencing desired region of SgrS	TGGGATGACCGCAATTCTGAAA
4	Reverse primer for sequencing desired region of SgrS	GAGCCTTTCGTTTTATTTGATGGATCC
MBP251F	Forward primer for PCR amplification of the <i>cat-sacB</i> cassette	GCAATTTTATTTTCCCTATATTAAGTCAATAATTCCTAACAAA ATGAGACGTTGATCGGCACGTAAG
MBP251R	Reverse primer for PCR amplification of the <i>cat-sacB</i> cassette	TTATCCAGATCATACGTTCCCTTTTTAGCGCGGCGAGAATGTA TCAAAGGGAAACTGTCCATATGC
OSA766	Forward primer for PCR amplification of <i>sgrS</i> , for allelic exchange between <i>sgrS</i> and the <i>cat-sacB</i> cassette	GCAATTTTATTTTCCCTATATTAAGTCAATAATTCCTAACgat GAAGCAAGGGGGTGCCC
MBP252R	Reverse primer for PCR	TTATCCAGATCATACGTTCCCTTTTTAGCGCGGCGAGAATAAAA AAAAACCAGCAGGTATAATCTGCTGGCGGG

	amplification of <i>sgrS</i> , for allelic exchange between <i>sgrS</i> and the <i>cat-sacB</i> cassette	
OSA768	Reverse primer for PCR amplification of <i>sgrS</i> T181A, for allelic exchange between <i>sgrS</i> and the <i>cat-sacB</i> cassette	<p>TTATCCAGATCATACGTTCCCTTTTTAGCGCGGCGAGAATaaa</p> <p>AAAAACCAGCAGGTATAATCTGCTGGCGGGTGATTTTACACCA</p> <p>TTACTCAGTCACACATGATGCAGGCA</p>
OSA769	Reverse primer for PCR amplification of <i>sgrS</i> T182A, for allelic exchange between <i>sgrS</i> and the <i>cat-sacB</i> cassette	<p>TTATCCAGATCATACGTTCCCTTTTTAGCGCGGCGAGAATaaa</p> <p>AAAAACCAGCAGGTATAATCTGCTGGCGGGTGATTTTACACCT</p> <p>ATACTCAGTCACACATGATGCAGGC</p>
MBP252R2	Reverse primer for PCR amplification of <i>sgrS</i> G215A, for allelic exchange between <i>sgrS</i> and the <i>cat-sacB</i> cassette	<p>TTATCCAGATCATACGTTCCCTTTTTAGCGCGGCGAGAATAAA</p> <p>AAAAACCAGTAGGTATAATCTGCTGGCGGG</p>
MBP252R3	Reverse primer for PCR amplification of <i>sgrS</i> T224G, for allelic exchange between <i>sgrS</i>	<p>TTATCCAGATCATACGTTCCCTTTTTAGCGCGGCGAGAATAAA</p> <p>CAAAACCAGTAGGTATAATCTGCTGGCGGG</p>

	and the <i>cat-sacB</i> cassette	
MBP252R4	Reverse primer for PCR amplification of <i>sgrS</i> T224A, for allelic exchange between <i>sgrS</i> and the <i>cat-sacB</i> cassette	TTATCCAGATCATACGTTCCCTTTTTAGCGCGGCGAGAATAAA TAAAACCAGTAGGTATAATCTGCTGGCGGG
OSA499	Primer to amplify <i>SgrS</i>	GATGAAGCAAGGGGGTGCCC
OSA500	Primer to amplify <i>SgrS</i>	CAATACTCAGTCACACATGATGCAGGC
OXM187	Primer to amplify <i>rrsA</i>	ATTCCGATTAACGCTTGAC
OXM188	Primer to amplify <i>rrsA</i>	AGGCCTTCGGGTTGTAAAGT
MBP201F		ACCTGACGCTTTTTATCGCAACTCTCTACTGTTTCTCCATATAA ATAAAGGGCGCTTAGATGCCCTGTAC
MBP201R		TACGCCAGGTTTTCCAGTCACGACGTTGTAAAACGACTTGC AGTTAGCAAATGCATTCTTAAACAT
A177T-F	Forward primer to generate <i>SgrS</i> A177T mutant	CTTGCCTGCATCATGTGTGACTGTGTATTGGTGTA AAAATC
A177T-F	Reverse primer to generate <i>SgrS</i> A177T mutant	GATTTTACACCAATACACAGTCACACATGATGCAGGCAA
G178T-F	Forward primer to generate <i>SgrS</i> G178T mutant	CTTGCCTGCATCATGTGTGACTGATTATTGGTGTA AAAATC
G178T-R	Reverse primer to generate <i>SgrS</i> G178T mutant	GATTTTACACCAATAATCAGTCACACATGATGCAGGCAAG

G178A-F	Forward primer to generate SgrS G178A mutant	CTTGCTGCATCATGTGTGACTGAATATTGGTGTAATC
G178A-R	Reverse primer to generate SgrS G178A mutant	GATTTTACACCAATTATCAGTCACACATGATGCAGGCAAG
G184A-F	Forward primer to generate SgrS G184A mutant	CCTGCATCATGTGTGACTGAGTATTGATGTAAATCACCC
G184A-R	Reverse primer to generate SgrS G184A mutant	GGGTGATTTTACATCAATACTCAGTCACACATGATGCAGG
C215A-F	Forward primer to generate SgrS C215A mutant	CCCGCCAGCAGATTATACCTACTGGTTTTTTTTATTCTC
C215A-R	Reverse primer to generate SgrS C215A mutant	GAGAATAAAAAAAACCAGTAGGTATAATCTGCTGGCGGG
T224G-F	Forward primer to generate SgrS T224G mutant	GATTATACCTGCTGGTTTTATTATTCTCGCCGCG
T224G-R	Reverse primer to generate SgrS T224G mutant	CGCGGCGAGAATAAAATAAAACCAGCAGGTATAATC
T224A-F	Forward primer to generate SgrS T224A mutant	GATTATACCTGCTGGTTTTGTTTATTCTCGCCGCG
T224A-R	Reverse primer to generate SgrS T224A mutant	CGCGGCGAGAATAAACAAAACCAGCAGGTATAATC
sgrS-bio	SgrS probe used in the Northern blot analysis	GCAACCAGCACAACTTCGCTGTGCGGGTAAATAGTG
ssrA-bio	5S rRNA probe used in Northern blot analysis	CGCCACTAACAACTAGCCTGACGCCACTAACAAA

SgrS	Probes* for smFISH	GTGCTGATAAAACTGACGCA ACTTCGCTGTCGCGGTAAAA CTTAACCAACGCAACCAGCA CATGGTTAATCGTTGTGGGA ATCCCACTGCATCAGTCCTT GTCAACTTTCAGAATTGCGG TCAGTCACACATGATGCAGG GCGGGTGATTTTACACCAAT AACCAGCAGGTATAATCTGC
<i>ptsG</i>	Probes* for smFISH	GCATCTAAGCGCCCTTTATT GCAGGTTAGCAAATGCATTC ATCAGCGATTTACCGACCTT CTGCCATAACATGCGATACA CATGTTTGCAAAGACGGAAC GACACCGATCGCAAAAATCA GATACGCCATCGTTATTGGT ATGATGCCATAGGCAACAAC AACCACGGCCATGGTTTTAA CAGGTGTTTAGAGGCGATTT TAAACATGTACGCTGCGATC GGCAGCTTAATACGGTAGAA GGCAAAGAAGCCAAGATACT CAGAAATGATCGGCACAAAG CCAAATGAAGGACAGCACAA ACTGAGAGAAGGTCTGGATT CAACGTTTCGATGAAACCGTA GGTGTATTACCAATCTGCA GGCAGACCGTACATTTTGAA CGGTTTTCTGGTTTAGCAGA AACGATGAAGTCGATCAGAC GCGGAAGATGGTGTAGTAAA CGTTTTTCAGATCCAGTGCTT TCGCTTTTGCATCTTCAGTC TCTTTACCACCAAATGCAGC TACATGCGTCGAGGTTAGTA TTAGTACCGAAAATCGCCTG AGTGGTTACGGATGTACTCA

576

577 *The probes were complementary sequences across the length of the RNAs.

578

579

580

581

582 **Supplementary Table 3. Rate constants for SgrS, *ptsG* mRNA association, dissociation and**
 583 **SgrS-*ptsG* complex codegradation.**

	α_s (molecules- s ⁻¹)	β_s (s ⁻¹)	α_p (molecules- s ⁻¹)	β_p (s ⁻¹)	k_{on} (M ⁻¹ -s ⁻¹) x 10 ⁵	k_{off} (s ⁻¹)	k_{cat} (s ⁻¹)
Wild Type	0.35	0.0013	0.13 ± 0.02	0.0037	1.9	0.22	0.3
Wild Type RNase E Mutant	0.35	0.0013	0.11 ± 0.02	0.0037	1.9	0.22	0.0062
A177U	0.36	0.0021	0.14 ± 0.02	0.0039	1.5	0.25	0.31
A177U RNase E Mutant	0.36	0.0021	0.12 ± 0.02	0.0039	1.5	0.25	0.0060
G178A	0.36	0.0021	0.14 ± 0.03	0.0038	1.3	0.27	0.3
G178A RNase E Mutant	0.36	0.0021	0.11 ± 0.03	0.0038	1.3	0.27	0.0078
G178U	0.36	0.0021	0.14 ± 0.03	0.0039	1.3	0.27	0.32
G178U RNase E Mutant	0.36	0.0021	0.12 ± 0.02	0.0039	1.3	0.27	0.0075
U181A	0.36	0.0022	0.13 ± 0.02	0.0037	1.4	0.26	0.34
U181A RNase E Mutant	0.36	0.0022	0.11 ± 0.02	0.0037	1.4	0.26	0.0065
U182A	0.34	0.0023	0.14 ± 0.02	0.0040	1.4	0.265	0.3
U182A RNase E Mutant	0.34	0.0023	0.13 ± 0.02	0.0040	1.4	0.265	0.0060

G184A	0.35	0.0034	0.15 ± 0.03	0.0040	0.95	0.293	0.32
G184A RNase E Mutant	0.35	0.0034	0.12 ± 0.02	0.0040	0.95	0.293	0.0080
G184A-C195U	0.35	0.0014	0.14 ± 0.03	0.0039	1.85	0.225	0.33
G184A-C195U RNase E Mutant	0.35	0.0014	0.12 ± 0.02	0.0039	1.85	0.225	0.0068
G215A	0.36	0.0025	0.15 ± 0.02	0.0040	1.2	0.28	0.30
G215A RNase E Mutant	0.36	0.0025	0.12 ± 0.02	0.0040	1.2	0.28	0.0082
U224A	0.34	0.0024	0.14 ± 0.03	0.0038	1.28	0.258	0.33
U224A RNase E Mutant	0.34	0.0024	0.11 ± 0.02	0.0038	1.28	0.258	0.0080
U224G	0.35	0.0022	0.14 ± 0.02	0.0038	1.3	0.27	0.32
U224G RNase E Mutant	0.35	0.0022	0.11 ± 0.02	0.0038	1.3	0.27	0.0075

584

585

Supplementary Table 4. Goodness of fit for the time dependent curves.

	Global R^2	R^2 for SgrS	R^2 for ptsG	R^2 for complex	χ^2 for complex	α for complex
Wild-type	0.999	0.999	0.995	-	0.37	0.01
Wild-type RNase E Mutant	0.999	0.999	0.963	0.902	-	-
A177U	0.998	0.998	0.993	-	0.33	0.001
A177U with WT k_{on} and k_{off}	0.990	0.996	0.970	-	0.27	0.001
A177U RNase E Mutant	0.998	0.999	0.927	0.805	-	-
A177U RNase E Mutant with WT k_{on} and k_{off}	0.990	0.998	0.796	0.581	-	-
G178A	0.999	0.999	0.990	-	0.09	0.001
G178A with WT k_{on} and k_{off}	0.990	0.993	0.931	-	0.15	0.001
G178A RNase E Mutant	0.999	0.999	0.962	0.700	-	-
G178A RNase E Mutant with WT k_{on} and k_{off}	0.990	0.998	0.749	-	17.73	0.99
G178U	0.999	0.999	0.994	-	0.13	0.001
G178U with WT k_{on} and k_{off}	0.991	0.994	0.959	-	0.15	0.001
G178U RNase E Mutant	0.999	0.999	0.970	0.795	-	-
G178U RNase E Mutant with WT k_{on} and k_{off}	0.991	0.999	0.772	-	21.36	0.999
U181A	0.998	0.998	0.997	-	0.27	0.001
U181A with WT k_{on} and k_{off}	0.982	0.982	0.979	-	2.63	0.15
U181A RNase E Mutant	0.998	0.998	0.989	0.789	-	-
U181A RNase E Mutant with WT k_{on} and k_{off}	0.982	0.988	0.978	-	24.59	0.9995

U182A	0.997	0.998	0.986	-	0.69	0.01
U182A with WT k_{on} and k_{off}	0.987	0.995	0.968	-	2.57	0.15
U182A RNase E Mutant	0.997	0.997	0.990	0.854	-	-
U182A RNase E Mutant with WT k_{on} and k_{off}	0.987	0.994	0.975	-	17.26	0.99
G184A	0.998	0.998	0.996	-	0.12	0.001
G184A with WT k_{on} and k_{off}	0.982	0.987	0.837	-	0.18	0.001
G184A RNase E Mutant	0.998	0.999	0.997	0.704	-	-
G184A RNase E Mutant with WT k_{on} and k_{off}	0.982	0.999	0.969	-	5.47	0.5
G184A-C195U	0.999	0.999	0.976	-	0.28	0.001
G184A-C195U with WT k_{on} and k_{off}	0.996	0.997	0.984	-	0.29	0.001
G184A-C195U RNase E Mutant	0.999	0.999	0.957	0.953	-	-
G184A-C195U RNase E Mutant with WT k_{on} and k_{off}	0.996	0.997	0.975	0.905	-	-
G215A	0.998	0.998	0.992	-	0.04	0.001
G215A with WT k_{on} and k_{off}	0.988	0.990	0.913	-	0.11	0.001
G215A RNase E Mutant	0.998	0.998	0.836	0.712	-	-
G215A RNase E Mutant with WT k_{on} and k_{off}	0.988	0.998	0.928	-	4.56	0.4
U224A	0.998	0.998	0.982	-	0.06	0.001
U224A with WT k_{on} and k_{off}	0.989	0.999	0.913	-	0.12	0.001
U224A RNase E Mutant	0.998	0.998	0.912	0.702	-	-
U224A RNase E Mutant with WT k_{on} and k_{off}	0.989	0.997	0.645	-	37.39	0.999995
U224G	0.998	0.998	0.964	-	0.08	0.001

U224G with WT k_{on} and k_{off}	0.988	0.991	0.888	-	0.13	0.001
U224G RNase E Mutant	0.998	0.998	0.933	0.941	-	-
U224G RNase E Mutant with WT k_{on} and k_{off}	0.988	0.997	0.981	-	5.731	0.55

587

588

589 **Supplementary Note 1**

590 **Impact of SgrS mutations on *ptsG* mRNA intrinsic degradation rates**

591 In order to solve the deterministic model (equations shown in Fig. 1), we also needed to obtain
592 the SgrS-independent degradation rates of *ptsG* mRNA. To determine this in various SgrS
593 mutant strains, we grew cells without SgrS induction and added rifampicin to stop transcription.
594 Samples were collected over time and fixed using paraformaldehyde. The fixed cells were then
595 subjected to the same imaging and analysis protocol and the average copy number of *ptsG*
596 mRNA per cell was calculated as a function of time after transcription inhibition. The
597 degradation rate thus determined was 0.0037 s^{-1} (4.5 min lifetime) for the wild type strain and
598 remained similar for all the mutants (Fig. S24-S34, S39). This verified that the mutations in the
599 SgrS by themselves do not affect the *ptsG* mRNA stability in the absence of sugar stress and co-
600 degradation.

601

602

603

604

605

606

607

608

609 **References**

- 610 1. Aiba, H., Adhya, S. & de Crombrughe, B. Evidence for two functional gal promoters in
611 intact Escherichia coli cells. *J. Biol. Chem.* **256**, 11905–10 (1981).
- 612 2. Schneider, C. A., Rasband, W. S. & Eliceiri, K. W. NIH Image to ImageJ: 25 years of
613 image analysis. *Nature Methods* (2012). doi:10.1038/nmeth.2089
- 614 3. Bobrovskyy, M. & Vanderpool, C. K. Diverse mechanisms of post-transcriptional
615 repression by the small RNA regulator of glucose-phosphate stress. *Mol. Microbiol.* **99**,
616 254–273 (2016).
- 617 4. Morita, T., Kawamoto, H., Mizota, T., Inada, T. & Aiba, H. Enolase in the RNA
618 degradosome plays a crucial role in the rapid decay of glucose transporter mRNA in the
619 response to phosphosugar stress in Escherichia coli. *Mol. Microbiol.* **54**, 1063–1075
620 (2004).
- 621 5. Fei, J. *et al.* Determination of in vivo target search kinetics of regulatory noncoding RNA.
622 *Science* (80-.). **347**, 1371–1374 (2015).
- 623 6. Kawamoto, H., Koide, Y., Morita, T. & Aiba, H. Base-pairing requirement for RNA
624 silencing by a bacterial small RNA and acceleration of duplex formation by Hfq. *Mol.*
625 *Microbiol.* **61**, 1013–1022 (2006).
- 626 7. Wadler, C. S. & Vanderpool, C. K. Characterization of homologs of the small rna sgrs
627 reveals diversity in function. *Nucleic Acids Res.* **37**, 5477–5485 (2009).

628